November 2018

Fatty Acid Amides and Their Biosynthetic Enzymes Found in Insect Model Systems

Ryan L. Anderson
University of South Florida, rlander6@mail.usf.edu

Fatty Acid Amides and Their Biosynthetic Enzymes Found in Insect Model Systems

by

Ryan L. Anderson

A dissertation submitted in partial fulfillment
of the requirements for the degree of
Doctor of Philosophy
Department of Chemistry
College of Arts and Sciences
University of South Florida

Major Professor: David J. Merkler, Ph.D.
Abdul Malik, Ph.D.
James Leahy, Ph.D.
Andreas Seyfang, Ph.D.

Keywords: Arylalkylamine *N*-acyltransferase, *N*-acylarylalkylamides, *Bombyx mori*, *Drosophila melanogaster,* upstream activator sequence, Gal4, SiRNA, knockdown

DEDICATION

This work is dedicated to my sister and father. I carry them with me every day and I know they would be proud of my accomplishments. I also dedicate this work to the rest of my loving, supportive family and friends.

ACKNOWLEDGEMENTS

I have had the pleasure of experiencing so many meaningful interactions on my journey to becoming a Ph.D. and am so grateful for each and every one of them. My efforts would not be possible if Dr. Kristen Jeffries had not created the preliminary space for me to start doing research on a graduate level at one of my lowest points in life. She became part of my first lab family and meaningful mentors, along with Dr. David Merkler, Dr. Daniel Dempsey and Dr. Matthew Battistini. Their compassion and skills as good leaders will always be looked up to as I continue my career in hopes of spreading, not only knowledge, but also comradery to instill a sense of family and friendship in the lab. As I quickly became the senior student in the lab, I then had the pleasure of being a bridge between the old and new students in Dr. Merkler's lab. It was also a great experience getting to know new colleagues such as Brian O'Flynn, Gabriela Suarez, John Dillashaw and Amanda Pierce, who quickly became my second lab family and were wonderful people with whom I could continue to learn and solve problems. To add to this, I became a mentor to a group of very bright undergraduates including Sydney Balgo, Carly Gunderson, Dean Holliday, Sydney Innes, Joseph Mira, Alexandria Musick, Alexander Aguirre, and Dylan Wallis. All these bright undergraduates became my friends as well as pupils. One of them even became my roommate and created a lifelong friendship. I would also like to thank my best friends in the area, Christine Bornberg, Miranda Betagglio and Francesca Kerns, for being supportive when I needed it the most. There were several other colleagues and friends who played a role in keeping me sane and productive throughout graduate school and I cannot thank them all enough.

TABLE OF CONTENTS

LIST OF TABLES

LIST OF FIGURES

LIST OF ABBREVIATIONS

AANAT	Arylalkylamine *N*-acyltransferase
AracSer	*N*-arachidonoylserotonin
Bm-iAANAT	Bombyx mori insect arylalkylamine *N*-acyltransferase
*Bmi*1	*Bombyx mori* instar 1
*Bmi*2	*Bombyx mori* instar 2
*Bmi*3	*Bombyx mori* instar 3
*Bmi*4	*Bombyx mori* instar 4
*Bmi*5	*Bombyx mori* instar 5
bp	base pair
CB	cannabinoid receptor
cDNA	complimentary deoxyribonucleic acid
CID	collision induced dissociation
CoA	coenzyme A
CT	cycle threshold
dsDNA	double-stranded DNA
FAA	fatty acid amide
FAAH	fatty acid amide hydrolase
GPR	G-protein receptor
GLYAT	glycine *N*-acyltrasnferase
HPLC	high performance liquid chromatography
LC-QToF-MS	Liquid chromatography time-of-flight mass spectrometry
LinGly	*N*-linoleoylglycine

Lino	linoleamide
mRNA	messenger RNA
MS/MS	tandem mass spectrometry
NADA	*N*-acetyldopamine
NAE	*N*-acylethanolamine
NAG	*N*-acylglycine
ND	not detected
pAb	polyclonal antibody
Palm	palmitamide
PalmDop	*N*-palmitoyldopamine
Palmle	palmitoleamide
PalmSer	*N*-Palmitoylserotonin
PALDA	*N*-palmitoyldopamine
Ole	oleamide
OleDop	*N*-oleoyldopamine
OleEth	*N*-oleoylethanolamine
OleSer	*N*-oleoylserotonin
OleTrp	*N*-oleoyltryptamine
PalmGly	*N*-palmitoylglycine
PAM	peptidylglycine-α-amidating monooxygenase
PFAM	primary fatty acid amide
OleGly	*N*-oleoylglycine
RISC	RNA induced silencing complex
RNA	ribonucleic acid
RT	reverse transcriptase

RT-qPCR	reverse transcriptase – quantitative polymerase chain reaction
Sb[1]	stubble gene
SDS-PAGE	sodium dodecyl sulfate – polyacrylamide gel electrophoresis
siRNA	small interfering RNA
ssRNA	single-stranded RNA
SteSer	*N*-stearoylserotonin
THC	tetrahydrocannabinol
TRPM8	transient receptor potential melastatin type 8
TRPV1	transient receptor potential vanilloid type 1
UAS	upstream activator sequence

ABSTRACT

A fatty acid amide is precisely as the name suggests: A fatty acid (CH_n-COOH), in which the hydroxyl group of the carboxylic acid is displaced by an amine functional group from a biogenic amine (R-NH_2), ultimately forming an amide bond. Furthermore, these fatty acid amides can be composed of a variety of different acyl chain lengths donated by the fatty acid and a myriad of different biogenic amines. Thus, these molecules can be subdivided in a number of different ways including the separation of short chain (acetyl to heptanoyl) and long chain (palmitoyl to arachidonoyl) and also based off the biogenic amine type. The long chain fatty acid amides quickly gained the interest of the scientific community through the discovery of anandamide (*N*-arachidonoylethanolamide), which was found to be the endogenous ligand for the cannabinoid receptor-1 (CB_1) found in the mammalian brain. This particular neural molecule is an *N*-acylethanolamide, which is one specific classification of long chain fatty acid amide. However, there exist other types of long chain fatty acid amides including the *N*-acylglycines, primary fatty acid amides (PFAMs) and *N*-acylarylalkylamides. Yet, despite the type of fatty acid amide, it has been shown many of these types of molecules are synthesized using a type of *N*-acyltransferase. These *N*-acyltransferases are believed to be members of the GCN5-related superfamily of *N*-acyltransferases (GNAT), which share the feature of being able to accept acyl-CoA thioester substrates. This dissertation will discuss and demonstrate the extraction of all types of the aforementioned classifications of long chain fatty acid amides but will have a particular focus on the *N*-acylarylalkylamides. Elucidating more about the biosynthetic pathways and metabolic routes of the long chain fatty acid amides could lead to the development of potential therapeutics and pest control agents. We have determined *Drosophila melanogaster* arylalkylamine N-acyltransferase like 2 is responsible for the in vivo biosynthesis of *N*-acyldopamines. We have also demonstrated *Bombyx mori* is another suitable model systems for the study of long chain fatty acid amides, as three insect arylalkylamine N-

acyltrasnferase from Bombyx mori (*Bm*-iAANAT) were found to share some homology in primary sequence (25-29%) to AAANTL2 in *Drosophila melanogaster*. We show herein that one of these enzymes is able to catalyze the formation of long chain *N*-acylarylalkylamides *in vivo*. The change in the transcription of these enzymes was tracked to try and understand if these enzymes serve a focused purpose in the physiological development of the insect. If it is found one of these *Bm*-iAANAT are crucial for growth, it may elucidate a general function of the enzyme, which may be able to inhibit growth of specific insects that are known pests, while not targeting endangered insects like *Apis melliferra* (honey bee). Understanding this would help in the eventual creation of targeted insecticides on specific insect pests Furthermore, a novel panel of fatty acid amides was characterized and quantified in extracts from this organism via LC-QToF-MS, ultimately showing it is very possible the *Bm*-iAANATs are performing this catalysis *in vivo*.

CHAPTER ONE

Introduction and literature review

1.1 Fatty acid amide research stems from studies done on cannabis and are biologically significant

Fatty acid amides are encompassed by the class of molecules known as endocannabinoids. These biomolecules have structural similarities to the most popular (and somewhat controversial) cannabinoid, Tetrahydrocannabinol (THC) and some have been found to be the endogenous ligands for the same receptors [1]. Cannabis has been widely used in the past as a medicine and for ritualistic practices and is known to have an array of physiological effects on mammals through the binding of molecules known as cannabinoids [2]. After an elucidation of the structure of THC by the Mechoulam group in 1964 [3], the avenue for THC binding studies was opened in order to understand how these molecules from a plant can have effects on mammals. The Howlett group took advantage of this opportunity and characterized the cannabinoid receptors (CB_1) in rat brains and proposed there must be endogenous molecules giving these receptors a purpose *in vivo* [4]. This ultimately led to the discovery of *N*-Arachidonoylethanolamide (anandamide), which is an endogenous ligand for the cannabinoid receptors in mammalian brains [5]. All this, ultimately, unlocked a broad field of research involving these lipid-signaling molecules, which attain similar structural motifs and use related *N*-acyltransferases for biosynthesis.

A fatty acid amide is precisely as the name implies: A fatty acid ($CH3(CH_2)_nCOOH$) where the hydroxyl at the head is replaced by an amine-containing compound ($R\text{-}NH_2$) to create an amide group. This nitrogenous group has been found to be donated by a number of different possibilities, which has, in turn, created several subclasses when combined with various alkyl chain lengths [6-7]. The groups of particular importance to this research include *N*-acylethanolamines (NAE), *N*-acylglycines (NAG), primary fatty acid amides (PFAM), and the *N*-acylarylalkylamides (NAAs). Due to its association with the cannabis field, the NAEs received the most amount of attention when considering research efforts.

However, this left a door open for the experimentation of other fatty acid amides. Although this research regards all proposed fatty acid amide subgroupings, the *N*-acylarylalkylamines will be of particular interest.

1.1.a Biosynthetic pathway of fatty acid amides

The fatty acid amides are linked through a single biosynthetic pathway and through the fact they all require a *N*-acyltransferase in the catalysis of their formation. This generally starts with a fatty acid of varying chain length, which is used as a substrate for the creation of an acyl-CoA using acyl-CoA synthase. This "activated" fatty acid now contains a good leaving group in the form of coenzyme A and can utilize a number of different acyltransferase enzymes capable of accepting fatty acid CoA thioester substrates and substituting the CoA leaving group for a biogenic amine [8-10]. If an arylalkylamine *N*-acyltransferase (AANAT) is used, an arylalkylamine, like dopamine or serotonin, can be used to create an *N*-acylarylalkylamide (NAAA) [11]. Alternatively, a glycine *N*-acyltransferase (GLYAT) can attach a glycine molecule to make the *N*-acylglycine (NAG) [6, 12]. Peptidylglycine α-amidating monooxygenase can finally use the *N*-acylglycine to make a primary fatty acid amide (PFAM), which simply has a simple amide group attached the acyl chain [13]. An alternative route has also been noted, which uses an *N*-acylethanolamide as a starting substrate and uses an *N*-acyglycinal intermediate for the creation of NAGs [14-15]. A putative pathway has been drafted for the biosynthetic pathway of fatty acid amides, starting from a fatty acid and going to a primary fatty acid amide (Figure 1.1) [16].

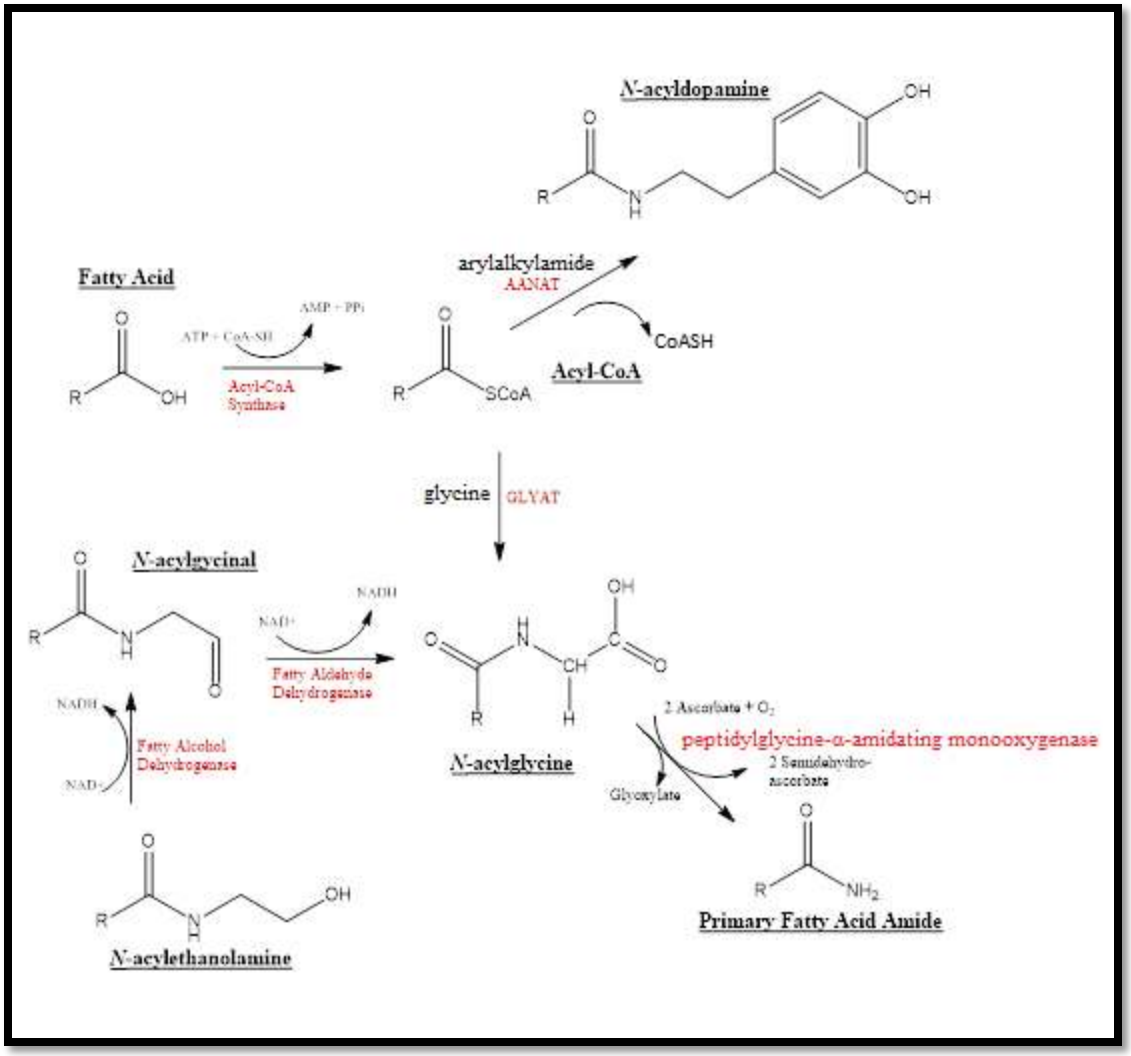

Figure 1.1 Biosynthetic pathway of fatty acid amides

1.1.b N-acylethanolamines

Many long chain *N*-acylethanolamines have been extracted and characterized from the mammalian brain with the highest concentrations consisting of acyl chains such as *N*-palmitoyl (16:0)-, *N*-stearoy l (18:0)-and *N*-oleoyl- (18:1) [7, 17]. However, other, less concentrated, long chains have been recognized with an ethanolamine moiety within mammalian brains, including *N*-linoleoyl(18:2)ethanolamine, *N*-linolenoyl(18:3)ethanolamine, *N*-docosatetraenoyl(22:4)ethanolamine [7]. The long chain *N*-acylethanolamines are probably the most well-known of the fatty acid amides due to the discovery of *N*-arachidonoylethanolamine. This was previously found to be the endogenous ligand to the cannabinoid receptors, CB_1, and its existence is the reason THC has physiological effects on the

mammalian brain [18]. Anandamide binds to other non-cannabinoid receptors such as the peroxisome proliferator-activated receptors (PPARα) [19], the transient receptor potential vanilloid type 1 (TRPV1) channels [20] and the transient receptor potential melastatin type 8 (TRPM8) [21]. Yet, the precise physiological effect elicited by anandamide binding to the non-cannabinoid receptors remains somewhat elusive. It is known anandamide plays a role in the regulation of body temperature, feeding, nociception, anxiety, fear and locomotion [1, 22-23]. The physiological effect of other *N*-acylethanolamines have yet to be fully elucidated and most have not been found to bind directly to the CB_1 and CB_2 receptors, but their names, suggested effects and known receptors can be seen in Table 1.1.

Table 1.1 Some *N*-acylethanolamines and their known receptors

N-acylethanolamine	Receptor Binding	Reference
N-dihomo-γ-linoleoylethanolamine	CB_1, CB_2	[20], [24], [25]
N-docosatetraenoylethanolamine	CB_1, CB_2	[20], [24], [25]
N-Oleoylethanolamine	PPARα, PPARβ, TRPV1, GPR119	[19], [24], [26], [27]
N-Stearoylethanolamine	CB_1(non-specific), CB_2	[28]
N-palmitoylethanolamine	PPARα, GPR55	[29], [30]

The *N*-acylethanolamines (NAE) can use different routes for their biosynthesis. The most widely accepted route starts with the *N*-acylation of phosphatidylethanolamine via calcium activated transacylase. *N*-acylphosphatidylethanolamine (NAPE) and uses the NAPE-specific phospholipase D (NAPE-PLD) to cleave the NAPE to make the corresponding NAE and phosphatidic acid [31-32]. Although this has been widely accepted to be a main route for NAE generation, there is evidence showing PLD-independent pathways also exist. One such pathway uses the cleavage of NAPE, mediated by phospholipase C, to create a phospho-NAE (pNAE) intermediate, which is ultimately cleaved by a phosphatase to yield the NAE [33]. The existence of multiple biosynthetic routes for the NAEs suggests their biological

importance, as different organisms may have backup systems for their generation in the case of metabolic emergencies [34].

General degradation of NAEs is believed to occur through a hydrolysis pathway to generate the fatty acid and the ethanolamine: R-CO-NH-CH_2-OH + H_2O $\longrightarrow$ R-COOH + NH_2-CH_2-OH. There has been detection of three different enzymes capable of performing this chemistry: Two of them are isoforms of fatty acid amide hydrolase (FAAH-1 and FAAH-2), which attain different acyl group specificity [35]. The third is an *N*-acylethanolamine-hydrolyzing acid amidase [36]. It should be noted that potential analgesic therapeutics are being based of the inhibition of FAAH [37].

1.1.c N-acylglycines

This section of the chapter has been previously published as the following review article: Anderson, R.L., Merkler, D. J., N-Fatty Acylglycines: Underappreciated endocannabinoid-like fatty acid amides? *Journal of Biology and Nature* 2017, 8 (4), 156-165. Ryan Anderson and David J. Merkler wrote the article. David J. Merkler is responsible for the idea to review this material. The article has been reproduced in Appendix A with the no extra permission required from Elsevier Limited.

1.1.d Primary Fatty Acid Amides

Structurally speaking, the primary fatty acid amides (PFAMs) can be viewed as the most simplistic due to the amide bond being formed by ammonia (NH_3). Yet, despite their simple structure, these compounds have been found to play a number of different roles in the physiology of both vertebrates and invertebrates. The first recorded detection of primary fatty acid amides included the characterization of palmitamide, palmitoleamide, oleamide, elaidamide and linoleamide., which were extracted from luteal phase plasma in 1989 [13]. Another significant detection of the PFAMs occurred when Cravatt et al. isolated oleamide and erucamide from the cerebrospinal fluid (CSF) of cats, rats and humans. Yet, the function of the PFAMs remained elusive until it was found injecting rats with nanomolar quantities of oleamide induced sleep in rats, which was a very exciting finding for the field as one of the molecules of this long chain fatty acid amide subclass now had a known phenotype in the sleep/wake cycle of mammalian system [38]. Several other phenotypic relationships of oleamide were

quickly found after these initial discoveries. For instance, it has now been shown oleamide also plays significant roles in signaling pathways regarding gap junction communication in glial cells, memory regulation, body temperature, locomotor activity, Ca^{2+} release, depressant drug receptor transduction and allosteric activation of the gamma amino butyric acid A ($GABA_A$) receptors [39-40]. Therefore, oleamide received a significant amount of attention at the forefront of PFAM discovery. However, other functions of different long chain PFAMs were recognized after these findings. For instance, linoleamide has been found to increase Ca^{2+} flux [41] and inhibits the *erg* current in pituitary cells [42]. Also, erucamide has been found to stimulate growth in blood vessels and regulates fluid imbalance, while elaidamide might function as an endogenous inhibitor of epoxide hydrolase. Ultimately the PFAMs are useful target of molecules to study within different model systems as many of their functions have yet to be generally defined. The Merkler lab previously characterized a novel panel of endogenous long chain fatty acid amides in the head and thorax-abdomen of *Drosophila melanogaster*, which included several PFAMs [16]. Much work remains to be done on elucidating the exact function of these molecules in both vertebrates and invertebrates, which may ultimately lead to the creation of targeted insecticides as well as information on general fatty acid amide biosynthesis in all organisms. As far as a degradative pathway is concerned, the PFAMs are believed to be degraded by FAAH to yield ammonia and a free fatty acid [26, 43].

1.1.e N-acylarylalkylamides are biologically significant and underappreciated

Out of the long chain fatty acid amides mentioned thus far, the *N*-acylethanolamides are the most widely studied due to their connection to anandamide and THC. However, many other long chain fatty acid amides of different chain length and biogenic amine have also been found to be biologically active. The biological function of some NAGs and PFAMs have been elucidated, as there is data showing *N*-oleoylglycine (NAG) and oleamide (PFAM) both decrease locomotion and body temperature in mammals [44]. However, the long chain *N*-acylarylalkylamides are arguably the most understudied and underappreciated of the fatty acid amides. This could be due to the fact they are generally seen as lowly abundant in comparison to the classifications of long chain fatty acid amides and are, therefore, more

difficult to detect. *N*-Acylarylalkylamides include the compounds containing arylalkylamine functional groups as part of the chemical structure. Out of all *N*-acylarylalkylamides in possible existence, the most widely seen in the literature are the *N*-acyldopamines (Figure 1.2) [45] and *N*-acylserotonins (Figure 1.3) [46-47] and have been discovered in a myriad of different living systems with varying chain lengths (Table 1.2).

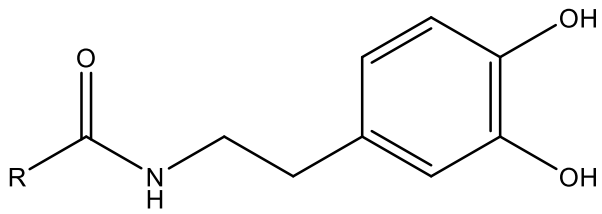

Figure 1.2 General structure of an *N*-acyldopamine. R is an alkyl group.

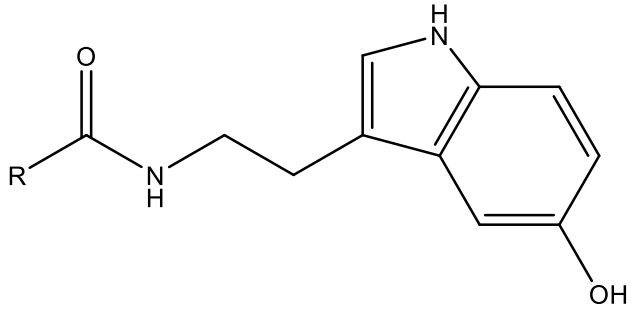

Figure 1.3 General structure of an *N*-acylserotonin. R is an alkyl group.

Table 1.2 *N*-acylarylalkylamides characterized in various organisms

N-acylarylalkylamide	Organism	Localization	Reference
N-Myristoyldopamine (14:0)	Rat	Brain	[48]
N-Palmitoyldopamine (16:0)	Rat Mouse Fruit Fly	Striatum $N_{18}TG_2$ cells Head Thorax-abdomen	[49] [50] [16]

Table 1.2 *N*-acylarylalkylamides characterized in various organisms

N-Stearoyldopamine (18:0)	Bovine	Brain	[48]
	Rat	Brain	[51]
N-Oleoyldopamine (18:1)	Rat	Striatum	[49]
	Mouse	$N_{18}TG_2$ cells	[50]
	Fruit Fly	Head	[16]
		Thorax-abdomen	
N-Arachidonoyldopamine (20:4)	Rat	Striatum	[49]
	Mouse	$N_{18}TG_2$ cells	[50]
	Fruit Fly	Head	[16]
		Thorax-abdomen	
N-Palmitoylserotonin (16:0)	Porcine	Intestinal tract	[47]
	Fruit fly	Thorax-abdomen	[52]
N-Stearoylserotonin (18:0)	Porcine	Intestinal tract	[47]
	Fruit fly	Thorax-abdomen	[52]
N-Oleoylserotonin (18:1)	Porcine	Intestinal tract	[47]
	Fruit fly	Thorax-abdomen	[52]
N-Arachidonoylserotonin (20:4)	Porcine	Intestinal tract	[47]
	Fruit fly	Thorax-abdomen	[16]
	Human	Brain	[53]
	Bovine	Brain	[53]

Clearly these molecules play an important role to life, which is indicative by their ubiquitous presence throughout the animal kingdom. Yet, there is much to be understood in regard to the biological synthesis and functionality of the *N*-acylarylalkylamides. Also, there are other biogenic amines other than serotonin and dopamine capable of being present in a long chain fatty acid amide structure and these molecules have yet to be extracted from or studied.

The degradation of N-acylarylalkylamides may be diverse due to the different possibilities of biogenic arylalkylamide attachment. However, one recognized degradative pathway for the *N*-acyl dopamines includes FAAH hydrolysis. Another way in which the *N*-acyldopamines can be degraded is through the use of *O*-methylation via *O*-methyltransferase [54].

1.2 Insect model systems as candidates to study fatty acid amide metabolism

1.2.a *Drosophila melanogaster*

Insects are quite pragmatic tools to use for the study of how biomolecules are generally metabolized and or synthesized. There have been many significant scientific discoveries made by using insects as the primary organisms of study. In the case of *Drosophila melanogaster*, or the common fruit fly, there have been six Nobel prizes, including the 2017 Nobel prize in Physiology and Medicine, won from its use as a scientific model [55]. Part of the reason these insects make such good candidates for biological and biochemical research is because their genome sequence has been elucidated, which has allowed them to be used in loss-of-function and gain-of-phenotype experiments. Furthermore, several cases directly involving fatty acid amide-related areas of human health have been completed, can be seen in Table 1.3.

Table 1.3 *Drosophila's* potential to study fatty acid amide systems involved in health and physiology

Type of Model System	Fatty Acid Amide Correlation	How *Drosophila* was/could be used
Aging	Aging decreases endogenous levels of anandamide and increases neuropathic pain [56]	Mutated *Indy* and lifespan [57]; Overexpressing fatty acid-β-oxidation-related genes and dietary restriction [58]. Feeding curcumin [59]
Alzheimer's Disease	*N*-palmitoylethanolamine is an anti-inflammatory and neuroprotective therapeutic [60], might treat memory impairments [61]	UAS controlling amyloid beta (Aβ) precursor proteins (stocks available at Bloomington Labs)
Huntington's Disease	Therapeutics based on endocannabinoid signaling [62] and biomarkers [63]	RNAi of *Huntington* or *Huntington-interaction protein 14* via UAS (Bloomington Lab)
Obesity	Ingested linoleate promotes weight gain via endocannabinoids and increases risk of obesity [64]	Fed high fat diet or express *human synphilin-1* protein via UAS control [65]
Pain	Anandamide [66-68], *N*-oleoylethanolamine [69], *N*-palmitoylethanolamine [70], N-arachidonoylglycine [71], *N*-arachidonoylserine [72] are analgesics	Exposure to UV radiation or heat [73]
Parkinson's Disease	Interactions between dopaminergic and cannabinoid signaling [74], endocannabinoid signaling [75-76], endocannabinoid-based therapeutics [62]	RNAi of pink1 or parkin via UAS [77] Loss of porin function in dopaminergic neurons via UAS/Gal4 [78]
Schizophrenia	Interactions between dopaminergic and cannabinoid signaling [74]	Use of Drosophila neuromuscular junction as model synapse [79]

Therefore, due to its high use and the availability of commercial strains, the fruit fly was a prime candidate for the study of fatty acid amide biosynthesis and metabolism. Also, the Merkler lab already had preliminary data in their discovery of seven N-acyltransferases, of which, two confidently seemed to

have the characteristics of AANAT enzymes [80]. They had then further discovered arylalkylamine N-acyltransferase-like 2 (AANATL2) in *D. melanogaster* indeed had the capability to catalyze the *in vitro* formation of long chain *N*-acylserotonins and *N*-acyldopamines [81]. Yet, there was still lacking evidence elucidating whether the chemistry was occurring *in vivo*.

1.2.b *Bombyx mori*

The domesticated silkworm, or *Bombyx mori*, has also been investigated as another insect model system for biochemical and biological research. This insect belonging to the *Lepidoptera* family has attained an economic value through its domestication over the last 5000 years, but is also considered a relatively new, scientific, insect model system since its genome was sequenced in 2009 [82-83]. Due its late arrival into the field of model systems, less mutant strains and genetic experiments have been done in comparison to *Drosophila*, zerba fish and *C. elegans*. Nonetheless, transgenic lines using different technologies to manipulate the expression of endogenous or exogenous genes have been used for various studies and can be seen in Table 1.4. Due to the fact many genes have unknown functions in this insect, many of the experiments still being done are to elucidate phenotypes and functions within the actual insect, rather than using it as a disease model for higher vertebrates, such as seen in *Drosophila*.

Table 1.4 Genetic engineering *Bombyx mori*

Method of genetic manipulation	Biochemical system(s) engineered
UAS/Gal4	Enhanced expression of calcium indicator protein (GCaMP5G) for improved visualization of neural activity, expression of tetanus toxin light chain (TeTxLC) to block synaptic transmission in sex pheromone receptors [84]; Expression of *dTrpA1* under UAS control [85]
CRISPR/Cas9	Testing the heritability of edited genomes using four test loci *Bm-ok*, *BmKMO*, *BmTH* and *Bmtan* [86]
Zinc-finger nucleases (ZFNs)	Somatic and germline mutations are caused by ZFN mRNA injections affecting the epidermal color marker gene (BmLOS2) via NHEJ [87]

However, this holds useful merit, as understanding more about general insect biochemistry yields the potential to uncover potential targets for insecticides to aid agriculture industries [88]. Furthermore, *Bombyx mori* is an ideal candidate for the study of fatty acid amides, particularly the *N*-

acylarylalkylamides and AANAT (iAANAT) [89]. Several enzymes were detected through a BLAST search and found to have some sequence homology (~29%) with *Drosophila* AANATL2 [90]. Furthermore, work has been done on two of these *Bombyx mori* insect AANATs (*Bm*-iAANAT) to show they played a role in the pigmentation and cuticle morphology of the silkworm through production of fatty acid amides, like *N*-acetyldopamine (NADA) [91]. However, none of these enzymes had been investigated for their potential to produce longer chain fatty acid amides, more specifically the *N*-acylarylalkylamides. Our goal is to investigate further these *Bm*-iAANATs to see if they catalyzed the formation of long chain fatty acid amides and how they might eventually be good candidates for targeted insecticides.

1.3 Lipidomics

The lipidome refers to the different lipid molecules found from a biological source. However, unlike nucleic acids, proteins, and carbohydrates, lipids include a more diverse class of relatively low molecular weight compounds. They do not all share a structural motif, but rather are consumed by the term due to their lack of solubility in water. The main classes are the neutral lipids, which include long-chain acylglycerols, fatty acids and their oxygenated derivatives. Then there are the more complex lipids, which include molecules like phospholipids, sphingolipids, glycolipids, and the various steroids and derivatives. Ultimately, lipids are a large and diverse group of biomolecules found ubiquitously in different innerworkings of cellular life and the entirety, and/or portions of this spectrum of compounds in a biological system are potentially useful areas of research.

The mapping of this spectrum would then be called lipidomics, which is a rising field of experimentation done to elucidate the form and function of various, simple and complex lipids within a cellular context. Furthermore, lipidomics can be divided into three separate, analytical schemes: untargeted, focused, and targeted lipidomics. Untargeted lipidomics refers to the method development for comprehensive lipid profiling from biological sources. Focused lipidomics investigates lipids of several different categories, usually with the employment of tandem mass spectrometry (MS-MS). Product-ion

scanning, precursor-ion scanning, and neutral-loss scanning can also be used to characterize lipids focused in limited categories. For example,Wang *et al.* completed a study first using untargeted lipidomics to identify 295 lipid species in the liver of mice. They then continued the study using focused lipidomics to find 39 out of the 295 hepatic lipids had significantly increased concentrations due to the knockout of the low density lipoprotein receptor (LDLR) [92]. Furhtermore, targeted lipidomics aims to determine target specific classifications of lipids and can be accomplished via selected reaction monitoring (SRM) or multiple reaction monitoring (MRM), as the fragmentation patterns of many lipids are known [93]. Ultimately, the field of lipidomics attains a spectrum in the quantity and classification of lipids being studied, in which the focus can be either very broad or very narrow, and the methodology can vary as well.

High performance liquid chromatography (HPLC) happens to be the most common technique used for lipidomic analysis. This is due to its good reproducibility and high resolution when compared to other methods [93]. Furthermore, the coupling of HPLC to electrospray ionization (ESI)-MS provides an even better platform for the analysis of many different lipid classes, or individual lipids, and is the most common separation technique and ionization source in lipidomics today. Both normal phase (NP) and reversed phase (RP) HPLC are applicable to the study of lipids depending on the structural features of the targeted molecule(s). NP-LC is used typically for the separation of classes of lipids containing different polar head groups, while RP-LC is often employed for the separation of species within the same lipid class, in which the difference in fatty-acyl chains are the main basis for separation [93]. Although ESI maintains a good reputation for the analysis of lipids, other ionization sources can be used with the HPLC-MS system. For instance, atmospheric pressure ionization (APCI) is also used frequently in lipidomics has been shown to be appropriate for the analysis of weak polar lipids, such as fatty acids, mono and diacyl-glycerols (MAG, DAG) [94], neutral sphingolipids, and cholesterol [95]. As for mass spec analyzers for the detection of lipids, Time of flight (ToF) tubes coupled with LC-MS are the most common in lipidomics and the Merkler lab previously characterized a novel panel of fatty acid amides

from *Drosophila melanogaster* using LC-QToF-MS [16]. Therefore, this is an adequate method for the continuation in detecting fatty acid amides in the same model system and other insects as well.

1.4 References

[1] Walker, J. M.; Huang, S. M.; Strangman, N. M.; Tsou, K.; Sanudo-Pena, M. C., Pain modulation by release of the endogenous cannabinoid anandamide. *Proc Natl Acad Sci U S A* **1999,** *96* (21), 12198-203.

[2] Ibeas Bih, C.; Chen, T.; Nunn, A. V.; Bazelot, M.; Dallas, M.; Whalley, B. J., Molecular Targets of Cannabidiol in Neurological Disorders. *Neurotherapeutics : the journal of the American Society for Experimental NeuroTherapeutics* **2015,** *12* (4), 699-730.

[3] Gaoni, Y.; Mechoulam, R., Isolation, Structure, and Partial Synthesis of an Active Constituent of Hashish. *Journal of the American Chemical Society* **1964,** *86* (8), 1646-1647.

[4] Devane, W. A.; Dysarz, F. A., 3rd; Johnson, M. R.; Melvin, L. S.; Howlett, A. C., Determination and characterization of a cannabinoid receptor in rat brain. *Molecular pharmacology* **1988,** *34* (5), 605-13.

[5] Farrell, E. K.; Merkler, D. J., Biosynthesis, degradation and pharmacological importance of the fatty acid amides. *Drug discovery today* **2008,** *13* (13-14), 558-68.

[6] van der Sluis, R.; Ungerer, V.; Nortje, C.; A, A. v. D.; Erasmus, E., New insights into the catalytic mechanism of human glycine N-acyltransferase. *Journal of biochemical and molecular toxicology* **2017,** *31* (11).

[7] Mechoulam, R.; Fride, E.; Di Marzo, V., Endocannabinoids. *European Journal of Pharmacology* **1998,** *359* (1), 1-18.

[8] Vetting, M. W.; S. de Carvalho, L. P.; Yu, M.; Hegde, S. S.; Magnet, S.; Roderick, S. L.; Blanchard, J. S., Structure and functions of the GNAT superfamily of acetyltransferases. *Archives of Biochemistry and Biophysics* **2005,** *433* (1), 212-226.

[9] Salah Ud-Din, I. A.; Tikhomirova, A.; Roujeinikova, A., Structure and Functional Diversity of GCN5-Related N-Acetyltransferases (GNAT). *International Journal of Molecular Sciences* **2016,** *17* (7).

[10] Zheng, W.; Cole, P. A., Serotonin N-acetyltransferase: mechanism and inhibition. *Current medicinal chemistry* **2002,** *9* (12), 1187-99.

[11] De Angelis, J.; Gastel, J.; Klein, D. C.; Cole, P. A., Kinetic analysis of the catalytic mechanism of serotonin N-acetyltransferase (EC 2.3.1.87). *The Journal of biological chemistry* **1998,** *273* (5), 3045-50.

[12] Jeffries, K. A.; Dempsey, D. R.; Farrell, E. K.; Anderson, R. L.; Garbade, G. J.; Gurina, T. S.; Gruhonjic, I.; Gunderson, C. A.; Merkler, D. J., Glycine N-acyltransferase-like 3 is responsible for long-chain N-acylglycine formation in N18TG2 cells. *Journal of lipid research* **2016,** *57* (5), 781-90.

[13] Arafat, E. S.; Trimble, J. W.; Andersen, R. N.; Dass, C.; Desiderio, D. M., Identification of fatty acid amides in human plasma. *Life Sciences* **1989,** *45* (18), 1679-1687.

[14] Aneetha, H.; O'Dell, D. K.; Tan, B.; Walker, J. M.; Hurley, T. D., Alcohol dehydrogenase-catalyzed in vitro oxidation of anandamide to N-arachidonoyl glycine, a lipid mediator: synthesis of N-acyl glycinals. *Bioorganic & medicinal chemistry letters* **2009,** *19* (1), 237-41.

[15] Ivkovic, M.; Dempsey, D. R.; Handa, S.; Hilton, J. H.; Lowe, E. W., Jr.; Merkler, D. J., N-acylethanolamines as novel alcohol dehydrogenase 3 substrates. *Arch Biochem Biophys* **2011,** *506* (2), 157-64.

[16] Jeffries, K. A.; Dempsey, D. R.; Behari, A. L.; Anderson, R. L.; Merkler, D. J., Drosophila melanogaster as a model system to study long-chain fatty acid amide metabolism. *FEBS letters* **2014,** *588* (9), 1596-602.

[17] Koga, D.; Santa, T.; Fukushima, T.; Homma, H.; Imai, K., Liquid chromatographic-atmospheric pressure chemical ionization mass spectrometric determination of anandamide and its analogs in rat brain and peripheral tissues. *Journal of Chromatography B: Biomedical Sciences and Applications* **1997,** *690* (1), 7-13.

[18] Palmer, S. L.; Thakur, G. A.; Makriyannis, A., Cannabinergic ligands. *Chemistry and physics of lipids* **2002,** *121* (1-2), 3-19.

[19] O'Sullivan, S. E., Cannabinoids go nuclear: evidence for activation of peroxisome proliferator-activated receptors. *British journal of pharmacology* **2007,** *152* (5), 576-82.

[20] Starowicz, K.; Nigam, S.; Di Marzo, V., Biochemistry and pharmacology of endovanilloids. *Pharmacology & therapeutics* **2007,** *114* (1), 13-33.

[21] De Petrocellis, L.; Starowicz, K.; Moriello, A. S.; Vivese, M.; Orlando, P.; Di Marzo, V., Regulation of transient receptor potential channels of melastatin type 8 (TRPM8): effect of cAMP, cannabinoid CB(1) receptors and endovanilloids. *Experimental cell research* **2007,** *313* (9), 1911-20.

[22] Williams, C. M.; Kirkham, T. C., Anandamide induces overeating: mediation by central cannabinoid (CB1) receptors. *Psychopharmacology* **1999,** *143* (3), 315-7.

[23] Marsicano, G.; Wotjak, C. T.; Azad, S. C.; Bisogno, T.; Rammes, G.; Cascio, M. G.; Hermann, H.; Tang, J.; Hofmann, C.; Zieglgansberger, W.; Di Marzo, V.; Lutz, B., The endogenous cannabinoid system controls extinction of aversive memories. *Nature* **2002,** *418* (6897), 530-4.

[24] Fu, J.; Gaetani, S.; Oveisi, F.; Lo Verme, J.; Serrano, A.; Rodriguez De Fonseca, F.; Rosengarth, A.; Luecke, H.; Di Giacomo, B.; Tarzia, G.; Piomelli, D., Oleylethanolamide regulates feeding and body weight through activation of the nuclear receptor PPAR-alpha. *Nature* **2003,** *425* (6953), 90-3.

[25] Lambert, D. M.; Di Marzo, V., The palmitoylethanolamide and oleamide enigmas : are these two fatty acid amides cannabimimetic? *Current medicinal chemistry* **1999,** *6* (8), 757-73.

[26] Movahed, P.; Jonsson, B. A.; Birnir, B.; Wingstrand, J. A.; Jorgensen, T. D.; Ermund, A.; Sterner, O.; Zygmunt, P. M.; Hogestatt, E. D., Endogenous unsaturated C18 N-acylethanolamines are vanilloid receptor (TRPV1) agonists. *The Journal of biological chemistry* **2005,** *280* (46), 38496-504.

[27] Overton, H. A.; Babbs, A. J.; Doel, S. M.; Fyfe, M. C.; Gardner, L. S.; Griffin, G.; Jackson, H. C.; Procter, M. J.; Rasamison, C. M.; Tang-Christensen, M.; Widdowson, P. S.; Williams, G. M.; Reynet, C., Deorphanization of a G protein-coupled receptor for oleoylethanolamide and its use in the discovery of small-molecule hypophagic agents. *Cell metabolism* **2006,** *3* (3), 167-75.

[28] Maccarrone, M.; Cartoni, A.; Parolaro, D.; Margonelli, A.; Massi, P.; Bari, M.; Battista, N.; Finazzi-Agro, A., Cannabimimetic activity, binding, and degradation of stearoylethanolamide within the mouse central nervous system. *Molecular and cellular neurosciences* **2002,** *21* (1), 126-40.

[29] Lo Verme, J.; Fu, J.; Astarita, G.; La Rana, G.; Russo, R.; Calignano, A.; Piomelli, D., The nuclear receptor peroxisome proliferator-activated receptor-alpha mediates the anti-inflammatory actions of palmitoylethanolamide. *Molecular pharmacology* **2005,** *67* (1), 15-9.

[30] Ryberg, E.; Larsson, N.; Sjogren, S.; Hjorth, S.; Hermansson, N. O.; Leonova, J.; Elebring, T.; Nilsson, K.; Drmota, T.; Greasley, P. J., The orphan receptor GPR55 is a novel cannabinoid receptor. *British journal of pharmacology* **2007,** *152* (7), 1092-101.

[31] Schmid, H. H.; Berdyshev, E. V., Cannabinoid receptor-inactive N-acylethanolamines and other fatty acid amides: metabolism and function. *Prostaglandins, leukotrienes, and essential fatty acids* **2002,** *66* (2-3), 363-76.

[32] Sugiura, T.; Kondo, S.; Sukagawa, A.; Tonegawa, T.; Nakane, S.; Yamashita, A.; Ishima, Y.; Waku, K., Transacylase-mediated and phosphodiesterase-mediated synthesis of N-

arachidonoylethanolamine, an endogenous cannabinoid-receptor ligand, in rat brain microsomes. Comparison with synthesis from free arachidonic acid and ethanolamine. *European journal of biochemistry* **1996,** *240* (1), 53-62.

[33] Simon, G. M.; Cravatt, B. F., Endocannabinoid biosynthesis proceeding through glycerophospho-N-acyl ethanolamine and a role for alpha/beta-hydrolase 4 in this pathway. *The Journal of biological chemistry* **2006,** *281* (36), 26465-72.

[34] Liu, J.; Wang, L.; Harvey-White, J.; Huang, B. X.; Kim, H. Y.; Luquet, S.; Palmiter, R. D.; Krystal, G.; Rai, R.; Mahadevan, A.; Razdan, R. K.; Kunos, G., Multiple pathways involved in the biosynthesis of anandamide. *Neuropharmacology* **2008,** *54* (1), 1-7.

[35] Wei, B. Q.; Mikkelsen, T. S.; McKinney, M. K.; Lander, E. S.; Cravatt, B. F., A second fatty acid amide hydrolase with variable distribution among placental mammals. *The Journal of biological chemistry* **2006,** *281* (48), 36569-78.

[36] Tsuboi, K.; Takezaki, N.; Ueda, N., The N-acylethanolamine-hydrolyzing acid amidase (NAAA). *Chemistry & biodiversity* **2007,** *4* (8), 1914-25.

[37] Maccarrone, M., Fatty acid amide hydrolase: a potential target for next generation therapeutics. *Current pharmaceutical design* **2006,** *12* (6), 759-72.

[38] Cravatt, B. F.; Prospero-Garcia, O.; Siuzdak, G.; Gilula, N. B.; Henriksen, S. J.; Boger, D. L.; Lerner, R. A., Chemical characterization of a family of brain lipids that induce sleep. *Science (New York, N.Y.)* **1995,** *268* (5216), 1506-9.

[39] Mendelson, W. B.; Basile, A. S., The hypnotic actions of the fatty acid amide, oleamide. *Neuropsychopharmacology* **2001,** *25* (5 Suppl), S36-9.

[40] Hiley, C. R.; Hoi, P. M., Oleamide: a fatty acid amide signaling molecule in the cardiovascular system? *Cardiovascular drug reviews* **2007,** *25* (1), 46-60.

[41] Lo, Y. K.; Tang, K. Y.; Chang, W. N.; Lu, C. H.; Cheng, J. S.; Lee, K. C.; Chou, K. J.; Liu, C. P.; Chen, W. C.; Su, W.; Law, Y. P.; Jan, C. R., Effect of oleamide on Ca(2+) signaling in human bladder cancer cells. *Biochemical pharmacology* **2001,** *62* (10), 1363-9.

[42] Liu, Y. C.; Wu, S. N., Block of erg current by linoleoylamide, a sleep-inducing agent, in pituitary GH3 cells. *Eur J Pharmacol* **2003,** *458* (1-2), 37-47.

[43] Grazia Cascio, M.; Minassi, A.; Ligresti, A.; Appendino, G.; Burstein, S.; Di Marzo, V., A structure-activity relationship study on N-arachidonoyl-amino acids as possible endogenous inhibitors of fatty acid amide hydrolase. *Biochemical and biophysical research communications* **2004,** *314* (1), 192-6.

[44] Chaturvedi, S.; Driscoll, W. J.; Elliot, B. M.; Faraday, M. M.; Grunberg, N. E.; Mueller, G. P., In vivo evidence that N-oleoylglycine acts independently of its conversion to oleamide. *Prostaglandins & other lipid mediators* **2006,** *81* (3-4), 136-49.

[45] Akimov, M. G.; Gretskaia, N. M.; Shevchenko, K. V.; Shevchenko, V. P.; Miasoedov, N. F.; Bobrov, M.; Bezuglov, V. V., [New aspects of biosynthesis and metabolism of N-acyldopamines in rat tissues]. *Bioorganicheskaia khimiia* **2007,** *33* (6), 648-52.

[46] Nguyen, M. D.; Nguyen, D. H.; Yoo, J. M.; Myung, P. K.; Kim, M. R.; Sok, D. E., Effect of endocannabinoids on soybean lipoxygenase-1 activity. *Bioorganic chemistry* **2013,** *49*, 24-32.

[47] Verhoeckx, K. C.; Voortman, T.; Balvers, M. G.; Hendriks, H. F.; H, M. W.; Witkamp, R. F., Presence, formation and putative biological activities of N-acyl serotonins, a novel class of fatty-acid derived mediators, in the intestinal tract. *Biochimica et biophysica acta* **2011,** *1811* (10), 578-86.

[48] Walker, J. M.; Krey, J. F.; Chen, J. S.; Vefring, E.; Jahnsen, J. A.; Bradshaw, H.; Huang, S. M., Targeted lipidomics: fatty acid amides and pain modulation. *Prostaglandins & other lipid mediators* **2005,** *77* (1-4), 35-45.

[49] Ferreira, S. G.; Lomaglio, T.; Avelino, A.; Cruz, F.; Oliveira, C. R.; Cunha, R. A.; Kofalvi, A., N-acyldopamines control striatal input terminals via novel ligand-gated cation channels. *Neuropharmacology* **2009,** *56* (3), 676-83.

[50] Jeffries, K. A.; Dempsey, D. R.; Farrell, E. K.; Anderson, R. L.; Garbade, G. J.; Gurina, T. S.; Gruhonjic, I.; Gunderson, C. A.; Merkler, D. J., Glycine N-acyltransferase-like 3 is responsible for long-chain N-acylglycine formation in N(18)TG(2) cells. *Journal of Lipid Research* **2016,** *57* (5), 781-790.

[51] Chu, C. J.; Huang, S. M.; De Petrocellis, L.; Bisogno, T.; Ewing, S. A.; Miller, J. D.; Zipkin, R. E.; Daddario, N.; Appendino, G.; Di Marzo, V.; Walker, J. M., N-oleoyldopamine, a novel endogenous capsaicin-like lipid that produces hyperalgesia. *The Journal of biological chemistry* **2003,** *278* (16), 13633-9.

[52] Dempsey, D. R.; Jeffries, K. A.; Anderson, R. L.; Carpenter, A. M.; Rodriquez Opsina, S.; Merkler, D. J., Identification of an arylalkylamine N-acyltransferase from Drosophila melanogaster that catalyzes the formation of long-chain N-acylserotonins. *FEBS letters* **2014,** *588* (4), 594-9.

[53] Siller, M.; Goyal, S.; Yoshimoto, F. K.; Xiao, Y.; Wei, S.; Guengerich, F. P., Oxidation of endogenous N-arachidonoylserotonin by human cytochrome P450 2U1. *The Journal of biological chemistry* **2014,** *289* (15), 10476-87.

[54] Huang, S. M.; Bisogno, T.; Trevisani, M.; Al-Hayani, A.; De Petrocellis, L.; Fezza, F.; Tognetto, M.; Petros, T. J.; Krey, J. F.; Chu, C. J.; Miller, J. D.; Davies, S. N.; Geppetti, P.; Walker, J. M.; Di Marzo, V., An endogenous capsaicin-like substance with high potency at recombinant and native vanilloid VR1 receptors. *Proc Natl Acad Sci U S A* **2002,** *99* (12), 8400-5.

[55] Huang, R.-C., The discoveries of molecular mechanisms for the circadian rhythm: The 2017 Nobel Prize in Physiology or Medicine. *Biomedical Journal* **2018,** *41* (1), 5-8.

[56] Bishay, P.; Haussler, A.; Lim, H. Y.; Oertel, B.; Galve-Roperh, I.; Ferreiros, N.; Tegeder, I., Anandamide deficiency and heightened neuropathic pain in aged mice. *Neuropharmacology* **2013,** *71*, 204-15.

[57] Wang, P. Y.; Neretti, N.; Whitaker, R.; Hosier, S.; Chang, C.; Lu, D.; Rogina, B.; Helfand, S. L., Long-lived Indy and calorie restriction interact to extend life span. *Proc Natl Acad Sci U S A* **2009,** *106* (23), 9262-7.

[58] Lee, S. H.; Lee, S. K.; Paik, D.; Min, K. J., Overexpression of fatty-acid-beta-oxidation-related genes extends the lifespan of Drosophila melanogaster. *Oxidative medicine and cellular longevity* **2012,** *2012*, 854502.

[59] Shen, L. R.; Parnell, L. D.; Ordovas, J. M.; Lai, C. Q., Curcumin and aging. *BioFactors (Oxford, England)* **2013,** *39* (1), 133-40.

[60] Scuderi, C.; Steardo, L., Neuroglial roots of neurodegenerative diseases: therapeutic potential of palmitoylethanolamide in models of Alzheimer's disease. *CNS & neurological disorders drug targets* **2013,** *12* (1), 62-9.

[61] D'Agostino, G.; Russo, R.; Avagliano, C.; Cristiano, C.; Meli, R.; Calignano, A., Palmitoylethanolamide Protects Against the Amyloid-β25-35-Induced Learning and Memory Impairment in Mice, an Experimental Model of Alzheimer Disease. *Neuropsychopharmacology* **2012,** *37* (7), 1784-1792.

[62] Fernandez-Ruiz, J., The endocannabinoid system as a target for the treatment of motor dysfunction. *British journal of pharmacology* **2009,** *156* (7), 1029-40.

[63] Bari, M.; Battista, N.; Valenza, M.; Mastrangelo, N.; Malaponti, M.; Catanzaro, G.; Centonze, D.; Finazzi-Agro, A.; Cattaneo, E.; Maccarrone, M., In vitro and in vivo models of Huntington's disease show alterations in the endocannabinoid system. *The FEBS journal* **2013,** *280* (14), 3376-88.

[64] Alvheim, A. R.; Torstensen, B. E.; Lin, Y. H.; Lillefosse, H. H.; Lock, E. J.; Madsen, L.; Froyland, L.; Hibbeln, J. R.; Malde, M. K., Dietary linoleic acid elevates the endocannabinoids 2-AG and anandamide and promotes weight gain in mice fed a low fat diet. *Lipids* **2014,** *49* (1), 59-69.

[65] Liu, J.; Li, T.; Yang, D.; Ma, R.; Moran, T. H.; Smith, W. W., Synphilin-1 alters metabolic homeostasis in a novel Drosophila obesity model. *International journal of obesity (2005)* **2012,** *36* (12), 1529-36.

[66] Cravatt, B. F.; Demarest, K.; Patricelli, M. P.; Bracey, M. H.; Giang, D. K.; Martin, B. R.; Lichtman, A. H., Supersensitivity to anandamide and enhanced endogenous cannabinoid signaling in mice lacking fatty acid amide hydrolase. *Proc Natl Acad Sci U S A* **2001,** *98* (16), 9371-6.

[67] Martin, B. R.; Lichtman, A. H., Cannabinoid transmission and pain perception. *Neurobiology of disease* **1998,** *5* (6 Pt B), 447-61.

[68] Greco, R.; Mangione, A. S.; Sandrini, G.; Maccarrone, M.; Nappi, G.; Tassorelli, C., Effects of anandamide in migraine: data from an animal model. *The journal of headache and pain* **2011,** *12* (2), 177-83.

[69] Suardiaz, M.; Estivill-Torrus, G.; Goicoechea, C.; Bilbao, A.; Rodriguez de Fonseca, F., Analgesic properties of oleoylethanolamide (OEA) in visceral and inflammatory pain. *Pain* **2007,** *133* (1-3), 99-110.

[70] Jaggar, S. I.; Hasnie, F. S.; Sellaturay, S.; Rice, A. S., The anti-hyperalgesic actions of the cannabinoid anandamide and the putative CB2 receptor agonist palmitoylethanolamide in visceral and somatic inflammatory pain. *Pain* **1998,** *76* (1-2), 189-99.

[71] Succar, R.; Mitchell, V. A.; Vaughan, C. W., Actions of N-arachidonyl-glycine in a rat inflammatory pain model. *Molecular pain* **2007,** *3*, 24.

[72] Barbara, G.; Alloui, A.; Nargeot, J.; Lory, P.; Eschalier, A.; Bourinet, E.; Chemin, J., T-type calcium channel inhibition underlies the analgesic effects of the endogenous lipoamino acids. *The Journal of neuroscience : the official journal of the Society for Neuroscience* **2009,** *29* (42), 13106-14.

[73] Milinkeviciute, G.; Gentile, C.; Neely, G. G., Drosophila as a tool for studying the conserved genetics of pain. *Clinical genetics* **2012,** *82* (4), 359-66.

[74] El Khoury, M.-A.; Gorgievski, V.; Moutsimilli, L.; Giros, B.; Tzavara, E. T., Interactions between the cannabinoid and dopaminergic systems: Evidence from animal studies. *Progress in Neuro-Psychopharmacology and Biological Psychiatry* **2012,** *38* (1), 36-50.

[75] Giuffrida, A.; Seillier, A., New insights on endocannabinoid transmission in psychomotor disorders. *Progress in neuro-psychopharmacology & biological psychiatry* **2012,** *38* (1), 51-8.

[76] Centonze, D.; Finazzi-Agro, A.; Bernardi, G.; Maccarrone, M., The endocannabinoid system in targeting inflammatory neurodegenerative diseases. *Trends in pharmacological sciences* **2007,** *28* (4), 180-7.

[77] Haywood, A. F.; Staveley, B. E., Parkin counteracts symptoms in a Drosophila model of Parkinson's disease. *BMC neuroscience* **2004,** *5*, 14.

[78] M'Angale, P. G.; Staveley, B. E., Loss of porin function in dopaminergic neurons of Drosophila is suppressed by Buffy. *Journal of biomedical science* **2016,** *23* (1), 84.

[79] Wentzel, C.; Delvendahl, I.; Sydlik, S.; Georgiev, O.; Müller, M., Dysbindin links presynaptic proteasome function to homeostatic recruitment of low release probability vesicles. *Nature Communications* **2018,** *9*, 267.

[80] Dempsey, D. R.; Jeffries, K. A.; Handa, S.; Carpenter, A. M.; Rodriguez-Ospina, S.; Breydo, L.; Merkler, D. J., Mechanistic and Structural Analysis of a Drosophila melanogaster Enzyme, Arylalkylamine N-Acetyltransferase Like 7, an Enzyme That Catalyzes the Formation of N-Acetylarylalkylamides and N-Acetylhistamine. *Biochemistry* **2015,** *54* (16), 2644-58.

[81] Dempsey, D. R.; Jeffries, K. A.; Anderson, R. L.; Carpenter, A.-M.; Ospina, S. R.; Merkler, D. J., Identification of an arylalkylamine N-acyltransferase from Drosophila melanogaster that catalyzes the formation of long-chain N-acylserotonins. *FEBS letters* **2014,** *588* (4), 594-599.

[82] Goldsmith, M. R.; Shimada, T.; Abe, H., The genetics and genomics of the silkworm, Bombyx mori. *Annual review of entomology* **2005,** *50*, 71-100.

[83] Xia, Q.; Guo, Y.; Zhang, Z.; Li, D.; Xuan, Z.; Li, Z.; Dai, F.; Li, Y.; Cheng, D.; Li, R.; Cheng, T.; Jiang, T.; Becquet, C.; Xu, X.; Liu, C.; Zha, X.; Fan, W.; Lin, Y.; Shen, Y.; Jiang, L.; Jensen, J.; Hellmann, I.; Tang, S.; Zhao, P.; Xu, H.; Yu, C.; Zhang, G.; Li, J.; Cao, J.; Liu, S.; He, N.; Zhou, Y.; Liu, H.; Zhao, J.; Ye, C.; Du, Z.; Pan, G.; Zhao, A.; Shao, H.; Zeng, W.; Wu, P.; Li, C.; Pan, M.; Li, J.; Yin, X.; Li, D.; Wang, J.; Zheng, H.; Wang, W.; Zhang, X.; Li, S.; Yang, H.; Lu, C.; Nielsen, R.; Zhou, Z.; Wang, J.; Xiang, Z.; Wang, J., Complete resequencing of 40 genomes reveals domestication events and genes in silkworm (Bombyx). *Science (New York, N.Y.)* **2009,** *326* (5951), 433-6.

[84] Hara, C.; Morishita, K.; Takayanagi-Kiya, S.; Mikami, A.; Uchino, K.; Sakurai, T.; Kanzaki, R.; Sezutsu, H.; Iwami, M.; Kiya, T., Refinement of ectopic protein expression through the GAL4/UAS system in Bombyx mori: application to behavioral and developmental studies. *Scientific Reports* **2017,** *7*, 11795.

[85] Kiya, T.; Morishita, K.; Uchino, K.; Iwami, M.; Sezutsu, H., Establishment of tools for neurogenetic analysis of sexual behavior in the silkmoth, Bombyx mori. *PLoS One* **2014,** *9* (11), e113156.

[86] Wei, W.; Xin, H.; Roy, B.; Dai, J.; Miao, Y.; Gao, G., Heritable Genome Editing with CRISPR/Cas9 in the Silkworm, Bombyx mori. *PLoS ONE* **2014,** *9* (7), e101210.

[87] Takasu, Y.; Kobayashi, I.; Beumer, K.; Uchino, K.; Sezutsu, H.; Sajwan, S.; Carroll, D.; Tamura, T.; Zurovec, M., Targeted mutagenesis in the silkworm Bombyx mori using zinc finger nuclease mRNA injection. *Insect biochemistry and molecular biology* **2010,** *40* (10), 759-65.

[88] O'Flynn, B. G.; Hawley, A. J.; Merkler, D. J., Insect Arylalkylamine N-Acetyltransferases as Potential Targets for Novel Insecticide Design. *Biochemistry & molecular biology journal* **2018,** *4* (1), 4.

[89] Hiragaki, S.; Suzuki, T.; Mohamed, A. A.; Takeda, M., Structures and functions of insect arylalkylamine N-acetyltransferase (iaaNAT); a key enzyme for physiological and behavioral switch in arthropods. *Frontiers in physiology* **2015,** *6*, 113.

[90] O'Flynn, B. G.; Suarez, G.; Hawley, A. J.; Merkler, D. J., Insect Arylalkylamine N-Acyltransferases: Mechanism and Role in Fatty Acid Amide Biosynthesis. *Frontiers in Molecular Biosciences* **2018,** *5*, 66.

[91] Tsugehara, T.; Iwai, S.; Fujiwara, Y.; Mita, K.; Takeda, M., Cloning and characterization of insect arylalkylamine N-acetyltransferase from Bombyx mori. *Comparative Biochemistry and Physiology Part B: Biochemistry and Molecular Biology* **2007,** *147* (3), 358-366.

[92] Wang, H. Y.; Quan, C.; Hu, C.; Xie, B.; Du, Y.; Chen, L.; Yang, W.; Yang, L.; Chen, Q.; Shen, B.; Hu, B.; Zheng, Z.; Zhu, H.; Huang, X.; Xu, G.; Chen, S., A lipidomics study reveals hepatic lipid signatures associating with deficiency of the LDL receptor in a rat model. *Biology Open* **2016,** *5* (7), 979-986.

[93] Li, M.; Zhou, Z.; Nie, H.; Bai, Y.; Liu, H., Recent advances of chromatography and mass spectrometry in lipidomics. *Analytical and bioanalytical chemistry* **2011,** *399* (1), 243-9.

[94] Suman, M.; Silva, G.; Catellani, D.; Bersellini, U.; Caffarra, V.; Careri, M., Determination of food emulsifiers in commercial additives and food products by liquid chromatography/atmospheric-pressure chemical ionisation mass spectrometry. *Journal of Chromatography A* **2009,** *1216* (18), 3758-3766.

[95] Farwanah, H.; Wirtz, J.; Kolter, T.; Raith, K.; Neubert, R. H.; Sandhoff, K., Normal phase liquid chromatography coupled to quadrupole time of flight atmospheric pressure chemical ionization mass spectrometry for separation, detection and mass spectrometric profiling of neutral sphingolipids and cholesterol. *Journal of chromatography. B, Analytical technologies in the biomedical and life sciences* **2009,** *877* (27), 2976-82.

CHAPTER TWO

Knockdown of arylalkylamine *N*-acyltransferase-like 2 (AANATL2) in *Drosophila melanogaster*

2.1 Note to reader

This chapter will be submitted to *Biochemistry* for peer review. The authors are Ryan L. Anderson, Dylan J. Wallis, Alexander Aguirre, Dean Holliday, and David. J. Merkler. Ryan L. Anderson completed the RT-qPCR, western blot and lipidomics. Dylan J. Wallis, Alexander Aguirre and Dean Holliday helped in the generation and collection of UAS/Gal4 AANATL2 knockdown flies. David J. merkler is responsible for the research design and is the corresponding author.

2.2 Significance statement

Previous work done in the Merkler lab has shown recombinant arylalkyamine *N*-acyltransferase-like 2 (AANATL2) from *Drosophila melanogaster* catalyzes the formation of long chain *N*-acyldopamines and long chain *N*-acylserotonins *in vitro*. However, this was not enough evidence to support the claim these metabolites were being formed *in vivo*. Showing a reduction in any *N*-acylarylalkylamides accompanying an *in vivo* siRNA knockdown of AANATL2 in *D. melanogaster* substantiates AANATL2 as major biosynthetic enzyme of at least some of these tertiary metabolites.

2.3 Abstract

Our lab is currently using *Drosophila melanogaster* as a model system to unravel the biosynthetic pathway of certain fatty acid amides. The work herein focuses on the biosynthesis of *N*-acylarylalkylamides in fruit flies. We previously characterized an arylalkylamine *N*-acyltransferase, named AANATL2, in *Drosophila* shown to catalyze the *in vitro* formation of these long chain *N*-acylserotonins and *N*-acyldopamines. Generating siRNA via the UAS/GAL4 bipartite approach for

targeted gene expression was shown, using RT-qPCR, to be an effective method for knocking down the endogenous levels of AANATL2 transcripts in *D. melanogaster*. Furthermore, the AANATL2 knockdown, fly offspring protein expression was also shown to be significantly reduced in a Western blot using a primary, anti-AANATL2 antibody. Finally, reduced expression of AANATL2 resulted in reduction in the cellular levels of *N*-palmitoyldopamine. This result provides strong evidence AANATL2 is responsible for the biosynthesis of *N*-palmitoyldopamine *in vivo*. This is the first time an AANAT has been knocked down in *Drosophila melanogaster* to confidently show it is a major biosynthetic enzyme for *N*-acylarylalkylamides. This supports *in vitro* data showing the enzyme has the capacity to catalyze the formation of these long chain fatty acid amides.

2.4 Abbreviations

Aryalkylamine *N*-acyltransferase-like 2, AANATL2; Upstream activator sequence ,UAS; Cannabinoid receptor, CB; *N*-palmitoyldopamine, PALDA; RNA-induced silencing complex, RISC; Single-stranded RNA, ssRNA; Silencing RNA, siRNA; Liquid chromatography time-of-flight mass spectrometry, LC-QToF-MS;

2.5 Introduction

Endocannabinoids are a widely studied family of lipids stemming from the discovery of the cannabinoid receptors (CB_1 and CB_2) and anandamide (*N*-arachidonoylethanolamide), the endogenous ligand for CB_1. Furthermore, endocannabinoids are also in the family of fatty acid amides, which can be subdivided into the *N*-acylethanolamides, *N*-acylamino acids, *N*-acylarylalkylamides and the primary fatty acid amides. These molecules are biologically significant as they are thought to serve a myriad of different functions throughout the animal kingdom, ranging from inducing sleep in mammals to the hardening of cuticles (sclerotization via *N*-acetyldopamine) in arthropods [1-2]. However, due to their diverse importance, there is much to be learned to further understand how these molecules are biosynthesized and able to serve such different purposes in different types of organisms. Our lab is

currently using *Drosophila melanogaster* as a model system to unravel the synthetic pathway of certain fatty acid amides. The work herein has a particular focus on the *N*-acylarylalkylamides in fruit flies, as we previously characterized an arylalkylamine *N*-acyltransferase, named AANATL2, in *Drosophila* shown to catalyze the *in vitro* formation of long chain *N*-acylserotonins and *N*-acyldopamines [3]. The catalytic chemistry of AANATL2 is similar to that of serotonin *N*-acetyl transferase, which is the penultimate enzyme in the biosynthesis of melatonin [3-4]. However, *N*-acetylserotonin from melatonergic systems only contains a 2-carbon acyl group and much more is currently unknown about the *N*-acylarylalkylamides containing longer acyl chains (> 14 carbons). The study of these long chain lipids' biosynthesis in a model system like *D. melanogaster* is valuable because only some of their functions have been fully elucidated in mammals but are seemingly significant. For instance, *N*-oleoyldopamine is a modulator of midbrain activity in dopaminergic neurons [5]. This involves the use of an activated acyl-CoA and either serotonin or dopamine to make an *N*-acylserotonin or *N*-acyldopamine, respectively [6]. The AANATs in *Drosophila* are still widely understudied and underappreciated for their ability to provide insight into the formation of these *N*-acylarylalkylamides and what purpose they might serve in the fruit fly and vertebrates. Our studies up to this point have led to the belief endogenous AANATL2 is responsible for the biosynthesis of the long chain *N*-acyldopamines and or *N*-acylserotonins *in vivo*. A panel of endogenous, long chain *N*-acylarylalkylamides has been characterized and quantified in wild type *D.* melanogaster, which included *N*-acyldopamines and *N*-acylserotonins [7]. Yet, the question still remained: If AANATL2 is removed or its expression reduced, are the levels of endogenous fatty acid amides affected? A strategy for achieving an *in vivo* knockdown of AANATL2 is through the use of silencing RNA to reduce the expression of the protein in living fruit flies.

RNA silencing (siRNA) is a gene regulatory mechanism conserved in eukaryotes and is used endogenously to rid organisms of invading viral RNA or regulate mRNA abundance of certain endogenous genes [8-13]. The eukaryotic cells use small segments of RNA (21-26 nucleotides) able to target RNA for degradation using a series of proteins: First, RNA silencing is induced by the presence of double-stranded RNAs (dsRNAs) or structured single-stranded RNAs (ssRNAs), which are processed

into siRNA by RNase III-like enzymes, such as Dicer [14-15]. These siRNA are then used as a guide by the RNA induced silencing complex (RISC) to degrade RNA with complementary base pairs to the siRNAs [15]. In addition to the siRNA, other short regulatory RNA known as micro RNA (miRNA) are also incorporated into the RNA silencing machinery. These mRNA are the product of endogenous noncoding genes, which are also Dicer-derived from an inverted-repeat mRNA precursor containing short dsRNA stem-loops and aid in mRNA targeting [16-19]. Therefore, the siRNA system can be controlled and deliberately induced through the introduction of dsRNA or RNA hairpin that is recognized by the degradative proteins and has matching nucleotides to a gene of interest [20]. However, transfection of synthetic RNA and targeting of genes becomes a more challenging problem when faced with a living organism with a myriad of different cell types, such as an adult fruit fly.

One method capable of knocking down the expression of AANATL2 in living fruit flies via siRNA is through use of the UAS/Gal4 bipartite approach for targeted gene expression [20-21]. This system uses two different parent mutants to create an offspring with targeted gene expression of either native or transposed genes [22]. One parent is a mutant containing a chosen responder gene with an activator sequence transposed upstream of transcription and attracts the protein, Gal4. This protein discovered in yeast is a known activator of gene transcription through binding of the upstream activator sequence (UAS), which can be transposed into *D. melanogaster*'s genome with no overtly deleterious, phenotypic effects [23]. The next parent contains the transposed, functional gene for Gal4 in a predetermined pattern of expression for targeting and is known as the driver. When the two mutants are mated together, the gene of interest in some offspring is rendered under the transcriptional control of the UAS/Gal4 combination in the same expression pattern delineated by the Gal4 driver. Furthermore, offspring with targeted gene expression can be differentiated based off the negative selection of a visible, inheritable phenotype from a balancer chromosome in the Gal4 driver [21].

In order to use this system to successfully knockdown AANATL2, a mutant fly housing a transposed, synthetic gene for an inverted-repeat, hairpin mRNA precursor containing complementary nucleotides to the AANATL2 transcript, the UAS and short dsRNA stem-loops was obtained. Then a

Gal4 driver was chosen with a specific transcriptional pattern. Since the precise cellular location of *N*-acylarylalkylamide biosynthesis is unknown in fruit flies, ubiquitous expression of Gal4 would increase the probability of higher degree of knockdown. The confirmation of AANATL2 knockdown was aptly shown in the chosen offspring before proposing any biosynthetic responsibility for *N*-acylarylalkylamides. This was accomplished through quantitative reverse transcriptase polymerase chain reaction (RT-qPCR) and Western blot analysis. Indeed, the qPCR and Western blot showed a significant reduction in AANATL2 in both transcripts and translated protein due to siRNA via UAS/Gal4 knockdown. The lipids were then extracted from the knockdown and the UAS parent, purified via silica column chromatography, and prepared for liquid chromatography quadrupole time-of-flight mass spectrometry (LC-QToF-MS) analysis. The mass spectra were targeted-screened for matching m/z and retention time of fatty acid amide standards and found significant differences in some fatty acid amide levels, including a disappearance of *N*-palmitoyldopamine (PALDA) in the knockdown flies. These data suggest AANATL2 is responsible for the *in vivo* biosynthesis of PALDA in *Drosophila melanogaster*. We have yet to fully elucidate a phenotype associated with the expression of AANATL2 in *D. melanogaster*. However, the hardening of many insect cuticles occurs through the cross-linking of acetylated quinones of monoamines, in which longer chain acyl groups may be used directly or indirectly [24]. Furthermore, *N*-palmitoyldopamine was found to repress the sonic hedgehog (Shh) pathway in ShhLIGHT2 cells, which is a pathway commonly studied for growth regulation and cell differentiation, which has direct ties to cancer research [25]. One last idea is the possibility of AANATL2 products interacting with TRPV receptors and other TRPs due to its structural similarities to capsaicin [26]. Therefore, a better understanding of AAANT-like enzyme product biosynthesis in fruit flies is significant due the importance of the long chain *N*-acyldopamines in varying organisms.

2.6 Materials and Methods

2.6.a General care of fly stocks

Drosophila UAS stocks (CG9486) were purchased from Vienna Drosophila Resource Center (VDRC) and are homozygous for an AANTAL2 siRNA hairpin that has been transposed into the second chromosome. The Gal4 drivers were purchased from Bloomington Labs (5138), have ubiquitous expression of Gal4 and a balancer chromosome (inserted into the third chromosome) containing the stubble (Sb[1]) phenotype. Both strains were cultured on Instant Drosophila Medium from Carolina Biological in Fisherbrand Drosophila vials capped with BuzzPlugs™ from Fisher Scientific.

2.6.b UAS/Gal4 Crossing scheme to generate AANATL2 knockdown flies

The Gal4 drivers were chosen to be all female in the crossing scheme to reduce the collection of false positive offspring. The UAS flies would then provide the males for the cross. The Gal4 adult flies were first split into new culturing tubes, then procreated and laid eggs for 7 days. After this period, all adults were removed from the culturing tubes, leaving only the larvae to remain. The larvae could then enter pupation and were closely monitored. Once the newly hatched flies began to emerge, virgin female, Gal4 drivers were swiftly collected in the morning and in the afternoon using Fly Nap and a low-powered magnification microscope. Virgin females were collected based off the positive identification of proper size, banding pattern, and present meconium. 5 virgin females were placed into freshly prepared tubes, to which 5, anesthetized UAS males were added. The UAS males and Gal4 females were left for 5 days before they were separated into new vials. Once the offspring of the cross hatched, AANATL2 knockdown flies were chosen based off the negative identification of the stubble (Sb[1]) gene using the same collection method as the virgin females. The depiction of the Sb[1] can be seen in figure 2.1 below

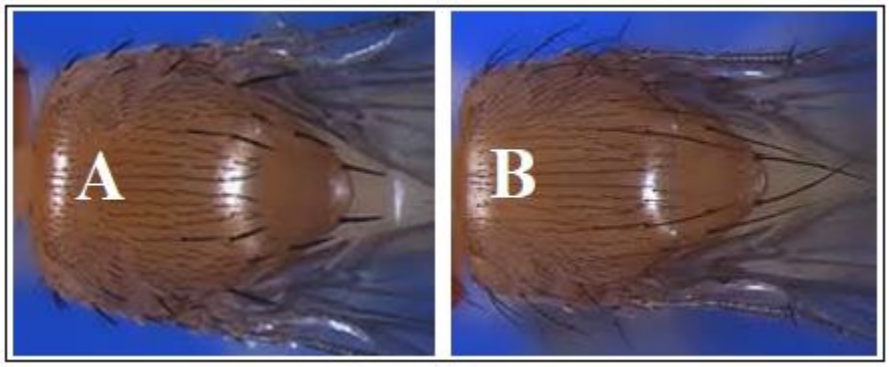

Figure 2.1 Depiction of Sb[1] phenotype in *Drosophila melanogaster*; A represents the dorsal thorax of *D. melanogaster* exhibiting the stubble (Sb[1]) phenotype from balancer chromosomes; B shows the dorsal thorax of a AANATL2 knockdown *D. melanogaster*.

Collected flies were flash frozen in liquid nitrogen and stored at -80°C until needed for downstream experiments. UAS flies were collected by putting the culturing tubes on ice, pouring the flies into a conical vial to separate the adults from larvae and media, then flash freezing and storing at -80°C.

2.6.c Detection of AANATL2 transcripts via RT-qPCR

AANATL2 qPCR primers were designed to amplify 75-150 base pair regions of the open reading frame of both the target AANATL2 and an endogenous control. Actin-42A was chosen as an endogenous control for qPCR. Primers were designed for the endogenous control in the same fashion as AANATL2 and their sequences and projected product sizes can be seen in Table 2.1.

Table 2.1 Primer Design for *Drosophila* AANATL2 and Actin-42A

Target	Forward Primer	Reverse Primer	Product Size
AANATL2	CATACGCGCCATGACAATC	GACACCTCGCTCTGCTTG	120 bp
Actin-42A	CACAGGTATCGTGTTGGACTC	AGGTAGTCGGTTAAATCGCG	123 bp

Above shows the forward and reverse primers for both the AANATL2 target and the actin-42A endogenous control. Primer sequences were generated using Integrated DNA Technologies (IDT) and were checked to have low spontaneity in the formation of hairpins and a less likelihood to form primer dimers. All primers were designed to have an annealing temperature of approximately 60°C. Primers were designed to target the 5' end of the mRNA, as it was previously found primer designations closer to the 3' end had the possibility of not showing mRNA degradation. This was due to the possibility of left over Dicer-degraded fragments long enough to be amplified in PCR [27].

mRNA stocks were gathered in the same manner for both the UAS parent and knockdown offspring: Dempsey *et. al* previously discovered AANATL2 transcripts to be concentrated in the thorax-abdomen of D. melanogaster [3]. For this reason, flies were collected and then flash frozen in liquid nitrogen to separate the heads from the thorax-abdomen. A sieve was used to segregate the body

segments of the organism and then total RNA was extracted from 200 mg of thorax-abdomen using TRIzol and collected via Pure Link RNA Minikit by Invitrogen. The mRNA was isolated using the PolyA-Tract from Promega and concentrated using a 10kD spin filte. Genomic DNA was removed through the use of DNase I by Invitrogen (modifications were made to the manufacturer's protocol: 2 µL of Dnase I, $MgCl_2$ buffer, and EDTA were used per 1 µg of mRNA). All purified mRNA stocks were made into 10 ng/µL aliquots and then stored at -20°C. The qPCR reactions were set up on a 96-well plate using mRNA from either the UAS parent or AANATL2 knockdown offspring and the parameters for each well can be seen in Table 2.2.

Table 2.2 qPCR Reactions on 96-Well Plate

Sample	**mRNA**	**SYBR**	**Actin-F**	**Actin-R**	**AANATL2-F**	**AANATL2-R**	**RT**	**Water**
UAS	30 ng	10 µL	200 nM	200nM	200 nM	100 nM	40U	To 20 µL
KD	30 ng	10 µL	200 nM	200nM	200 nM	100 nM	40U	To 20 µL

Power Up SYBR Green from Fisher Scientific was used for all reactions. UAS stands for the parent strain of flies, while KD refers to the AANATL2 knockdown offspring. Actin-F and Actin-R respectively refer to the forward and reverse primers of the endogenous control. Likewise, AANATL2-F and AANATL2-R refer to the forward and reverse primers of the target gene. RT stands for reverse transcriptase, in which MMLV-RT from Promega was used. All reactions were brought to a total of 20 µL using nuclease-free water.

All qPCR experiments were setup for ΔΔCT analysis and carried out on an Applied Biosystems QuantStudio 3 by Thermo Fisher Scientific. The first step of heating was a hold at 50°C for 45 minutes for the creation of cDNA by reverse transcriptase (RT). The temperature was then held at 95°C for 10 minutes to inactivate the RT. Subsequent PCR thermal cycles are as follows: 95°C for 15 seconds and then a decrease of 1.6 °C/s to hold at 60°C for 1 minute. This method was repeated for 40 cycles. Melting curves were completed using the same cycling temperatures, times and rates as the PCR cycling.

2.6.d Detection of AANATL2 protein via SDS-PAGE/ western blot

Proteins were collected from the UAS parent and knockdown offspring, separately, in the following way: 5 mL of a lysis buffer was made by combining 2500 µL 2x lysis solution (40 mM Tris-

HCl pH 7.4, 4 mM $MgCl_2$, 2 mM EDTA, 2 mM EGTA, 300 mM NaCl, 2.0% Triton-X-100), 300 µL PIC, 25 µL PMSF (200 mM), 50 µL Na_3VO_4 (100 mM) and 2125 µL of DI water. All protease inhibitors were prepared fresh before lysis. Approximately 20 flash-frozen, fruit fly thorax-abdomen were collected using the same method as the RNA extraction. These were placed into the 5 mL of lysis buffer in a mortar and pestle and the solution was ground to lyse the cells. The homogenate was pipetted into a scintillation vial, sonicated for 3 minutes on ice (30 second pulses with 30 seconds of rest at 50% amplitude) and then centrifuged at 13,400 rpm for 5 minutes. The resulting supernatant containing the cellular proteins was collected and the pellet was discarded. The supernatant was placed into a microcentrifuge tube on ice and then transferred to a 10 kD spin filter and centrifuged at max speed to concentrate the proteins larger than 10 kD. A Bradford assay was then done to assess the concentration of proteins in the solution and the volume containing 22 µg of protein was collected in a 1.5 mL microcentrifuge tube. An equal volume of 2x Laemmli Buffer containing BME was added to the solution and then placed into a water bath at 100°C for 3 minutes. The tube was then briefly centrifuged to collect all of the sample at the bottom. 7 µL of the Biorad color marker from NEB, 5 µL of Magic Marker from NEB, 5ng of recombinant AANATL2 with a 6X Histidine tag and linker region, and the decided volume of denatured proteins was loaded into respective wells of a 15% acrylamide gel immersed in 1X TGS buffer. Electrophoresis was started at 90V until the protein bands in the gel reached the bottom of the stacking layer, at which time the voltage was increased to 120V for approximately 2 hrs. The proteins on the acrylamide gel were transferred to a nitrocellulose membrane using the sandwich method. The assembled sandwich was placed into the proper cassette and then placed into an electrophoresis transfer apparatus holding transfer buffer (25 mM Tris-base, 192 mM glycine, 10% methanol). Electrophoresis was completed in a cold room at 4°C while stirring at 100V for approximately 1 hr. The nitrocellulose membrane was removed from all apparatus, washed in TBST (20 mM Tris, 500 mM NaCl, 20 µL of tween), placed into a solution containing 2.0 g of nonfat dry milk in 40 mL TBST and was allowed to rock for 2 hrs. The membrane was washed in TBST and cut horizontally at the 40 kDa molecular weight marker. The top half of the membrane was placed into a solution containing 25 µg/mL rabbit anti-α-tubulin pAb (*Drosophila*) primary antibody (from Santa

Cruz Biotech) in 40 mL TBST, while the bottom half was placed into a separate solution containing 0.5 µg/mL rabbit anti-AANATL2 (*Drosophila*) pAb (custom synthesized by Genscript) in 40 mL TBST. Both solutions were rocked overnight at 4°C. Each half of the nitrocellulose was transferred into separate containers with identical solutions of 0.5 µg/mL goat anti-rabbit IgG, HRP, pAb, secondary antibody in 40 mL TBST and rocked at room temperature for 2 hrs. Each half was placed into separate solutions containing 10 mL HRP substrate (1:1 stable peroxide: enhancer solution) and was allowed to sit for 5 minutes while lightly rocking. Membrane halves were removed and allowed to completely dry before piecing back together, exposure and X-Ray development. The X-Ray film was exposed to the irradiating membrane for 10 minutes in a dark room and immediately developed.

2.6.e Liquid extraction and purification of lipids from Drosophila thorax-abdomen

Frozen thorax abdomen (0.4 grams) from both the UAS parent and AANATL2 knockdown offspring were collected separately in triplicate samples (1.2 g total for each variety of fly and 6 samples total) and all replicates were treated using the same techniques following Sultana and Johnson [39]. Each replicate was dissolved in 14 mL of HPLC grade methanol from Fisher and transferred to mortar and pestle. A solvent blank containing 14 mL of methanol was also prepared and treated in the exact same manner as all *Drosophila* samples. The thorax-abdomen were ground in methanol for 5 mins and transferred to a 25 mL scintillation vial placed on ice. The remaining, loosely broken up, fly bodies were sonicated for 15 minutes on ice to further lyse the cells and expose the lipids in solution. Homogenates were centrifuged for 10 minutes and the supernatants were collected into a large test tube and capped. Cell pellets were re-suspended in 14mL chloroform: methanol: water (1:1:0.1, v/v/v) and then sonicated for 10 minutes. Supernatants were collected and compiled onto the methanol extracts in the same test tube of the appropriate sample. Cell pellets were reconstituted in 14 mL chloroform: methanol (2:1, v/v) and 2.4 mL 0.5 M KCl/ 0.08 M phosphoric acid (aq) was added to create an emulsion. Homogenates were sonicated for 2 minutes, briefly vortexed and centrifuged for 10 minutes. The organic layer containing chloroform (bottom) was consolidated into the same test tube as before, with all three solvent types now

containing biomaterial from the same type of thorax-abdomen. All extracts were dried under inert nitrogen overnight on a sand bath at 40°C.

Dried extracts were constituted in 1 mL HPLC-grade n-hexane from Fisher Scientific. The sides of the tube were thoroughly washed in hopes of dissolving all organic material and the resulting solution was transferred to a new, small test tube, ensuring to leave most insoluble material behind. This process was repeated for another 1 mL of hexane and placed into the same, small test tube. The n-hexane crude extracts were dried under inert nitrogen at 40°C. 500 mg DSC-silica from Sigma Aldrich was placed into a 5 mL drip column and analytical grade sand was placed atop the silica in an approximately 0.3 cm layer. The dried extracts were suspended in 150 µL n-hexane, while the silica was equilibrating in 5 mL n-hexane. Once the bottom of the meniscus of the equilibrant reached the top of the sand, the entire dissolved extract was injected onto the silica/sand bed and allowed to fully adsorb into the adsorbent. Hexane (4 mL) was added and dripped into a waste container. The solvent level got very low, without drying the column, before adding a new solvent, while the flow continued to be directed to the waste. This was continued for the following solvents after n-hexane: 1 mL hexane: acetic acid (99:1, v/v), 1 mL hexane: ethyl acetate (90:10, v/v), 1 mL hexane: ethyl acetate (80:20, v/v). After the 80:20 solvent has almost finished eluting, add 1 mL hexane: ethyl acetate (70:30, v/v) and begin collecting the eluent in a small test tube. Continue to collect the elution fractions in the same test tube for the remaining solvents: 1.5 mL chloroform: 2-propanol (2:1, v/v) and 1 mL HPLC-grade methanol. The collected elution was capped and finally dried under inert nitrogen at 40°C.

2.6.f LC-QToF-MS/MS detection of fatty acid amides from Drosophila thorax-abdomen

Purified extracts were dissolved in 90 µL methanol: acetonitrile (1:1, v/v), to which 50 pmoles of *N*-arachidonoyldopamine and 50 pmoles of *N*-arachidonoylserotonin were added to make a total volume of 100 µL, which was transferred to the appropriate insert of a clear 12 x 32 mm vial. These two compounds were chosen as internal standards because they were not detected in an initial pilot experiment containing 0.4 g of fruit fly thorax-abdomen. A volume of 25 µL was chosen for injection onto an Agilent 6540 liquid chromatography/quadrupole time-of-flight mass spectrometer (LC/QToF-

MS) in positive ion mode and a cutoff of 3200 m/z. A Kinetix 2.6 µm C_{18} 100 Å (50 x 2.1 mm) reverse phase column was used for the separation of lipid extracts from both the UAS parent and AANATL2 knockdown offspring. Mobile phase A was 0.1% formic acid in water while mobile phase B was 0.1% formic acid in acetonitrile and the flow rate was set to 0.6 mL/min. The elution profile is as follows: Linear increase from 10% to 100% B in 5 min and a hold for 3 min at 100% B. The column was then re-equilibrate with 10% for 8 minutes after each run. In addition, a wash step was completed after each run, which is identical to the method just stated, except there is a 50 µL injection and the flow rate is 1.0 mL/min until the equilibration step is reached. The retention time and m/z of fatty acid amides (FAAs) were found by matching them to pure standard solutions of the compound and the intensity recorded for each compound found to have a match. The instrument was then instructed to collect certain FAAs by their corresponding m/z and retention time and fragment each compound with a collision energy of 15-20 mV. The resulting mass spectra were then analyzed to find the precursor ion and fragments indicative of that particular fatty acid amide.

2.7 Results and Discussion

2.7.a AANATL2 transcripts are reduced in AANATL2 knockdown offspring

ΔΔCT analysis was used to determine the fold change of AANATL2 transcripts in the AANATL2 knockdown offspring of the UAS/Gal4 cross in *D. melanogaster*. Show in Table 2.3 are the CT values recorded for the AANATL2 target and actin-42A endogenous control for both the UAS parent and knockdown offspring.

Table 2.3 ΔCT Values calculated for ΔΔCT analysis

	CT_{Actin}	$CT_{AANATL2}$	ΔCT
UAS	17.14 ± 0.02	25.82 ± 0.09	8.676 ± 0.09
Knockdown	18.24 ± 0.09	29.45 ± 0.19	11.21 ± 0.21

The average CT values of three replicates for the actin-42A and AANATL2 amplicons in both the UAS parent and AANATL2 knockdown offspring are shown. CTs reflect the amplification of a single product, as there was no amplification detected in the "no-RT" and "no-template", negative controls. Also, all sequencing results from Eurofins Genomics came back positive for the appropriate amplicon. The ΔΔCT is used to find the change in abundance of a particular target amplicon relative to an endogenous control in a control and treated sample. In this experiment, the control is the UAS parent, while the treated sample is the AANATL2 knockdown offspring. This value is calculated by subtracting the ΔCT of the UAS from that of the knockdown, which provides a value of 2.537 ± 0.23. In order to find the fold change, the ΔΔCT is then plugged into the equation $2^{-\Delta\Delta CT}$, which provides a fold change of 0.15 - 0.19 in the knockdown compared to the UAS parent. In other words, the AANATL2 transcripts are 81-85% reduced in the offspring when compared to the UAS parent. These data ultimately convey the effectiveness of the UAS/Gal4 mating cross to produce a particular kind offspring having significantly less AANATL2 mRNA via siRNA interference. In order to further conclude the amplicons attained the proper identity, 40 µL of each amplicon were taken from the 96-well plate and combined with 10 µL of purple loading dye (NEB) and injected into respective wells of a 1.8% agarose gel with 127 nM ethidium bromide. Electrophoresis was run for 1.5 hr at 50 V, at which time the gel was irradiated with UV light and the bands were lined up with the ladder for approximate size matching and then cut out of the gel. The resulting gel can be seen in Figure 2.2.

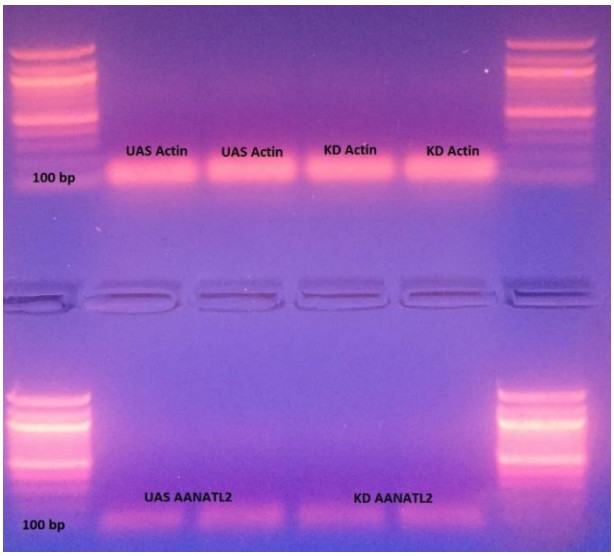

Figure 2.2 Agarose Gel with cDNA products from RT-qPCR; depicts the cDNA products run on a 1.8% agarose gel. Lanes 1, 6, 7 and 12 each contain 11µL of 100bp ladder (NEB). Lanes 2-3 show the actin amplicons of the UAS parents, while lanes 4-5 show the actin amplicons for the AANATL2 knockdowns. Lanes 8-9 show the AANATL2 amplicons from the UAS parent, while lanes 10-11 show the AANATL2 amplicons from the knockdown flies. All actin and AANATL2 amplicons are seen to be approximately the correct product sizes (actin = 123 bp ; AANATL2 = 120 bp). All excised bands were shown to have the correct matching sequences via sequencing by Eurofins Genomics.

DNA was extracted from the agarose gel slices using the Wizard SV Gel and PCR Clean-up System from Promega. Extracted DNA bands were then shown to have the correct base pair sequence via luciferase analysis by Eurofins Genomics. However, the level of transcripts does not always directly correlate the level of translated protein in the cell. Therefore, a Western blot showing a qualitative reduction of AANATL2 would complement the reduction of transcripts and deduce the UAS/Gal4 mating cross is ultimately producing an effective protein knockdown via RNA silencing.

2.7.b Drosophila AANATL2 protein abundance is reduced in knockdown offspring

Shown in Figure 2.3is the knockdown of AANATL2 protein expression in the non-stubble (Sb[1]) offspring of the UAS/Gal4 cross in the outlined bands in the figure. These bands weigh about 25 kD each, which likely correspond to endogenous AANATL2 that has a molecular weight of approximately 24.3 kD. These bands are also the only bands in the blot slightly lighter than the recombinant protein, which has six histidine molecules and a linker region attached, adding almost 2 kD of weight to the recombinant protein. Therefore, the endogenous protein in an extract would be expected

to be slightly lighter than the recombinant, which is seen here. Furthermore, the AANATL2 band seen in the knockdown looks fainter than the band seen in the lane corresponding to the UAS parent. This would suggest the AANATL2 expression in the thorax-abdomen of the knockdown offspring is not as abundant as the AANATL2 expression in the thorax-abdomen of the UAS parent. Ultimately, these data, in conjunction with the confirmed knockdown of AANATL2 transcripts, show the UAS/Gal4 bipartite approach is successful in generating a mutant *Drosophila melanogaster* strain with reduced AANATL2.

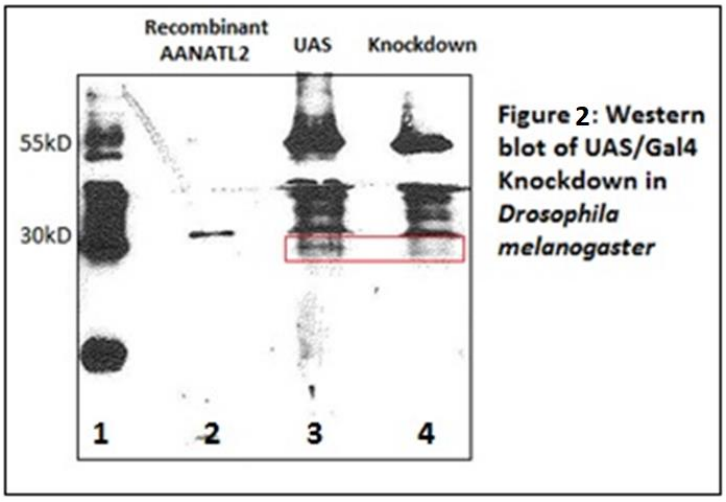

Figure 2.3 AANATL2 knockdown western blot; contains representations of the proteins extracted from the thorax-abdomen of the knockdowns and UAS parents. Lane 1 shows the Magic Marker protein ladder. Lane 2 represents a positive control of recombinant AANATL2 from E.coli containing a 6X-Histidine tag. Lane 3 shows 22 µg of total protein from the thorax-abdomen of the UAS parent and lane 4 shows 22 µg of total protein from the thorax-abdomen of the AANATL2 knockdown offspring. The bands outlined are proposed to be AANATL2 at around 25 kD.

2.7.c Detection of PALDA reduced abundance in AANATL2 knockdown flies via subtraction

After triplicate LC-QToF-MS injections of the six collected samples (3 UAS and 3 knockdown), the resulting total ion chromatograms were scanned for m/z and retention time values matching that of pure, commercially available, fatty acid amide standards. These standards were placed into 1.5 mL of methanol: acetonitrile (1:1 v/v) at a concentration of 5 µM for each compound and injected using the same column, injection volume and gradient elution as all purified extracts. Once the retention time and m/z was confirmed for each identified fatty acid amide, targeted, tandem mass spectrometry was

completed on each molecule using a 5 µL injection volume and a collision energy (CID) of 15-20 mV. The list of detected fatty acid amides in both the UAS mutant and AANATL2 knockdown mutant can be seen in table 4 and the resulting list of fragments can be seen in table 2.5.

Table 2.4: Matching m/z and Retention Times of Fatty Acid Amides Detected in the Thorax-Abdomen

Fatty Acid Amide	m/z			Retention Time (min)		
	Standard	UAS	KD	Standard	UAS	KD
N-Palmitoyldopamine	392.3164	392.3183	ND	5.998	5.933	ND
N-Palmitoylglycine	314.2694	314.2695	314.2690	5.832	5.908	5.830
N-Palmitamide	256.2640	ND	256.2636	6.040	ND	6.048
N-Palmitoleamide	254.2483	254.2456	254.2478	5.683	5.667	5.680
N-Oleoylethanolamine	326.3064	326.3057	326.3056	5.907	5.909	5.915
N-Oleamide	282.2797	282.2783	282.2799	6.115	6.116	6.134

The panel of fatty acid amides detected in the thorax-abdomen of the UAS parent and/or AANATL2 knockdown offspring. A m/z detected in a purified extract was considered to be a match to its corresponding standard if it was ± 0.05 m/z and ± 0.2 min from the standard m/z and retention time respectively. If a found m/z did not match these parameters, "ND" was placed for "not detected".

Table 2.5: Tandem mass spectrometry fragmentation of detected fatty acid amides

	m/z								
	Precursor			**Amine**			**Acyl**		
FAA	Std	UAS	KD	Std	UAS	KD	Std	UAS	KD
Ole	282.2785	282.2811	282.2858	100.0752	100.0756	100.0712	135.1136	135.116	135.1175
OleEth	326.3076	326.3060	326.3055	62.059	62.0605	62.0600	135.1167	135.1164	135.1131
Palm	256.2665	ND	256.2624	100.0742	ND	100.0772	57.0698	ND	57.0687
Palmle	254.2456	254.2453	254.2522	100.0772	100.0752	100.0759	135.1155	135.1172	135.1166
PalmGly	314.2690	314.2880	314.269	76.0397	76.0398	76.0395	57.0700	57.0694	57.0708
PalmDop	392.3160	392.3223	ND	154.0835	154.0856	ND	57.0688	57.0708	nd

Looking at Table 2.4, no m/z value was detected in the knockdown offspring for *N*-palmitoyldopamine. The blank run for each extraction was also scanned for any matching lipids as well. Any quantifiable m/z found in the blank were subtracted from each sample replicate to reduce the likelihood of false positives. Once a compound was confirmed based off its matching m/z and retention time to the standard and blank subtraction, it was quantified using standard curves generated from concentrations of the standard compound ranging from 5-500 nM. The average intensity recorded by the mass spectrometer was converted into pmoles for each compound detected in each replicate. *N*-arachidonoylserotonin (50 pmoles) and *N*-arachidonoyldopamine (50 pmoles) were spiked into each sample before LC-QToF-MS injection, which was used as an internal standard to normalize fatty acid amide quantification between replicates. Both internal standards had a recovery of greater than 80%. Finally, all resulting values were divided by 0.4 g to give the pmoles of fatty acid amides per gram of *Drosophila melanogaster* thorax-abdomen. The list of values can be seen in Table 2.5.

Table 2.6 Quantification of fatty acid amides in AANATL2 knockdown *Drosophila melanogaster*

Fatty Acid Amide	UAS (pmole/g)	AANATL2 KD (pmole/g)
N-Palmitoyldopamine	3.49 ± 1.3	ND
N-Palmitoylglycine	13.1 ± 1.7	21.1 ± 7.5
N-Palmitamide	ND	4.94 ± 1.2
N-Palmitoleamide	19.0 ± 7.8	37.3 ± 10
N-Oleoylethanolamine	37.3 ± 8.6	14.1 ± 3.9
N-Oleamide	31.7 ± 1.3	374 ± 56.9

The pmoles/g of fatty acids detected in the thorax-abdomen of the UAS parent and AANATL2 knockdown mutant. Each average reflects triplacte LC-QToF-MS injections from three different replicates of thorax-abdomenl lipid extracts from each type of fly. “ND” refers to compounds not detected by either being to sparse for detection using the standard curves or being too similar in magnitude to the blank.

The difference in levels of fatty acid amides in the thorax-abdomen between the UAS mutant and AANATL2 knockdown mutant is shown in Table 2.6. The panel seen above shows significant differences in certain lipids, while others remain relatively similar. This leads to the belief that the greater differences are more significant. For instance, there is a clear reduction in the levels of *N*-palmitoyldopamine (PALDA), as it was not detected at all in the thorax-abdomen of the AANATL2 knockdown mutant, but was detected in the UAS mutant. It is important to note PALDA was also previously detected in wild type *Drosophila* by Jeffries *et al.,* suggesting its absence is not due to natural differences of expression of different mutant strains [7]. Furthermore, PALDA is an *N*-acylarylalkylamide previously shown to be biosynthesized by AANATL2 in *D. melanogaster in vitro*. This reduction is a key finding, as it concludes reducing the expression of AANATL2 in *Drosophila melanogaster* causes a loss of detection of PALDA. These data suggest AANATL2 is responsible for the *in vivo* biosynthesis of PALDA in *Drosophila melanogaster*. It is also quite possible there are other *N*-acylarylalkylamides being produced by this enzyme *in vivo*, but simply were not detected in the parental strains to constraints on sample size collection. It remains unclear what purpose the products of AANATL2 are serving in *D. melanogaster*. We are certain the knockdown in expression is not lethal to the insects, but any other phenotypes have yet to be discovered. It is known the hardening of many insect cuticles occurs through the cross-linking of acetylated quinones of monoamines, in which longer chain acyl groups may be used directly or indirectly, but that fact still remains to be tested [24]. Another possibility is that PALDA and other long chain *N*-acylarylalkylamides interact with different transient receptor potential (TRP) proteins, like TRPV1, due to its structural similarity to capsaicin. Furthermore, *N*-palmitoyldopamine was found to repress the sonic hedgehog (Shh) pathway in ShhLIGHT2 cells, which is a pathway commonly studied for growth regulation and cell differentiation. It is possible the long chain N-acylarylalkylamides are participating in some or all of these metabolic pathways occurring in *D. melanogaster*. Further studies on the biosynthesis and may eventually provide insights to cancer research efforts in mammals [25]. Therefore, a better understanding of PALDA biosynthesis and the other possible products of AANATL2 in fruit flies is significant due the importance of the *N*-acyldopamines in varying organisms.

2.8 Acknowledgements

This work has been supported, in part, by grants from the ShirleyW. and William L. Griffin Foundation and National Institute of General Medical Science of the National Institutes of Health (R15-GM107864) to D.J.M. A special thanks to Sydney Balgo for the collection of insect thorax-abdomen.

2.9 References

[1] Cravatt, B. F.; Prospero-Garcia, O.; Siuzdak, G.; Gilula, N. B.; Henriksen, S. J.; Boger, D. L.; Lerner, R. A., Chemical characterization of a family of brain lipids that induce sleep. *Science (New York, N.Y.)* **1995,** *268* (5216), 1506-9.

[2] Wright, T. R., The genetics of biogenic amine metabolism, sclerotization, and melanization in Drosophila melanogaster. *Advances in genetics* **1987,** *24*, 127-222.

[3] Dempsey, D. R.; Jeffries, K. A.; Anderson, R. L.; Carpenter, A. M.; Rodriquez Opsina, S.; Merkler, D. J., Identification of an arylalkylamine N-acyltransferase from Drosophila melanogaster that catalyzes the formation of long-chain N-acylserotonins. *FEBS letters* **2014,** *588* (4), 594-9.

[4] Zheng, W.; Cole, P. A., Serotonin N-acetyltransferase: mechanism and inhibition. *Current medicinal chemistry* **2002,** *9* (12), 1187-99.

[5] Sergeeva, O. A.; De Luca, R.; Mazur, K.; Chepkova, A. N.; Haas, H. L.; Bauer, A., N-oleoyldopamine modulates activity of midbrain dopaminergic neurons through multiple mechanisms. *Neuropharmacology* **2017,** *119*, 111-122.

[6] Hickman, A. B.; Klein, D. C.; Dyda, F., Melatonin Biosynthesis: The Structure of Serotonin N-Acetyltransferase at 2.5 Å Resolution Suggests a Catalytic Mechanism. *Molecular Cell* **1999,** *3* (1), 23-32.

[7] Jeffries, K. A.; Dempsey, D. R.; Behari, A. L.; Anderson, R. L.; Merkler, D. J., Drosophila melanogaster as a model system to study long-chain fatty acid amide metabolism. *FEBS letters* **2014,** *588* (9), 1596-602.

[8] Baulcombe, D., RNA silencing in plants. *Nature* **2004,** *431* (7006), 356-63.

[9] Hannon, G. J.; Conklin, D. S., RNA interference by short hairpin RNAs expressed in vertebrate cells. *Methods in molecular biology (Clifton, N.J.)* **2004,** *257*, 255-66.

[10] Meister, G.; Tuschl, T., Mechanisms of gene silencing by double-stranded RNA. *Nature* **2004,** *431* (7006), 343-9.

[11] Plasterk, R. H., RNA silencing: the genome's immune system. *Science (New York, N.Y.)* **2002,** *296* (5571), 1263-5.

[12] Voinnet, O., RNA silencing: small RNAs as ubiquitous regulators of gene expression. *Current opinion in plant biology* **2002,** *5* (5), 444-51.

[13] Zamore, P. D., Ancient pathways programmed by small RNAs. *Science (New York, N.Y.)* **2002,** *296* (5571), 1265-9.

[14] Bernstein, E.; Caudy, A. A.; Hammond, S. M.; Hannon, G. J., Role for a bidentate ribonuclease in the initiation step of RNA interference. *Nature* **2001,** *409* (6818), 363-6.

[15] Nykanen, A.; Haley, B.; Zamore, P. D., ATP requirements and small interfering RNA structure in the RNA interference pathway. *Cell* **2001,** *107* (3), 309-21.

[16] Ambros, V.; Lee, R. C.; Lavanway, A.; Williams, P. T.; Jewell, D., MicroRNAs and other tiny endogenous RNAs in C. elegans. *Current biology : CB* **2003,** *13* (10), 807-18.

[17] Carrington, J. C.; Ambros, V., Role of microRNAs in plant and animal development. *Science (New York, N.Y.)* **2003,** *301* (5631), 336-8.

[18] Lagos-Quintana, M.; Rauhut, R.; Lendeckel, W.; Tuschl, T., Identification of novel genes coding for small expressed RNAs. *Science (New York, N.Y.)* **2001,** *294* (5543), 853-8.

[19] Mourelatos, Z.; Dostie, J.; Paushkin, S.; Sharma, A.; Charroux, B.; Abel, L.; Rappsilber, J.; Mann, M.; Dreyfuss, G., miRNPs: a novel class of ribonucleoproteins containing numerous microRNAs. *Genes & development* **2002,** *16* (6), 720-8.

[20] Kalidas, S.; Smith, D. P., Novel Genomic cDNA Hybrids Produce Effective RNA Interference in Adult Drosophila. *Neuron* **2002,** *33* (2), 177-184.

[21] Duffy, J. B., GAL4 system in Drosophila: a fly geneticist's Swiss army knife. *Genesis (New York, N.Y. : 2000)* **2002,** *34* (1-2), 1-15.

[22] Brand, A. H.; Perrimon, N., Targeted gene expression as a means of altering cell fates and generating dominant phenotypes. *Development* **1993,** *118* (2), 401-415.

[23] Giniger, E.; Varnum, S. M.; Ptashne, M., Specific DNA binding of GAL4, a positive regulatory protein of yeast. *Cell* **1985,** *40* (4), 767-74.

[24] Hiragaki, S.; Suzuki, T.; Mohamed, A. A.; Takeda, M., Structures and functions of insect arylalkylamine N-acetyltransferase (iaaNAT); a key enzyme for physiological and behavioral switch in arthropods. *Frontiers in physiology* **2015,** *6*, 113.

[25] Khaliullina, H.; Bilgin, M.; Sampaio, J. L.; Shevchenko, A.; Eaton, S., Endocannabinoids are conserved inhibitors of the Hedgehog pathway. *Proc Natl Acad Sci U S A* **2015,** *112* (11), 3415-20.

[26] Chu, C. J.; Huang, S. M.; De Petrocellis, L.; Bisogno, T.; Ewing, S. A.; Miller, J. D.; Zipkin, R. E.; Daddario, N.; Appendino, G.; Di Marzo, V.; Walker, J. M., N-oleoyldopamine, a novel endogenous capsaicin-like lipid that produces hyperalgesia. *The Journal of biological chemistry* **2003,** *278* (16), 13633-9.

[27] Holmes, K.; Williams, C. M.; Chapman, E. A.; Cross, M. J., Detection of siRNA induced mRNA silencing by RT-qPCR: considerations for experimental design. *BMC Research Notes* **2010,** *3*, 53-53.

CHAPTER THREE

Bm-iAANAT and its potential role in fatty acid amide biosynthesis in *Bombyx mori*

3.1 Note to reader

This chapter was previously published in the following article: Anderson R.L., Battistini M.R., Wallis D.J., Shoji C., O'Flynn B.G., Dillashaw J.E., Merkler D.J. Bm-iAANAT and its potential role in fatty acid amide biosynthesis in *Bombyx mori*. *Prostaglandins Leukotrienes and Essential Fatty Acids*. 2018. 135; 10-17. Ryan Anderson designed the experiments, performed experiments, and wrote a majority of the manuscript for publication. Matthew R.Battistini made significant contributions involving enzyme kinetic data and helped write the manuscript. Dylan J. Wallis and Christopher Shoji contributed to the care of insects and completed certain enzyme kinetic experiments. John E. Dillashaw helped make the N-oleoyltryptamine standard for LC-QToF-MS analysis. David J. Merkler designed the scope of the entire research and is the corresponding author. This article has been reproduced in Appendix B and has been approved for reproduction by Elsevier Limited.

CHAPTER FOUR

Changes in expression of three insect arylalkylamine-*N*-acyltransferases and fatty acid amides detected in the different life stages of *Bombyx mori*.

4.1 Note to reader

This chapter will be submitted to FEBS Letters for peer review. The authors are Ryan L. Anderson, Dylan J. Wallis, Alexandria C. Musick, Sydney Innes and David J. Merkler. Ryan L. Anderson did a majority of the RT-qCPR and LC-QToF-MS analysis of fatty acid amides. Dylan J. Wallis helped rear silkworms and performed some RT-qPCR experiments. Alexandria C. Musick and Sydney Innes helped rear silkworms and do fatty acid amide purifications. David J. Merkler designed the research and is the corresponding author.

4.2. Significance statement

Insect model systems are a pragmatic tool to utilize for finding general synthesis patterns of fatty acid amides. This has the potential of providing insight into the biosynthesis of other organisms, like higher vertebrates. Furthermore, fatty acid amides serve unique, biological functions in insects and may provide information on future target proteins for novel insecticides. One set of insect proteins being looked into specifically for the purpose of pest control are the insect arylalkylamine *N*-acyltransferases (iAANAT). The data herein conveys the change in expression of three of these *Bombyx mori* iAANAT (*Bm*-iAANAT) in different life stages of the silkworm. Furthermore, novel panels of fatty acid amides have also been characterized and quantified for each instar of the growing insect. It has been shown the AANATs are important biosynthetic enzymes for insects in general, but remains unknown about the exact

function of the products of the iAANATs. This work gives potential to learn more about general long chain fatty acid amides for developing targeted insecticides and possibly future therapeutics.

4.3 Abstract

The purpose of this research is to track the change in transcripts of three insect arylalkylamine-*N*-acyltransferases (iAANATs) using RT-qPCR in the domesticated silkworm (*Bombyx mori*) as it transcends into each of its different life stages. The end goal being to note key differences in their expression at different times of the insect's life. Furthermore, knowing these enzymes are capable of biosynthesizing certain fatty acid amides *in vitro*, we also wanted to characterize and quantify a panel of such lipids via liquid chromatography time-of-flight mass spectrometry (LC-QToF-MS) from purified lipid extracts of each *B. mori* life stage. This would ultimately provide insight on how these fatty acid amides are being synthesized *in vivo*. The results show differences in expression for these separate iAANATs as well as a unique, novel panel of fatty acid amides at different time points in the silkworm's growth.

4.4 Abbreviations

Bm-iAANAT, *Bombyx mori* insect arylalkylamine *N*-acyltransferase; *Bm*i1, *Bombyx mori* instar 1; *Bm*i5, *Bombyx mori* instar 5; PalmGly, *N*-palmitoylglycine; PalmDop, *N*-palmitoyldopamine; PalmSer, *N*-Palmitoylserotonin; Palmle, Palmitoleamide; Palm, Palmitamide; OleGly, *N*-oleoylglycine; OleEth, *N*-oleoylethanolamine; OleDop, *N*-oleoyldopamine; OleSer, *N*-oleoylserotonin; OleTrp, *N*-oleoyltryptamine; Ole, Oleamide; AracSer, *N*-arachidonoylserotonin; LinGly, *N*-linoleoylglycine; Lino, Linoleamide; SteSer, *N*-stearoylserotonin

4.5 Introduction

The fatty acid amides encompass a family of biologically functional lipids known to play different roles in metabolic pathways unique to vertebrates and invertebrates [1-2]. The general form of these endocannabinoid-like molecules exists as R-CO-NH-R', where R is an alkyl chain of a certain

length, derived from a fatty acid, and NH-R' is representative of a biogenic amine [3-7]. This form gives rise to many subclasses capable of having different alkyl chain lengths and different amine groups. However, this research focuses on those fatty acid amides incorporating long chain acyl groups derived from fatty acids having 16 to 20 carbons. These long chain fatty acids can be conjugated with an $–NH_2$ to create the primary fatty acid amides (PFAM) [8], a glycine to make the *N*-fatty acylglycines [9-10], an ethanolamine to make the *N*-acylethanolamines [11], or an arylalkylamide, like serotonin, to make the *N*-fatty acylarylalkylamides [12-13]. Each of these classifications have been found to be related in a common, biosynthetic pathway and each attains its own biological function [1].

Long chain fatty acid amide bio-production has been shown to use a general scheme of a fatty acid first being activated to a long chain acyl-CoA thioester [14-15], in which the CoA group can be substituted by a number of different biogenic amines using different *N*-acyltransferases [16]. These *N*-acyltransferases are believed to be members of the GCN5-related superfamily of *N*-acyltransferases (GNAT), which share the feature of being able to accept acyl-CoA thioester substrates [17-19]. Examples of such enzymes exhibiting this chemistry include *N*-myristoyl transferase, glycine *N*-acyltrasnferases (GLYATs), and aryalkylamine *N*-acyltransferases (AANATs) [10, 20-21]. Yet despite the wealth of data showing the varying fatty acid amides exist with these enzymes in several different organisms, much work remains on bridging the gap to delineate their precise metabolic functions and chemical mechanisms of biosynthesis.

Insect model systems are a pragmatic tool to utilize for finding general synthesis patterns of fatty acid amides. This has the potential of providing insight into the biosynthesis of other organisms, like higher vertebrates. For example, our lab previously characterized a panel of fatty acid amides in *Drosophila melanogaster*, which was ultimately used to propose a general pathway of PFAM biosynthesis [14]. Furthermore, fatty acid amides serve unique, biological functions in insects and may provide information on future target proteins for novel insecticides [22-24]. One set of insect proteins being looked into specifically for the purpose of pest control are the insect arylalkylamine *N*-acyltransferases (iAANAT) [23]. These would provide more precise targets partly due to their low

sequence homology (20-40%) from insect to insect [24]. A phylogenetic analysis demonstrates this homology shared between the AANAT enzymes of different insect organisms (Figure 4.1). Unlike humans and most other vertebrates, which have been found to express only one AANAT, which is utilized in the penultimate step in melatonin biosynthesis [25-26], it is not uncommon for insects to attain an arsenal of these enzymes [12]. Although insects are generally accepted to also use AANAT expression for the regulation of circadian rhythms and photoperiodism, like vertebrates, they also serve different functions within the insect. This includes cuticle morphology/coloring, neurotransmitter deactivation and regulation of amino acid metabolism [15, 27-30]. The use of these enzymes is mainly due to a lack of monamine oxidases (MAO) in insects and monoamine metabolism is compensated through the use of the iAANAT [28]. Therefore, the enzymes seen in the neighbor joining tree in Figure 4.1 may be providing at least one of these functions in insect metabolism and or morphology. The fact these enzymes may be playing similar roles, despite low/moderate homology in primary structure due to distance in a common ancestor is promising to the field of targeted insecticides.

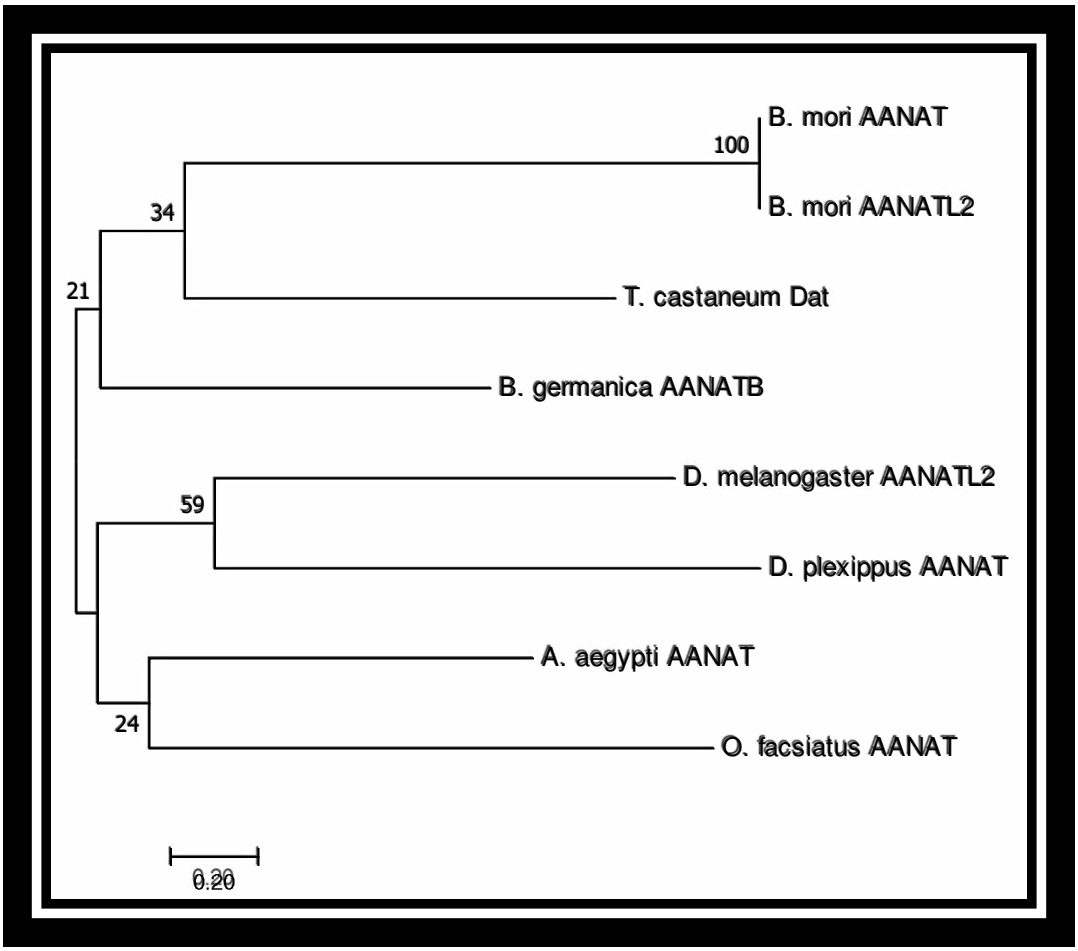

Figure 4.1 Neighbor-joining tree showing likelihood of common ancestry of different insect AANAT; The percentage of replicate trees where the associated taxa clustered in the bootstrap test (5000 replicates) are enumerated are shown next to the branches [31]. The tree has been constructed to scale, with lengths of branches being proportionate to the units of the evolutionary distances used to infer the phylogenetic tree. These distances were computed using the Poisson correction method and are represented as the number of amino acids substituted per site [32]. All analyses were carried out using MEGA7 [33].

Bombyx mori, or the domesticated silkworm, is a likely candidate for studying fatty acid amide metabolism and biosynthesis. This being especially true for those lipids stemming from iAANAT activity, as several iAANATs, as well as a panel of fatty acid amides, have already been identified in one instar of *B. mori* [34-35]. However, the literature currently available does not address how the expression of these proteins changes as the silkworm transcends each larval stage into its pupae and ultimate moth life stages. We have identified three different AANAT-like proteins in *Bombyx mori* that have sequence homology (25-39%) with AANATL2 in *Drosophila melanogaster*: an enzyme shown to catalyze the formation of long chain *N*-acylarylalkylamides *in vitro* [13]. It is unclear if *Bombyx mori* attains a set of

cannabinoid receptors, but receptors with sequence homology to a known cannabinoid receptor have been found, such as an octopamine receptor (28% identity to CB in *Xenopus laevis*). The exact, *in vivo* function of these enzymes and their metabolic products remain unknown. It is possible one of these proteins holds a particular importance to a specific life stage. Tracking the change in transcriptional expression of these *B. mori* insect AANAT: *Bm*-iAANAT, *Bm*-iAANAT2 and *Bm*-iAANAT3, has the potential to provide data on the temporal importance of these iAANAT's expression. It should be noted, we have used names consistent with previous literature about these enzymes, which can be confusing. Detection of the fatty acid amides in each life stage via LC-QToF-MS has the potential of determining if a change in transcriptional expression may be causing a change in fatty acid amide abundance. Characterizing a panel of fatty acid amides could also determine which life stages would be most efficient for future, genetic manipulation experiments on iAANAT, like CRISPR, in the silkworm.

4.6 Materials

Unless otherwise stated, all reagents and instruments were purchased from reputable, commercial sources and attained high quality for the purpose of scientific experimentation. All deuterated, internal standards were purchased from Cayman Chemical and have certificates of analysis indicative of high levels of purity.

4.7 Methods

4.7.a Silkworm rearing and sample collection

Bombyx mori eggs were purchased from Carolina Biological, immediately placed into a petri dish upon arrival and fed Silkworm Artificial Dry Diet from Carolina Biological after hatching. The different instars were identified based off the number of molts, such that the first instar (Bmi1) was collected before the first molt and the fifth instar (Bmi5) was collected after the fourth molt. The pupae and moth life stages were also collected, respectively. After collection, each sample type was immediately flash

frozen in liquid nitrogen and stored at -80°C before continuing any extraction of either nucleic acids or fatty acid amides.

4.7.b Extraction/ isolation of mRNA and gDNA decontamination

Total RNA was extracted using TRIzol® reagent and collected using the PureLink RNA Mini Kit® from Thermo Fisher. The mRNA was then sequestered via PolyATtract® mRNA Isolation Systems III from Promega. After the elution of mRNA in nuclease-free water, a 10 kDa centrifugal filter was used to concentrate the transcripts (15 min at 12,000 × g). A Nanodrop® from Thermo Fisher was used to determine the final concentration of the resulting mRNA isolations. DNase I from Thermo Fisher was employed for the removal of genomic DNA (gDNA) and modifications made to the manufacturer's protocol for full gDNA decontamination can be seen in Table 4.1.

Table 4.1 Decontamination of gDNA from mRNA isolations

Reagent	Recommended Protocol[a]	Modified Protocol
mRNA	1 µg	1 µg
DNase I	1 µL	2 µL
DNase I Buffer with $MgCl_2$	1 µL	2 µL
Nuclease-Free Water	to 10 µL	to 18 µL

[a]As recommended by the manufacturer.

The mRNA was incubated with DNase I, $MgCl_2$ buffer and nuclease-free water at 37° for 45 minutes, at which time 2 µL of EDTA was added while raising the temperature to 65°C for 10 minutes to inactivate the DNase I. After the completion of gDNA decontamination, the mRNA solution was diluted with nuclease-free water to a final concentration of 10 ng/µL.

4.7.c One-Step RT-qPCR of Tua1, Bm-iAANAT, Bm-iAANAT2 and Bm-iAANAT3

Separate, triplicate wells of a 96-well plate were initially loaded with 10 µL Power Up™ SYBR® Green Master Mix from Thermo Fisher, 30 ng mRNA from a specific *B. mori* life stage and 2 µL (20 U/µL) MMLV-RT from Promega. Next, the different primers were added to the wells, which essentially delineate the amplicon being replicated. The forward and reverse primers for each amplicon type were

designed to create 75-150 bp products and the primer sequences can be seen in Table 4.2. Alpha tubulin (Tua1) was chosen as the positive, endogenous control for all RT-qPCR experiments, as it is expressed in abundance throughout every post-embryonic life stage of the organism [36].

Table 4.2 RT-qPCR primers for Tua1, *Bm*-iAANAT, *Bm*-iAANAT2, and *Bm*-iAANAT3

Amplicon	Forward Primer	Reverse Primer
Tua1	AGATGCCCACAGACAAGACC	CAAGATCGACGAAGAGAGCA
Bm-iAANAT	CAAAATGTCCGTTCCAGCTT	GATTGACGGCGAGATTCATT
Bm-iAANAT2	GAACGAGGCAGTAGGGTTATATG	CCTTTCAGTAGCGAATCCCTG
Bm-iAANAT3	CCTTAGAACGTCTTTGCCTCG	TCGGTGGACTGCTTTATCTTC

200 nM *Bombyx mori* Tua1 forward primer and 200 nM Tua1 reverse primer were added to wells A1-A3; 200 nM *Bm*-iAANAT forward primer and 200 nM *Bm*-iAANAT reverse primer were added to wells B1-B3. 200 nM *Bm*-iAANAT2 forward primer and 200 nM *Bm*-iAANAT2 reverse primer were added to wells C1-C3. 50 nM *Bm*-iAANAT forward primer and 50 nM *Bm*-iAANAT reverse primer were added to wells D1-D3. Nuclease-free water was used to make each well have a final volume of 20 µL. A negative control substituting MMLV-RT for nuclease-free water was used to ensure total decontamination of gDNA. Another negative control substituting the mRNA template for nuclease-free water was run to ensure fluorescence was not being detected from primer dimer formation. This entire plate-loading process was repeated separately, using mRNA from a different life stage each time. Each prepared plate was capped and briefly centrifuged before placing into an Applied Biosystems QuantStudio3 qPCR thermal cycler. The one-step RT-qPCR conditions were as follows: The reverse transcriptase phase was completed by holding the temperature at 50°C for 45 minutes and then raising the temperature to 95°C for 10 minutes to inactivate the MMLV-RT. The PCR cycles then immediately began with an initial temperature hold at 95°C for 15 seconds and then lowered to 60°C for 1 minute

before returning to 95°C and was repeated for a total of 40 cycles. Melt curve analysis was employed after the completion of thermal cycling with holds at 95°C for 15 seconds, 60°C for 1 minute, and a final 95°C for 1 second. The cDNA products of the same amplicon were added together to make a final volume of 40 µL and mixed with 10 µL purple loading dye from New England Biolabs (NEB). This was done for Tua1, *Bm*-iAANAT, *Bm*-iAANAT2 and *Bm*-iAANAT3 amplicons separately. A 100 bp ladder from NEB and the resulting 50 µL mixtures of PCR products were injected, respectively, into the lanes of a 1.8% agarose gel containing ethidium bromide and electrophoresis was done at 50 V for 90 minutes. All bands denoting significant cDNA products were extracted using the Wizard® SV Gel and PCR Clean-Up System from Promega and sequenced commercially by Eurofins Genomics.

4.7.d Extraction and purification of fatty acid amides from different B. mori life stages

0.5-1.0 g (depending on the life stage) of a *Bombyx mori* larval instar, pupae or moth was collected in triplicate (1.5-3.0 g total) using the sample collection method described above. To extract the fatty acid amides, the insects were first placed into a mortar and pestle with 20.8 mL of methanol per gram of solid tissue used. The remaining extraction solvents and steps, as well as the silica and Zip Tip purification, closely follow the work done by Anderson et al [35]. Blanks using the same proportionate volumes of solvents, but containing no tissue, were prepared and treated in the exact same manner as each different extraction done.

4.7.e Injection of Bombyx mori Purified, Fatty Acid Amide Extracts on LC-QToF-MS

Fatty acid amide extract (90 µL) was eluted from the Zip Tip in 5:95 (water: acetonitrile) into an LC vial with glass insert and 10 µL of internal standard solution, containing 1 pmole/µL each of *N*-arachidonoylglycine d_8, *N*-arachidonoylethanolamine d_8, *N*-arachidonoyldopamine d_8 and *N*-oleoylserotonin d_{17}, was added. This was repeated for the extraction blanks as well. Each internal standard was quantified using standard curves generated from pure material ranging from 0.1 – 10 pmoles and having an R^2 value of at least 0.990. All deuterated internal standards were checked for, and found to be free of, any unlabeled compounds. *Bombyx mori* lipid extracts were injected on an Agilent 6540 liquid chromatography/quadrupole time-of-flight mass spectrometer (LC-QTOF-MS) in positive ion mode with

a Kinetex 2.6 µm C_{18} 100 Å (50 × 2.1 mm) column and the following mobile phase gradient at a flow rate of 0.6 mL/min: mobile phase A was 0.1% (v/v) formic acid in water, while mobile phase B was 0.1% (v/v) formic acid in acetonitrile. A linear gradient of 10% mobile phase B increased to 100% B over 5 minutes, followed by a hold of 3 minutes at 100% B for the analysis of the product. The column was then equilibrated with 10% mobile phase B for 10 minutes before subsequent injections. The column was thoroughly washed between injections using the same solvent gradient, but at a flow rate of 1.0 mL/min. A solution containing pure, targeted compounds was also injected onto the same column for retention time and m/z value comparison to facilitate fatty acid amide characterization in the extracts.

4.8 Results and Discussion

4.8.a Difference in expression of *Bm*-iAANAT, *Bm*-iAANAT2, *Bm*-iAANAT3 transcripts shown by RT-qPCR

CT values for all amplicons were compiled into Table 4.3. The subsequent fold changes for each iAANAT were calculated using the formula, $2^{-\Delta\Delta CT}$, and recorded in Figure 4.2. These data convey the change in abundance of each transcript relative to the change in abundance of the alpha tubulin as the silkworm grows from the first instar.

Table 4.3 CT values for Tua1, *Bm*-iAANAT, *Bm*-iAANAT2 and *Bm*-iAANAT3 in *Bombyx mori*

	Tua1 (CT)	Bm-iAANAT (CT)	Bm-iAANAT2 (CT)	Bm-iAANAT3 (CT)
Instar 1	16.48 ± 0.06	19.23 ± 0.06	18.85 ± 0.04	21.73 ± 0.09
Instar 2	14.25 ± 0.32	18.80 ± 0.16	19.48 ± 0.14	26.10 ± 0.12
Instar 3	17.56 ± 0.43	20.10 ± 0.12	22.06 ± 0.03	30.40 ± 0.42
Instar 4	14.80 ± 0.07	18.52 ± 0.09	19.98 ± 0.18	27.79 ± 0.22
Instar 5	17.86 ± 0.15	19.56 ± 0.08	20.66 ± 0.16	30.65 ± 0.16

Table 4.3 CT values for Tua1, *Bm*-iAANAT, *Bm*-iAANAT2 and *Bm*-iAANAT3 in *Bombyx mori*

Pupae	15.28 ± 0.22	18.82 ± 0.17	20.67 ± 0.12	25.47 ± 0.06
Moth	14.31 ± 0.10	16.36 ± 0.22	19.29 ± 0.04	27.84 ± 0.14

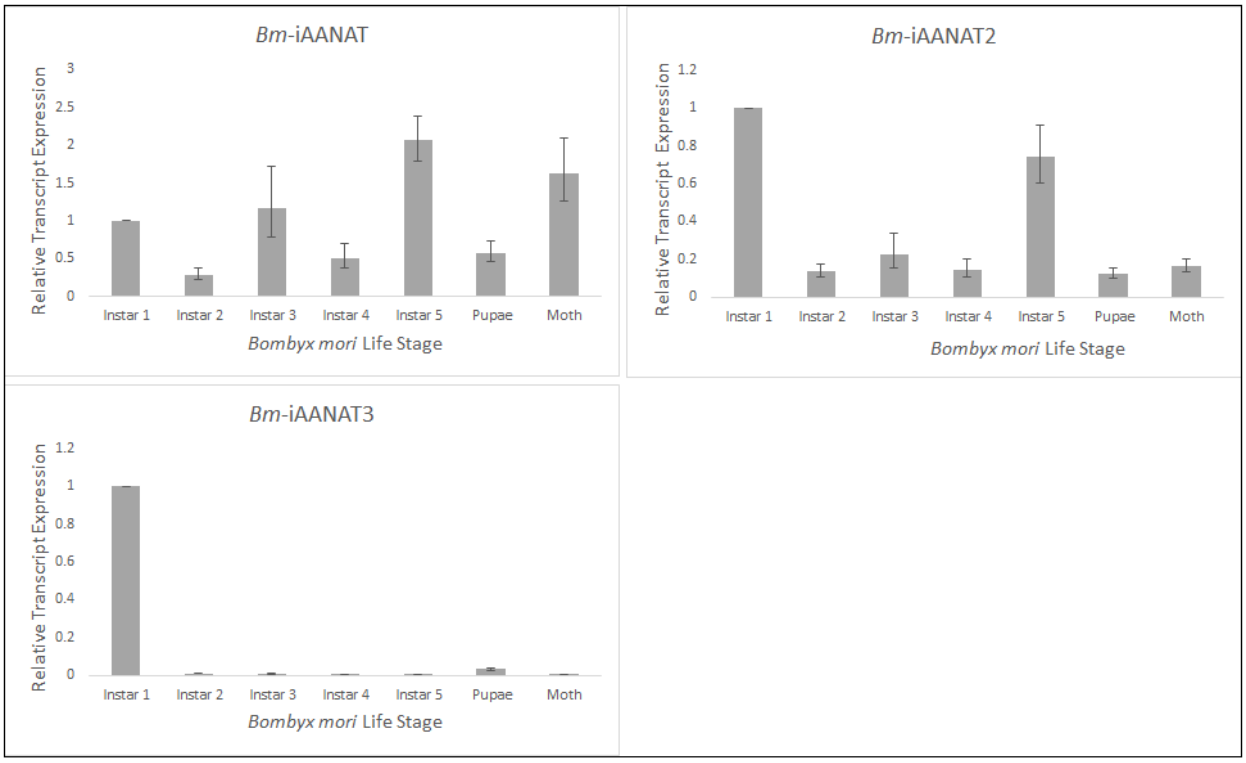

Figure 4.2 Relative transcript abundance of three *Bm*-iAANATs in different silkworm life stages

Looking at the bar graphs above, *Bm*-iAANAT has slight changes in transcript expression as the silkworm grows into each different instar and can be deduced to having a more general purpose to the organism, requiring similar amounts of expression in all life stages. In contrast, *Bm*-iAANAT2 and *Bm*-iAANAT3 transcripts are much more abundant in Bmi1 when compared to any other instar with this effect being more prominent in *Bm*-iAANAT3. This may denote an importance of purpose within the first several days of the insect's life. The explanation for such a higher level of *Bm*-iAANAT3 expression in the first instar may lie within the color of the insects. Silkworms erupt from their eggs a very dark, almost black, color and for this reason are called the "ant". No molting occurs between the ant stage and the first

instar, but the silkworms do seemingly develop a lighter color more rapidly during this time than any other life stage transition. Previous results demonstrate expression of both *Bm*-iAANAT and *Bm*-iAANAT2 are responsible for a lighter pigmentation in the cuticle of *B. mori* [34, 37]. These data infer this also may be the case for *Bm*-iAANAT, especially during the more rapid color transitioning of newly hatched silkworms. Extensive *in vitro* kinetic analysis of enzyme catalysis has been done on *Bm*-iAANAT and *Bm*-iAANAT3 and both are capable of synthesizing *N*-acetyldopamine (NADA). However, it was shown *Bm*-iAANAT3 exclusively accepted shorter chain acyl-CoA substrates and *Bm*-iAANAT much more promiscuous in its acceptance of longer chain CoA thioesters [35, 38]. These data would support a claim that *Bm*-iAANAT3 aids in the formation of NADA for the process of lighter pigmentation, especially in the first days of silkworm life.

4.8.b Novel panel of fatty acid amides quantified for Bombyx mori life stages

Total ion chromatograms (TIC) from all *Bombyx mori* purified extracts were searched for m/z values and retention times corresponding to pure, fatty acid amide standards. Current literature shows an acceptable error range for retention times to be within ± 0.2 minutes from the standard, while all m/z within ± 0.05 of the standard are considered a matching metabolite. For example, the detection of *N*-palmitoyldopamine in the first instar larvae can be seen in Figure 4.3.

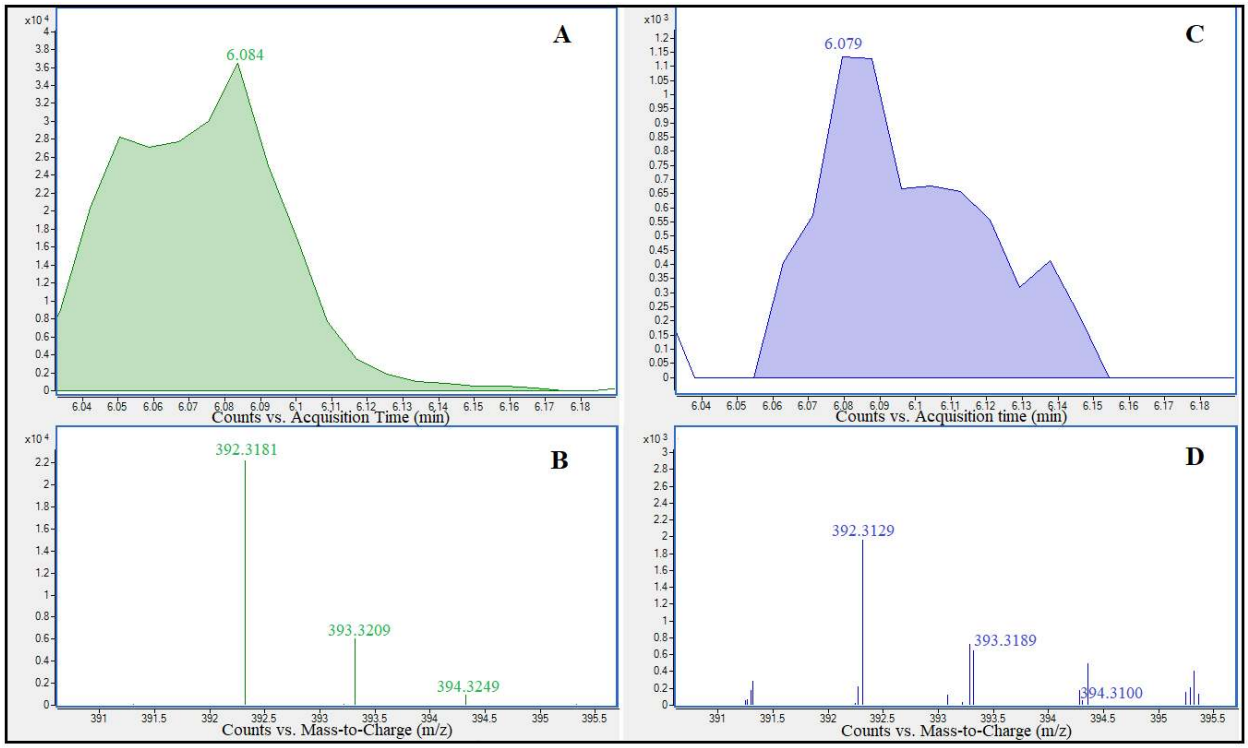

Figure 4.3 Identification of *N*-palmitoyldopamine in *Bombyx mori* first instar larvae by LC-QToF-MS; A.) Extracted ion chromatogram for the N-palmitoyldopamine standard. B.) Mass spectra for *N*-palmitoyldopamine standard. C) Extracted ion chromatogram for *B. mori* first instar larvae extract. D) Mass spectra for *B. mori* first instar larvae extract. The retention and m/z found in the *B. mori* first instar, purified extract closely matches that of the *N*-palmitoyldopamine standard.

Furthermore, all retention times and m/z of fatty acid amides detected in each instar and the pure, standard compounds can be seen in Tables 4.4 through 4.10. Quantification of all detected fatty acid amides was done by first converting integrated area intensity units from the mass spec to pmoles using standard curves generated from pure compounds. These values were then normalized based off the recovery of the internal standards spiked into each solution.

Table 4.4 Comparison of retention times and m/z values of *Bombyx mori* first instar larvae (*Bmi*1) and the pure standards used for detection.

Fatty Acid Amide	m/z		Retention Time (mins)	
	Standard	*Bmi*1	Standard	*Bmi*1
N-Palmitoylglycine	314.2709	314.2675	5.917	5.912
N-Palmitoyldopamine	392.3181	392.3129	6.084	6.079
Palmitamide	256.2593	256.2569	6.184	6.181
N-Oleoylethanolamine	326.3002	326.2992	6.059	6.046
N-Oleoyldopamine	418.3247	418.3194	6.200	6.204
N-Oleoyltryptamine	425.3548	425.3691	6.583	6.577

Table 4.5 Comparison of retention times and m/z values of *Bombyx mori* second instar larvae (*Bmi*2) and the pure standards used for detection.

Fatty Acid Amide	m/z		Retention Time (mins)	
	Standard	*Bmi*2	Standard	*Bmi*2
N-palmitoylglycine	314.2701	314.2667	5.902	5.898
N-Palmitoyldopamine	392.3177	392.3195	6.068	6.105
N-Oleoylglycine	340.2858	340.2844	5.993	5.839

Table 4.6 Comparison of retention times and m/z values of *Bombyx mori* third instar larvae (*Bm*i3) and the pure standards used for detection.

Fatty Acid Amide	m/z		Retention Time (mins)	
	Standard	*Bm*i3	Standard	*Bm*i3
N-Palmitoylglycine	314.2639	314.2601	5.972	5.971
N-Palmitoyldopamine	392.3095	392.3078	6.125	6.129
Palmitoleamide	254.2438	254.2411	5.830	5.830
Palmitamide	256.2593	256.2569	6.184	6.181
N-Oleoylethanolamine	326.3002	326.2992	6.059	6.046
N-Oleoyldopamine	418.3247	418.3194	6.200	6.204
N-Oleoylserotonin	441.3399	441.3142	6.229	6.295
Oleamide	282.2746	282.2715	6.254	6.254
N-Linoleoylglycine	338.2638	338.3091	5.806	5.797
N-Linoleamide	280.2590	280.2547	5.963	6.043

Table 4.7 Comparison of retention times and m/z values of *Bombyx mori* fourth instar larvae (*Bm*i4) and the pure standards used for detection.

Fatty Acid Amide	m/z		Retention Time (mins)	
	Standard	*Bm*i4	Standard	*Bm*i4
Palmitamide	256.2645	256.2631	6.214	6.213
N-Palmitoylserotonin	415.3322	415.2882	6.187	6.125
Palmitoleamide	254.2456	254.2463	5.857	5.859
N-Stearoylserotonin	443.3638	443.3505	6.542	6.576
Oleamide	282.2796	282.2786	6.289	6.277
N-Oleoyldopamine	418.3315	418.3306	6.248	6.246
N-Oleoylethanolamine	326.3057	3.26.3049	6.077	6.074
N-Oleoylglycine	340.2846	340.2847	6.094	5.945
N-Oleoylserotonin	441.3479	441.3483	6.262	6.322
Linoleamide	280.2643	280.2616	5.979	6.027
N-Arachidonoylserotonin	463.3326	463.3337	6.071	6.069

Table 4.8 Comparison of retention times and m/z values of *Bombyx mori* fifth instar larvae (*Bmi*5) and the pure standards used for detection.

Fatty Acid Amide	m/z		Retention Time (min)	
	Standard	*Bmi*5	Standard	*Bmi*5
N-Palmitoylglycine	314.2689	314.2975	5.899	6.001
N-Palmitoyldopamine	392.3163	392.3153	6.065	5.951
Palmitoleamide	254.2482	254.2445	5.757	5.777
N-Oleoylglycine	340.2848	340.3185	5.990	5.918
N-Oleoylethanolamine	326.3063	326.2927	5.982	5.986
N-Oleoyldopamine	418.3316	418.3356	6.140	6.124
Oleamide	282.2794	282.2749	6.173	6.167

Table 4.9 Comparison of retention times and m/z values of *Bombyx mori* pupae and the pure standards used for detection.

Fatty Acid Amide	m/z		Retention Time (mins)	
	Standard	*Bm*-Pupae	Standard	*Bm*-Pupae
N-Palmitoylglycine	314.2681	314.2670	5.926	5.9299
N-Palmitoyldopamine	392.3157	392.3156	6.096	6.093
N-Palmitoylserotonin	415.3318	415.3221	6.125	6.074
N-Oleoyldopamine	418.3303	418.3292	6.167	6.161
N-Oleoyltryptamine	425.3523	425.3339	6.587	6.617
N-Stearoylserotonin	443.3626	443.3415	6.471	6.475

Table 4.10 Comparison of retention times and m/z values of *Bombyx mori* moth and the pure standards used for detection.

Fatty Acid Amide	m/z		Retention Time (mins)	
	Standard	*Bm*-Moth	Standard	*Bm*-Moth
N-Palmitoyldopamine	392.3168	392.3146	6.082	5.966
N-Palmitoylserotonin	415.3333	415.3558	6.115	6.087
N-Oleoylethanolamine	326.3071	326.3058	6.003	5.982
N-Arachidonoylserotonin	463.3299	463.3395	6.174	6.054
Linoleamide	280.2647	280.2633	5.908	5.896

Finally, the pmoles were divided by the mass of starting tissue to give a final unit of pmole/g. Any fatty acid amide characterized/quantified within each instar's extract was placed into Table 4.11.

Table 4.11 Quantification of fatty acid amides from different life stages of *Bombyx mori*

	pmoles/g						
Fatty Acid Amide	Instar 1	Instar 2	Instar 3	Instar 4	Instar 5	Pupae	Moth
PalmGly	2.88 ± 0.92	11.3 ± 2.3	15.3 ± 0.40	N.D.	5.68 ± 1.3	2.08 ± 0.12	3.69 ± 1.5
PalmDop	5.46 ± 0.54	2.77 ± 1.1	N.D.	N.D.	1.12 ± 0.13	0.606 ± 0.29	N.D.
PalmSer	N.D.	N.D.	N.D.	9.85 ± 0.62	N.D.	0.927 ± 0.12	6.04 ± 4.4
Palmle	N.D.	N.D.	6.45 ± 1.2	21.6 ± 13	1.06 ± 0.32	N.D.	N.D.
Palm	N.D.	N.D.	21.8 ± 8.7	27.5 ± 19	N.D.	N.D.	N.D.
OleGly	N.D.	29.7 ± 11	N.D.	N.D.	31.9 ± 25	N.D.	N.D.
OleEth	1.62 ± 0.45	N.D.	2.48 ± 0.68	19.9 ± 15	4.52 ± 1.3	N.D.	0.225 ± 0.13

Table 4.11 Quantification of fatty acid amides from different life stages of *Bombyx mori*

OleDop	1.74 ± 1.0	N.D.	6.96 ± 5.5	5.96 ± 0.29	N.D.	2.97 ± 2.5	N.D.
OleSer	N.D.	N.D.	3.03 ± 0.81	3.51 ± 0.61	N.D.	N.D.	N.D.
OleTrp	1.90 ± 0.24	N.D.	N.D.	N.D.	N.D.	0.431 ± 0.10	N.D.
Ole	N.D.	N.D.	661 ± 135	N.D.	119 ± 93	N.D.	N.D.
AracSer	N.D.	N.D.	N.D.	13.8 ± 2.9	N.D.	N.D.	0.924 ± 0.66
LinGly	N.D.	N.D.	28.2 ± 7.2	N.D.	N.D.	N.D.	N.D.
Lino	N.D.	N.D.	9.23 ± 1.6	22.1 ± 14	N.D.	N.D.	N.D.
SteSer	N.D.	N.D.	N.D.	N.D.	N.D.	0.503 ± 0.10	6.06 ± 2.7

N.D. denotes the fatty acid amide not being detected in that instar using the above identification methods

Due to the wide and varying spread of fatty acid amides detected in the different instars, it is difficult to confidently ascertain if any change in abundance of lipids corresponds to a change in iAANAT abundance of any three of the *B.mori* enzymes. There were no definitive changes of fatty acid amide abundance due to a lower expression of any of the iAANATs. However, this does not conclude fatty acid amides are not biosynthesized by any of these iAANAT's *in vivo*. The concerted effort of different iAANAT within insects would appear to be a very complicated mechanism, which was not resolved by our data. Yet these fatty acid amides have only just begun to be researched in insects, and our main focus for these experiments was on general detection, as no fatty acid amides have yet been detected in any life stage of the silkworm until the emergence of this data. There has yet to be genetic manipulation experiments, like CRISPR, done on these iAANATs in the silkworm and seeing which instar provides the highest abundance of metabolites is useful knowledge for further experimentation on the catalytic capabilities of *Bm*-iAANATs. If a knockdown of a *Bm*-iAANAT were to be completed to check for a change in metabolites, it would appear knocking down iAANAT and extracting the fatty acid amides from the third or fourth instar would yield results with the most information on long chain fatty acid amide biosynthesis. This is because iAANAT has been shown to be more promiscuous in its acceptance

of long chain thioester substrates and the third and fourth instars seemingly have the highest abundance of fatty acid amides.

4.9 Acknowledgements

This work has been supported, in part, by grants from the ShirleyW. and William L. Griffin Foundation and National Institute of General Medical Science of the National Institutes of Health (R15-GM107864) to D.J.M.

4.10 References

[1] Farrell, E. K.; Merkler, D. J., Biosynthesis, degradation and pharmacological importance of the fatty acid amides. *Drug Discovery Today* **2008,** *13* (13), 558-568.

[2] Evans P.H., F. P. M., Enzymatic N-acetylation of indolealkylamines by brain homogenates of the honeybee, *Apis melifera*. *J. Insect Physiol.* **1975,** *21*, 343-353.

[3] Iannotti, F. A.; Di Marzo, V.; Petrosino, S., Endocannabinoids and endocannabinoid-related mediators: Targets, metabolism and role in neurological disorders. *Progress in Lipid Research* **2016,** *62*, 107-128.

[4] Witkamp, R., Fatty acids, endocannabinoids and inflammation. *European Journal of Pharmacology* **2016,** *785*, 96-107.

[5] Tabor H., M. A. H., Stadtman E.R., The enzymatic acetylation of amines. *J. Biol. Chem.* **1953,** *204*, 127-138.

[6] Weissbach H., R. B. G., Axelrod J., The enzymatic acetylation of serotonin and other naturally occurring amines. *Biochem. Biophys.* **1961,** *Acata 54*, 190-192.

[7] Puiroux J., M. R., Gourdoux L., Simultaneous estimation of dopamine, serotonin and related compounds in the brain of Pieris brassicoe pupae: degradation pathways of biogenic amines in insect nervous tissue. *Biogenic Amines* **1992,** *8*, 391-400.

[8] Driscoll, W. J.; Chaturvedi, S.; Mueller, G. P., Oleamide synthesizing activity from rat kidney: identification as cytochrome c. *The Journal of biological chemistry* **2007,** *282* (31), 22353-63.

[9] Waluk, D. P.; Schultz, N.; Hunt, M. C., Identification of glycine N-acyltransferase-like 2 (GLYATL2) as a transferase that produces N-acyl glycines in humans. *The FASEB Journal* **2010,** *24* (8), 2795-2803.

[10] Jeffries, K. A.; Dempsey, D. R.; Farrell, E. K.; Anderson, R. L.; Garbade, G. J.; Gurina, T. S.; Gruhonjic, I.; Gunderson, C. A.; Merkler, D. J., Glycine N-acyltransferase-like 3 is responsible for long-chain N-acylglycine formation in N(18)TG(2) cells. *Journal of Lipid Research* **2016,** *57* (5), 781-790.

[11] Schmid, H. H.; Berdyshev, E. V., Cannabinoid receptor-inactive N-acylethanolamines and other fatty acid amides: metabolism and function. *Prostaglandins, leukotrienes, and essential fatty acids* **2002,** *66* (2-3), 363-76.

[12] Dempsey, D. R.; Jeffries, K. A.; Bond, J. D.; Carpenter, A.-M.; Rodriguez-Ospina, S.; Breydo, L.; Caswell, K. K.; Merkler, D. J., Mechanistic and Structural Analysis of Drosophila melanogaster Arylalkylamine N-Acetyltransferases. *Biochemistry* **2014,** *53* (49), 7777-7793.

[13] Dempsey, D. R.; Jeffries, K. A.; Anderson, R. L.; Carpenter, A.-M.; Ospina, S. R.; Merkler, D. J., Identification of an arylalkylamine N-acyltransferase from Drosophila melanogaster that catalyzes the formation of long-chain N-acylserotonins. *FEBS letters* **2014,** *588* (4), 594-599.

[14] Jeffries, K. A.; Dempsey, D. R.; Behari, A. L.; Anderson, R. L.; Merkler, D. J., Drosophila melanogaster as a model system to study long-chain fatty acid amide metabolism. *FEBS letters* **2014,** *588* (9), 1596-1602.

[15] Dempsey, D. R.; Nichols, D. A.; Battistini, M. R.; Pemberton, O.; Ospina, S. R.; Zhang, X.; Carpenter, A. M.; O'Flynn, B. G.; Leahy, J. W.; Kanwar, A.; Lewandowski, E. M.; Chen, Y.; Merkler, D. J., Structural and Mechanistic Analysis of Drosophila melanogaster Agmatine N-Acetyltransferase, an Enzyme that Catalyzes the Formation of N-Acetylagmatine. *Scientific reports* **2017,** *7* (1), 13432.

[16] Merkler, D. J.; Merkler, K. A.; Stern, W.; Fleming, F. F., Fatty Acid Amide Biosynthesis: A Possible New Role for Peptidylglycine α-Amidating Enzyme and Acyl-Coenzyme A:GlycineN-Acyltransferase. *Archives of Biochemistry and Biophysics* **1996,** *330* (2), 430-434.

[17] Vetting, M. W.; S. de Carvalho, L. P.; Yu, M.; Hegde, S. S.; Magnet, S.; Roderick, S. L.; Blanchard, J. S., Structure and functions of the GNAT superfamily of acetyltransferases. *Archives of Biochemistry and Biophysics* **2005,** *433* (1), 212-226.

[18] Salah Ud-Din, I. A.; Tikhomirova, A.; Roujeinikova, A., Structure and Functional Diversity of GCN5-Related N-Acetyltransferases (GNAT). *International Journal of Molecular Sciences* **2016,** *17* (7).

[19] Zheng, W.; Cole, P. A., Serotonin N-acetyltransferase: mechanism and inhibition. *Current medicinal chemistry* **2002,** *9* (12), 1187-99.

[20] Resh, M. D., Covalent lipid modifications of proteins. *Current biology : CB* **2013,** *23* (10), R431-5.

[21] De Angelis, J.; Gastel, J.; Klein, D. C.; Cole, P. A., Kinetic analysis of the catalytic mechanism of serotonin N-acetyltransferase (EC 2.3.1.87). *The Journal of biological chemistry* **1998,** *273* (5), 3045-50.

[22] Han, Q.; Robinson, H.; Ding, H.; Christensen, B. M.; Li, J., Evolution of insect arylalkylamine N-acetyltransferases: structural evidence from the yellow fever mosquito, Aedes aegypti. *Proceedings of the National Academy of Sciences of the United States of America* **2012,** *109* (29), 11669-74.

[23] O'Flynn, B. G.; Hawley, A. J.; Merkler, D. J., Insect Arylalkylamine N-Acetyltransferases as Potential Targets for Novel Insecticide Design. *Biochemistry & molecular biology journal* **2018,** *4* (1), 4.

[24] O'Flynn, B. G.; Suarez, G.; Hawley, A. J.; Merkler, D. J., Insect Arylalkylamine N-Acyltransferases: Mechanism and Role in Fatty Acid Amide Biosynthesis. *Frontiers in Molecular Biosciences* **2018,** *5* (66).

[25] Coon, S. L.; Mazuruk, K.; Bernard, M.; Roseboom, P. H.; Klein, D. C.; Rodriguez, I. R., The human serotonin N-acetyltransferase (EC 2.3.1.87) gene (AANAT): structure, chromosomal localization, and tissue expression. *Genomics* **1996,** *34* (1), 76-84.

[26] Li, P.; Modica, Justin A.; Howarth, Ashlee J.; Vargas L, E.; Moghadam, Peyman Z.; Snurr, Randall Q.; Mrksich, M.; Hupp, Joseph T.; Farha, Omar K., Toward Design Rules for Enzyme Immobilization in Hierarchical Mesoporous Metal-Organic Frameworks. *Chem* **2016,** *1* (1), 154-169.

[27] Noh, M. Y.; Koo, B.; Kramer, K. J.; Muthukrishnan, S.; Arakane, Y., Arylalkylamine N-acetyltransferase 1 gene (TcAANAT1) is required for cuticle morphology and pigmentation of the adult red flour beetle, Tribolium castaneum. *Insect biochemistry and molecular biology* **2016,** *79*, 119-129.

[28] Hiragaki, S.; Suzuki, T.; Mohamed, A. A.; Takeda, M., Structures and functions of insect arylalkylamine N-acetyltransferase (iaaNAT); a key enzyme for physiological and behavioral switch in arthropods. *Frontiers in physiology* **2015,** *6*, 113.

[29] Andersen, S. O., Insect cuticular sclerotization: a review. *Insect biochemistry and molecular biology* **2010,** *40* (3), 166-78.

[30] Sloley, B. D., Metabolism of monoamines in invertebrates: the relative importance of monoamine oxidase in different phyla. *Neurotoxicology* **2004,** *25* (1-2), 175-83.

[31] Felsenstein, J., CONFIDENCE LIMITS ON PHYLOGENIES: AN APPROACH USING THE BOOTSTRAP. *Evolution; international journal of organic evolution* **1985,** *39* (4), 783-791.

[32] Zuckerkandl E., P. L., Evolutionary divergence and convergence in proteins. *Evolving Genes and Proteins* **1965**, 97-166.

[33] Kumar, S.; Stecher, G.; Tamura, K., MEGA7: Molecular Evolutionary Genetics Analysis Version 7.0 for Bigger Datasets. *Molecular biology and evolution* **2016,** *33* (7), 1870-4.

[34] Tsugehara, T.; Iwai, S.; Fujiwara, Y.; Mita, K.; Takeda, M., Cloning and characterization of insect arylalkylamine N-acetyltransferase from Bombyx mori. *Comparative Biochemistry and Physiology Part B: Biochemistry and Molecular Biology* **2007,** *147* (3), 358-366.

[35] Anderson, R. L.; Battistini, M. R.; Wallis, D. J.; Shoji, C.; O'Flynn, B. G.; Dillashaw, J. E.; Merkler, D. J., Bm-iAANAT and its potential role in fatty acid amide biosynthesis in Bombyx mori. *Prostaglandins, Leukotrienes and Essential Fatty Acids* **2018,** *135*, 10-17.

[36] Hachouf-Gherras, S.; Thérèse Besson, M.; Bosquet, G., Identification and developmental expression of a Bombyx moriα-tubulin gene. *Gene* **1998,** *208* (1), 89-94.

[37] Long, Y.; Li, J.; Zhao, T.; Li, G.; Zhu, Y., A New Arylalkylamine N-Acetyltransferase in Silkworm (Bombyx mori) Affects Integument Pigmentation. *Applied Biochemistry and Biotechnology* **2015,** *175* (7), 3447-3457.

[38] Battistini M. R., O. F. B. G., Shoji C., Suarez G., Galloway L.C., Anderson R.L., Merkler D.J., Bm-iAANAT3: Expression and Characterization of a Novel Arylalkylamine N-acyltransferase from Bombyx mori. *Archives of Biochemistry and Biophysics* **2018 (In Review)**.

APPENDIX A

N-Fatty Acylglycines: Underappreciated endocannabinoid-like fatty acid amides?

Ryan L. Anderson and David J. Merkler. *Journal of Biology and Nature* 2017, 8 (4), 156-165

Abstract

Long-chain *N*-fatty acylglycines, R-CO-NH-CH_2-COOH, are found in mammals and insects and are structurally related to the cell-signaling, lipid-like, *N*-fatty acylethanolamines, R-CO-NH-CH_2-CH_2-OH. Accumulating evidence demonstrates that the *N*-fatty acylglycines have important cellular functions, but much work remains in order to fully appreciate and understand these biomolecules including: (*a*) more work on their functions *in vivo*, (*b*) measuring their concentrations in the cell, (*c)* defining the pathways for the biosynthesis and degradation, and (*d*) understanding the metabolic interconversion(s) between the *N*-fatty acylglycines and other fatty acid amides. Our purpose in reviewing the current state-of-knowledge about the *N*-fatty acylglycines is to stimulate future research about this intriguing family of biomolecules.

Keywords

N-arachidonoylglycine, *N*-oleoylglycine, *N*-palmitoylglycine, *N*-linoleoylglycine, *N*-myrisotylglycine, *N*-fatty acylethanolamine, fatty acid amide hydrolase, oxidative metabolism, metabolic interconversion

1. Long Chain *N*-Fatty Acylglycines are Endocannabinoid-Like Compounds:

Endocannabinoids quickly became a popular focus of research after the discovery of anandamide (*N*-arachidonoylethanolamide) as the endogenous ligand for the cannabinoid receptor-1 (CB_1) [1]. The *N*-acylglycines are a subgroup of the family of *N*-acetyl- and *N*-acylamino acids exhibiting bioactivity in different cell types within a myriad of different organisms. Although there are a multitude of possible *N*-acylamino acids (copious combinations of different acyl chains covalently attached to the □-amino group of different amino acids), this review will focus on the *N*-fatty acylglycines, endocannibinoid-like fatty acid amides consisting of a glycine *N*-conjugated to an acyl chain containing at least 14 carbon atoms, R-$(CH_2)_n$-CO-NH-CH_2-COOH ($n \geq 12$). The acyl group attached to glycine can be saturated, monounsaturated, or polyunsaturated. We include in the commentary a discussion on the metabolism and function of the *N*-fatty acylglycines and a section on the N-myristoylation of proteins. In sum, we demonstrate the *N*-fatty acylglycines are noteworthy, yet understudied endocannabinoid-like fatty acid amides.

2. Biosynthesis of the *N*-Fatty Acylglycines

N-Fatty acylglycines have been isolated from both invertebrates and vertebrates and are, therefore, likely common in eukaryotes [2-6]. Examples include the identification of *N*-myristoylglycine and *N*-palmitoylglycine in human urine [6], *N*-palmitoyglycine, *N*-oleoylglycine, *N*-stearoylglycine, *N*-linoleoylglycine, *N*-arachidonoylglycine, and *N*-docosahexaenoylglycine from the CNS and tissues of the rat [3], and *N*-palmitoyglycine, *N*-oleoylglycine, *N*-stearoylglycine, and *N*-linoleoylglycine from *Drosophila melanogaster* [4, 5]. The pathways proposed for the biosynthesis of the *N*-fatty acylglycines fall broadly into two categories – the glycine-dependent pathway and the glycine-independent pathway (Fig. 1). Within the glycine-dependent pathway, one route to the *N*-fatty acylglycines is the reaction between glycine and a fatty acyl-CoA, catalyzed by a glycine *N*-acyltransferase (GLYAT, also called acyl-CoA:glycine *N*-acyltransferase or glycine-*N*-acylase) [7-9]. Acyl-CoA synthetases catalyze the ATP-dependent formation of the acyl-CoAs from coenzyme A and the corresponding fatty acid. A family of acyl-CoA synthetases have been described, each with a different acyl chain preference [10]. The GLYAT-catalyzed formation of *N*-fatty acylglycines was, at first, controversial because the only GLYATs known at the time of our proposal would not accept long-chain acyl-CoAs as substrates [11,12]. More recent work has identified GLYATs that will accept long-chain acyl-CoAs as substrates [8,13]. In addition, we have shown the RNAi-mediated knockdown of GLYAT-like-3 (GLYATL3) in cultured mouse $N_{18}TG_2$ cells resulted in a reduction in the levels of *N*-palmitoylglycine and *N*-oleoylglycine produced by these cells [9].

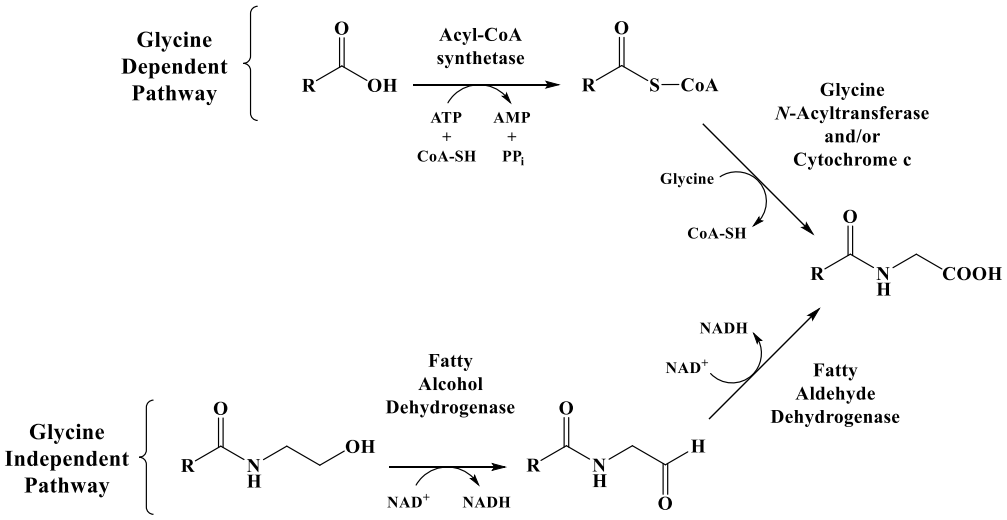

Fig. 1: N-fatty acylglycine biosynthesis. The number in the brackets refers to the appropriate references for the individual reactions.

The GLYAT-catalyzed formation of *N*-fatty acylglycines is not the only chemistry proposed to account for *N*-fatty acylglycine biosynthesis *in vivo*. Mueller and coworkers reported that cytochrome *c* catalyzed the H_2O_2-dependent formation of *N*-fatty acylglycines from the corresponding long-chain acyl-CoA and glycine [14, 15] – a reaction similar to the GLYAT-catalyzed reaction. Mueller and coworkers report further that the cytochrome *c* would accept other long-chain acyl-CoAs and amino acids to potentially yield a diversity of *N*-fatty acylamino acids [14, 16]. A different, but related, reaction to explain *N*-fatty acylglycine production is the direct conjugation of glycine to an inactivated fatty acid [17]. While thermodynamically unfavorable under biological conditions (pH ~ 7.0 and relatively low concentrations of the fatty acids and glycine), there is evidence supporting this chemistry. In fact, there are reports that fatty acid amide hydrolase (FAAH) will catalyze the direct conjugation reaction [18]. Explanations to account for these reports include a low, steady-state level of an acyl-CoA with the fatty acid moiety being supplied by the FAAH (or another hydrolase) catalyzed hydrolysis of a fatty acid amide or the possibility of different activated fatty acid, like a fatty acyl-adenylate, serving as an intermediate in *N*-fatty acylglycine biosynthesis.

The glycine-independent reactions involve a set of oxidation reactions between the *N*-fatty acylglycines and the *N*-fatty acylethanolamines (Fig. 1). *In vitro* studies demonstrate that alcohol dehydrogenase will catalyze the NAD^+-dependent oxidation of the *N*-fatty acylethanolamines to the *N*-fatty acylglycinals [19, 20]. Subsequent conversation of the *N*-fatty acylglycinal to the *N*-fatty acylglycine could occur either by the NAD^+-dependent oxidation as catalyzed by an aldehyde dehydrogenase or aldehyde dismutation as catalyzed by an alcohol dehydrogenase [21]. Studies in cultured cells demonstrate anandamide can serve as a precursor to *N*-arachidonoylglycine [22, 23], providing evidence that this chemistry could take place *in vivo*.

The multiple proposed pathways for the biosynthesis of the *N*-fatty acylglycines are not mutually exclusive. It is possible different organisms and/or tissues utilize different pathways to produce the *N*-fatty acylglycines or that the glycine-dependent pathway is the predominate route to one set of *N*-fatty acylglycines and the glycine-independent pathway is the predominate route to a different set of *N*-fatty acylglycines. Furthermore, it has been shown that both the glycine-dependent and glycine-independent pathways exist in cultured human endometrial HEC-1B cells [24] and in cultured C6 glioma cells where the dual pathways function to produce a constant level of *N*-arachidonoylglycine [23]. Inhibition of the glycine-dependent pathway in the C6 glioma cells did not result in a decrease in *N*-arachidonoylglycine, hinting at an effective "shunting" of *N*-arachidonoylglycine production to the glycine-independent pathway. In contrast to the C6 glioma cells, the glycine-dependent pathway is predominant, and potentially the sole pathway, for the production of the *N*-fatty acylglycines in cultured mouse macrophage RAW 267.4 cells [23] and mouse neuroblastoma $N_{18}TG_2$ cells [9]. Clearly more research is needed to fully understand the biosynthesis of the *N*-fatty acylglycines. The existence of multiple pathways for their biosynthesis and the results from the C6 glioma cells demonstrating a link between the different pathways to maintain cellular levels of *N*-arachidonoylglycine all point towards important function(s) for the *N*-fatty acylglycines *in vivo*.

3. Degradation and Metabolism of the *N*-Fatty Acylglycines

One key reaction in *N*-fatty acylglycine degradation is hydrolysis to the glycine and the fatty acid in a reaction catalyzed by FAAH: $R\text{-}(CH_2)_n\text{-}CO\text{-}NH\text{-}CH_2\text{-}COOH + H_2O \rightarrow R\text{-}(CH_2)_n\text{-}COOH + H_2N\text{-}CH_2\text{-}COOH$ [23]. To the best of our knowledge, *N*-fatty acylglycines have not been evaluated as potential substrates for other hydrolases that might function in *N*-fatty acylglycine degradation, including *N*-acylethanolamine-hydrolyzing acid amidase (NAAA) and ceramidase.

Reactions detailing the metabolic conversion of the *N*-fatty acylglycines to other fatty acid amides have been reported. Oxidative cleavage of the *N*-fatty acylglycines to the primary fatty acid amides in a reaction catalyzed by peptidylglycine □-amidating monooxygenase (PAM) *in vitro* was first described by Merkler *et al*. [7] (Fig. 2). Subsequent work in cultured $N_{18}TG_2$ cells found the inhibition of PAM led to an accumulation of the *N*-fatty acylglycines and a decrease in the primary fatty acid amides, strong support that PAM does have a cellular role in the conversion of the *N*-fatty acylglycines to the primary fatty acid amides [25]. Reduction of expression of GLYATL3 in the $N_{18}TG_2$ cells resulted in a decrease in the cellular levels of the both the *N*-fatty acylglycines and the primary fatty acid amides [9], further evidence that the *N*-fatty acylglycines are metabolic precursors for the primary fatty acid amides. In addition, Farrell *et al*. [26] demonstrated the metabolic flux of *N*-tridecanoylethanolamine, $CH_3\text{-}(CH_2)_{10}\text{-}CO\text{-}CH_2\text{-}CH_2\text{-}OH$, to tridecanamide, $CH_3\text{-}(CH_2)_{10}\text{-}CO\text{-}NH_2$, in $N_{18}TG_2$ and sheep choroid plexus (SCP) cells, data consistent with *N*-tridecanoylglycine serving as an intermediate between the *N*-acylethanolamine and the primary fatty acid amide.

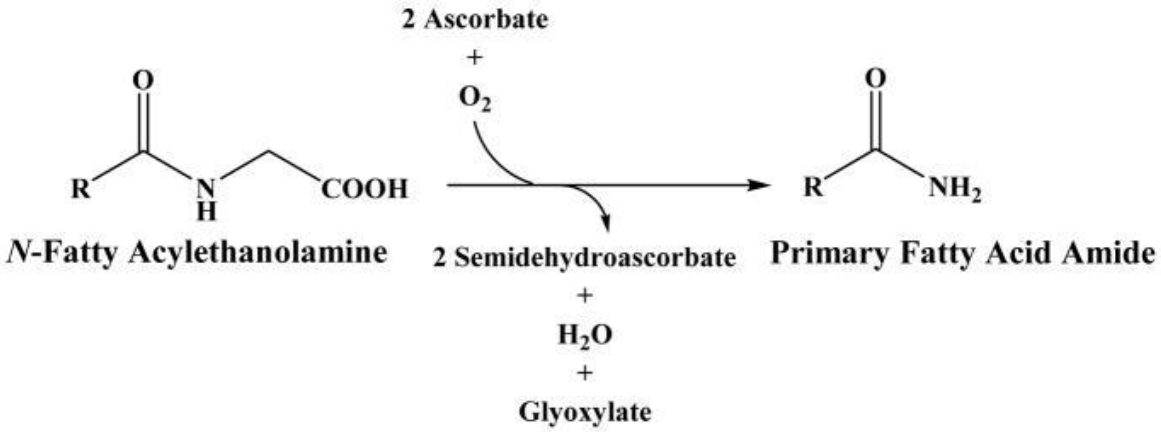

Fig 2: The PAM-mediated Oxidation of N-Fatty Acylglycines to the Primary Fatty Acid Amides.

The fatty acid moiety of *N*-palmitoylglycine and *N*-arachidonoylglycine are enzymatically oxidized, similar to the oxidative modifications of palmitate and arachidonate. *N*-Palmitoylglycine is an excellent substrate for cytochrome P450 BM-3 from *Bacillus megaterium* [27], yielding the □-1, □-2, and □-3 monohydroxylated palmitoyl-derivatives in a reaction that requires NADPH (Fig. 3). There are no other reports of *N*-palmitoylglycine serving as a substrate for a cytochrome P450 from other organisms and no data regarding the biological importance of this chemistry.

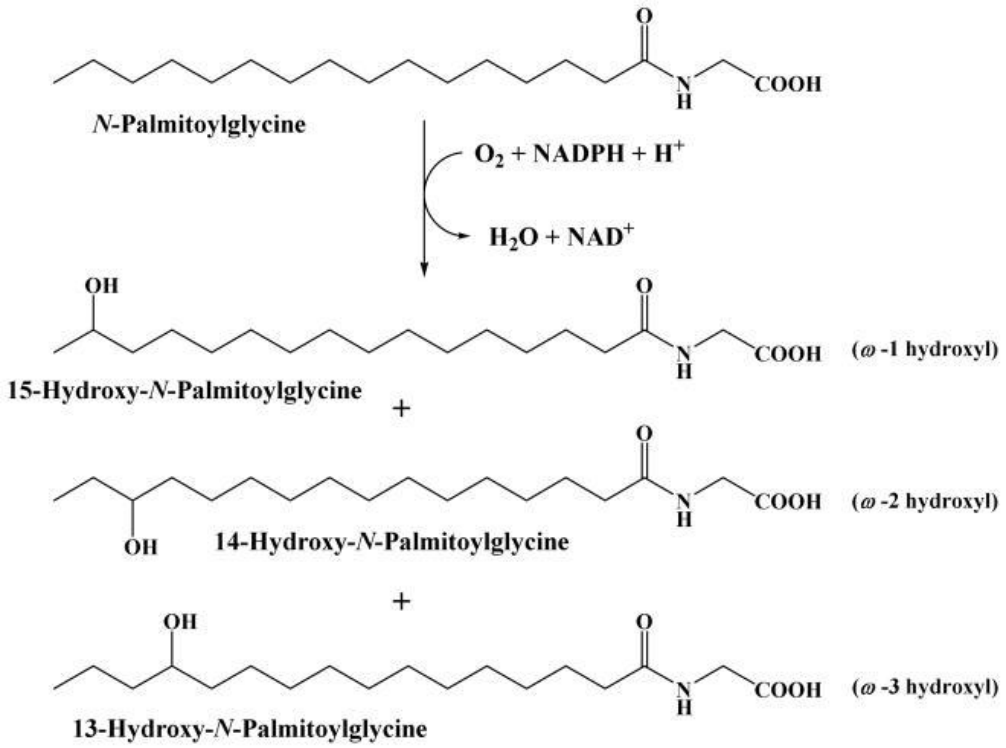

Fig. 3: The Cytochrome P450 BM-3 PAM-mediated Oxidation of N-Palmitoylglycine.

N-Arachidonoylglycine is oxidized by cytochrome P450, lipoxygenase, and cyclooxygenase to yield a number of different hydroxylated and epoxylated products, nicely summarized in a review by Rouzer and Marnet [28] (Fig. 4). With regard to the specific oxygenation of *N*-arachidonoylglycine, little is known about the *in vivo* significance of this chemistry. There is no evidence this chemistry occurs *in vivo* and the biological activity of the products of *N*-arachidonoylglycine oxidation are unknown. As

discussed in reviews by Rouzer and Marnet [28] and Maccarone [29], accumulating evidence shows anandamide and 2-arachidonoylglycerol oxidation does occur *in vivo* and that the oxidation products have biological activities distinct from anandamide and 2-arachidonoylglycerol [30, 31]. Future work on the oxidation of *N*-arachidonoylglycine and *N*-palmitoylglycine and their respective oxidation products are likely to demonstrate the *in vivo* significance of this chemistry.

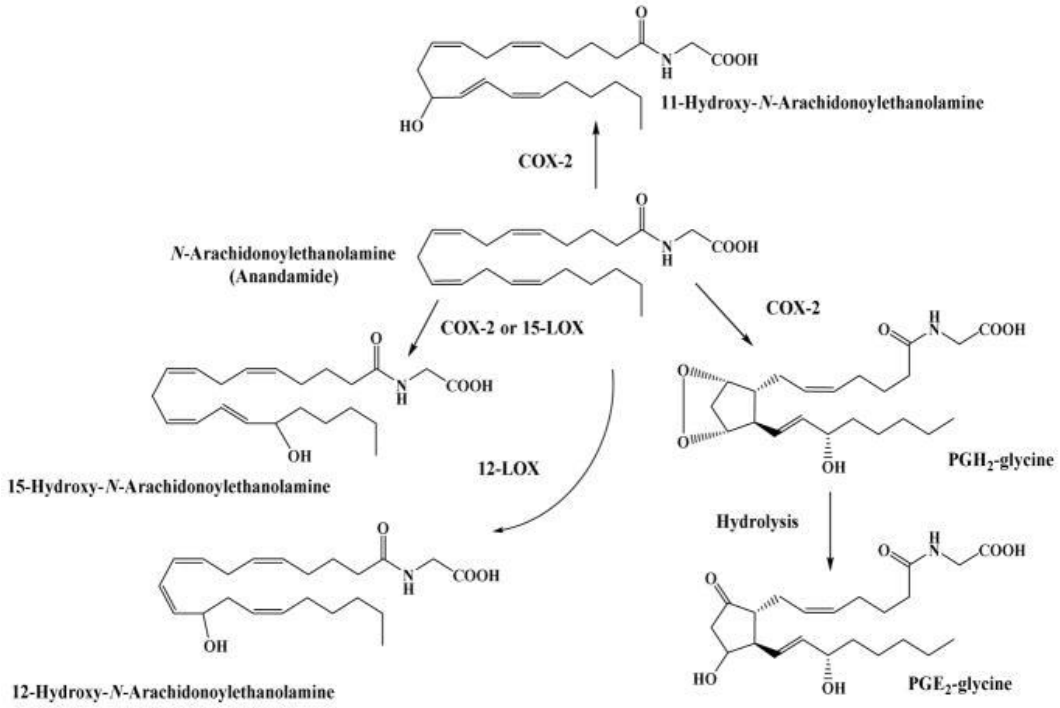

Fig 4: The Oxidative Metabolism of N-Arachidonoylglycine. COX-2 is cyclooxygenase-2, 12-LOX is 12-lipoxygenase, and 15-LOX is 15-lipoxygenase

The cellular concentrations for the N-fatty acylglycines is difficult to estimate from available data. Data from the N18TG2 cells is reported as pmoles N-fatty acylglycine per 107 cells. Assuming a mammalian cell volume of 2 pL [32], the concentration of N-oleoylglycine in the $N_{18}TG_2$ cells is 60 ± 40 μM and that for N-palmitoylglycine is 12 ± 2 μM [9]. Other data on the cellular abundance of the N-fatty acylglycines are reported as pmoles/gram of tissue (or gram of dry weight of tissue) – measurements that are challenging to convert to a cellular concentration in molarity. Assuming the dry weight of a mammalian cell is ~50% of the wet weight and the weight of a mammalian cell is ~3.5 ng [32], the cellular concentration

of N-arachidonoylglycine in the rat spinal cord cells is ~100 nM [2]. The cellular concentrations of the N-fatty acylglycines listed here are estimates, due to the experimental uncertainties in each of the measurements. Most likely, the cellular concentrations of the N-fatty acylglycines are in the high nM to low μM range.

4. Physiological Functions of *N*-Fatty Acylglycines

N-Arachidonoylglycine is the best studied of the *N*-fatty acylglycines due to its structural similarity to anandamide. Cellular functions attributed to ***N***-arachidonoylglycine include anti-inflammatory activity [32], analgesia [33], vasorelaxation [34], modulation of electrical signaling [35], and inhibition of T-channel currents (glycine and calcium) [36, 37]. The activities described for *N*-arachidonoylglycine must result from its binding to a receptor and/or another non-receptor protein.

N-Arachidonoylglycine binds to FAAH [38], the glycine T2 transporter [39, 40], GPR55 [41], GPR92 [42], and the $GABA_A$ [43] receptor with relatively low affinity, K_d values = 1-10 μM. *N*-Arachidonoylglycine is either an inhibitor [2, 38, 44] or a poor substrate [23] for FAAH; its binding to FAAH results in an increase in the cellular concentration of anandamide [45] – the "entourage effect". Some of the activities ascribed to *N*-arachidonoylglycine may result from the increase in the cellular concentration of anandamide. It is difficult to assess the biological significance of the low affinity interactions of *N*-arachidonoylglycine with these proteins since the *in vivo* concentration of *N*-arachidonoylglycine in the CNS is ≤50 nM [2]. *N*-Arachidonoylglycine does not bind to either CB_1 [46] or CB_2 [38], but does bind with relatively high affinity, $K_d \leq 100$ nM, to GPR18 [24, 41], an orphan G-protein coupled receptor. The binding of *N*-arachidonoylglycine to GPR18 is saturable and may be responsible for much of the bioactivity of *N*-arachidonoylglycine [24, 47, 48]. However, the binding of *N*-arachidonoylglycine to GPR18 is controversial because there are reports that *N*-arachidonoylglycine is not a ligand for GPR18 [49]. Less has been reported about potential biological functions of the other known *N*-fatty acylglycines relative to *N*-arachidonoylglycine. *N*-Oleoylglycine is an inhibitor of the glycine T2 transporter (K_d = 0.5-1.0 μM) [40] and paraoxonase ($K_d \approx$ 1.0 μM) [50], is a weak agonist for the PPAR-α

receptor [51], and has activities that overlap with oleamide: regulating body temperature and locomotion [52]. In fact, Chaturvedi *et al*. [52] report *N*-oleoylglycine and oleamide are equipotent in decreasing body temperature and locomotion in rats. *N*-Oleoylglycine is more potent than *N*-arachidonoylglycine as an inhibitor of the glycine T2 transporter by a factor of 5-10, based on the ratio of their estimated K_d values. The activities of *N*-oleoylglycine may result from its binding to the CB_1 receptor [53, 54]; however, there are no reports for the K_d value for the binding of *N*-oleoylglycine to CB_1. As detailed by Bradshaw *et al*. [3], *N*-palmitoylglycine may have a role in sensory neuronal signaling, resulting, perhaps, from its binding to the TRPC5 receptor [55]. *N*-Linoleoylglycine is reported to exhibit anti-inflammatory activity using the mouse peritonitis assay [56].

Also, the *N*-fatty acylglycines may prove useful as health-related biomarkers. Elevated biofluid levels of short chain *N*-acylglycines are indicators of inborn errors of metabolism [57, 58]. Examples include elevated levels of *N*-palmitoylglycine and *N*-myristoylglycine identified in the urine of women suffering from primary dysmenorrhea [6].

Protein Myristoylation

Our discussion has focused on the *N*-fatty acylglycines as individual molecules, rather than as a component of a larger biomolecule like an acylated protein. N-Myristoyltransferase (NMT) catalyzes the myristoyl-CoA-dependent myristoylation of an N-terminal glycine, an important co- or post-translational modification found in a number of proteins [59]. Glycine is not a substrate for NMT; thus, NMT cannot catalyze the production of *N*-myristoylglycine [60]. However, an enzyme, IpaJ from *Shigella flexneri* [61], has been identified that will release *N*-myristoylglycine from a myristoylated protein. Because of the potential to generate *N*-myristoylglycine from proteins myristoylated at the N-terminus, we have included a brief section on protein myristoylation. Myristoylation at the N-terminus serves to anchor the protein to the cell membrane and, also, regulates protein function, protein-protein interactions, protein stability, and cell metabolism [59]. Palmitoylation of an N-terminal glycine has been reported [62] and such palmitoylated proteins might provide a source for *N*-palmitoylglycine. The significance of N-terminal

palmitoylation is unclear because this modification may be an artifact resulting from intramolecular *S*- to *N*-transfer during sample preparation [63]. *S*-Palmitoylation at a Cys residue is a well characterized post-translation modifcation [59,64].

5. Conclusions

Much work remains to fully appreciate the biological significance of the *N*-fatty acylglycines; the work certainly suggests these are an important family of molecules. In moving forward, it is crucial to define the cellular concentrations of the *N*-fatty acylglycines to provide context for their reported activities. The design, synthesis, and implementation of reactive analogs of the *N*-fatty acylglycines as activity-based profiling probes, similar to the approach of Niphakis *et al*. [65] using analogs of the *N*-acylethanolamines, could prove especially useful in future studies to define receptors and other proteins that bind individual *N*-fatty acylglycines.

One final comment that relates to the metabolic conversions discussed herein. The conversion of the *N*-fatty acylethanolamines to the *N*-fatty acylglycines and then the *N*-fatty acylglycines to the primary fatty acid amides points towards a potential regulatory mechanism. If each of the metabolically linked fatty acid amides has a different function, then the reactions shown in Figs. 2, 3, and 4 are not just reactions in a biosynthetic pathway, but also serve to alter the function of a specific *N*-fatty acylated amine.

Acknowledgements

This work has been supported, in part, by grants from the University of South Florida (a Creative Scholarship grant), the Eppley Foundation for Research, the Shirley W. and William L. Griffin Charitable Foundation, the National Institute of Drug Abuse at the National Institutes of Health (R03-DA034323) and the National Institute of General Medical Science of the National Institutes of Health (R15-GM107864) to D.J.M.

Competing Interests

The authors declare no competing interests.

Authors' Contributions

R. L. A. and D. J. M. contributed equally to the writing and creation of this work.

References

1. Devane, W.A., Hanŭs, L., Breuer, A., Pertwee, R.G., Stevenson, L.A., Griffin, G., Gibson, D., Mandelbaum, A., Etinger, A., and Mechoulam, R. (1992) Isolation and structure of a brain constituent that binds to the cannabinoid receptor. *Science* **258**, 1946-1949.

2. Huang, S.M., Bisogno, T., Petros, T.J., Chang, S.Y., Zavitsanos, P.A., Zipkin, R.E., Sivakumar, R., Coop, A., Maeda, D.Y., De Petrocellis, L., Burstein, S., Di Marzo, V., and Walker, J.M. (2001) Identification of a new class of molecules, the arachidonyl amino acids, and characterization of one member that inhibits pain. *J. Biol. Chem.* **276**, 42639-42644.

3. Bradshaw, H.B., Rimmerman, N., Hu, S. S.-J., Burstein, S., and Walker, J.M. (2009) Novel endogenous *N*-acyl glycines identification and characterization. *Vitam. Horm.* **81**, 191-205.

4. Tortoriello, G., Rhodes, B.P., Takacs, S.M., Stuart J. M., Basnet, A., Raboune, S., Widlanski, T.S., Doherty P., Harkany T., and Bradshaw, H. (2013) Targeted lipidomics in *Drosophila melanogaster* identified novel 2-monoacylglycerols and *N*-acyl amides. *PLoS One* **8**:e67865.

5. Jeffries, K.A., Dempsey, D.R., Behari, A.L., Anderson, R.L., and Merkler, D.J. (2014) *Drosophila melanogaster* as a model system to study long-chain fatty acid amide metabolism. *FEBS Lett.* **588**, 1596-1602.

6. Lui, P., Duan, J., Wang, P., Qian, D., Guo, J., Shang, E., Su, S., Tang, Y., and Tang, Z. (2013) Biomarkers of primary dysmenorrhea and herbal formula intervention: an exploratory metabonomics study of blood plasma and urine. *Mol. BioSyst*. **9**, 77-87.

7. Merkler, D.J., Merkler, K.A., Stern, W., and Fleming, F.F. (1996) Fatty acid amide biosynthesis: a possible new role for peptidylglycine □-amidating enzyme and acyl-coenzyme A:glycine *N*-acyltransferase. *Arch. Biochem. Biophys*. **330**, 430-434.

8. Waluk, D.P., Schultz, N., and Hunt, M.C. (2010) Identification of glycine *N*-acyltransferase-like 2 (GLYATL2) as a transferase that produces *N*-acylglycines in humans. *FASEB J*. **24**, 2795-2803.

9. Jeffries, K.A., Dempsey, D.R., Farrell, E.K., Anderson, R.L., Garbade, G.J., Gurina, T.S., Gruhonjic, I., Gunderson, C.A., and Merkler, D.J. (2016) Glycine *N*-acyltransferase-like 3 is responsible for long-

chain *N*-acylglycine formation in $N_{18}TG_2$ cells. *J. Lipid Res*. **57**, 781-790.

10. Watkins, P.A., Maiguel, D., Jia, Z., and Pevsner, J. (2007) Evidence for 26 distinct acyl-coenzyme A synthetase genes in the human genome. *J. Lipid Res*. **48**, 2736-2750.

11. Schachter, D., and Taggart, J. V. (1954) Glycine *N*-acylase – purification and properties. *J. Biol. Chem*. **208**, 263-275.

12. Kelly, M., and Vessey, D. A. (1993) Isolation and characterization of mitochondrial acyl-CoA: glycine *N*-acyltransferases from kidney. *J. Biochem. Toxicol*. **8**, 63-69.

13. Dempsey, D.R., Jeffries, K.A., Anderson, R.L., Carpenter, A.-M., Rodriquez Ospina, S., and Merkler, D. J. (2014) Identification of an arylalkylamine N-acyltransferase from *Drosophila melanogaster* that catalyzes the formation of long-chain N-acylserotonins. *FEBS Lett*. **588**, 594-599.

14. Mueller, G.P., and Driscoll, W.J. (2007) *In vitro* synthesis of oleoylglycine by cytochrome *c* points to a novel pathway for the production of lipid signaling molecules. *J. Biol. Chem*. **282**, 22364-22369.

15. McCue, J.M., Driscoll, W.J., and Mueller, G.P. (2008) Cytochrome *c* catalyzes the *in vitro* synthesis of arachidonoyl glycine. Biochem. Biophys. Res. Commun. **365**, 322-327.

16. McCue, J.M., Driscoll, W.J., and Mueller, G.P. (2009) *In vitro* synthesis of arachidonoyl amino acids by cytochrome *c*. *Prostaglandins. Other Lipid Mediat*. **90**, 42-48.

17. Bachur, N.R., and Udenfriend, S. (1966) Microsomal synthesis of fatty acid amides, *J. Biol. Chem*. **241**, 1308-1313.

18. Arreaza, G., Devane, W.A., Omeir, R.L., Sajnani, G., Kunz, J., Cravatt, B.F., and Deutsch, D.G. (1997) The cloned rat hydrolytic enzyme responsible for the breakdown of anandamide also catalyzes it formation via the condensation of arachidonic acid and ethanolamine. *Neurosci. Lett*. **234** (1997) 59-62.

19. Aneetha, H., O'Dell, D.K., Tan, B., Walker, J. M., and Hurley, T. D (2009) Alcohol dehydrogenase-catalyzed in vitro oxidation of anandamide to *N*-arachidonoyl glycine, a lipid mediator: Synthesis of *N*-acyl glycinals. *Bioorg. Med. Chem. Lett*. **19**, 237-241.

20. Ivkovic, M., Dempsey, D.R., Handa, S., Hilton, J.H., Lowe, E.W. Jr., and Merkler, D.J. (2011) *N*-Acylethanolamines as novel alcohol dehydrogenase 3 substrates. *Arch. Biochem. Biophys*. **506**, 157-164.

21. Henehan, G.T.M., and Oppenheimer, N. J. (1993) Horse liver alcohol dehydrogenase-catalyzed oxidation of aldehydes: dismutation precedes net production of reduced nicotinamide adenine dinucleotide. *Biochemistry* **32**, 735–738.

22. Burstein, S.H., Rossetti, R.G., Yagen, B., and Zurier, R.B. (2000) Oxidative metabolism of anandamide. *Prostaglandins. Other Lipid Mediat*. **61**, 29-41.

23. Bradshaw, H.B., Rimmerman, N., Hu, S.S.-J., Benton, V.M., Stuart, J.M., Masuda, K. Cravatt, B.F., O'Dell, D.K., and Walker, J.M. (2009) The endocannabinoid anandamide is a precursor for the signaling lipid *N*-arachidonoyl glycine by two distinct pathways. *BMC Biochem.* 10:14.

24. McHugh, D., Page, J., Dunn, E., and Bradshaw, H.B. (2012) Δ^9-Tetrahydrocannabinol and *N*-arachidonoyl glycine are full agonist at GPR18 receptors and induce migration in human endometrial HEC-1B cells. *Br. J. Pharmacol*. **165**, 2414-2424.

25. Merkler, D.J., Chew, G.H., Gee, A.J., Merkler, K.A., Sorondo, J.-P.O., and Johnson, M.E. (2004) Oleic acid derived metabolites in mouse neuroblastoma cells. *Biochemistry* **43**, 12667-12674.

26. Farrell, E.K., Chen, Y., Barazanji, M., Jeffries, K.A., Cameroamortegui, F., and Merkler, D.J. (2012) Primary fatty acid amide metabolism: conversion of fatty acids and an ethanolamine in $N_{18}TG_2$ and SCP cells. *J. Lipid Res*. **53**, 247-256.

27. Haines, D.C., Tomchick, D.R., Machius, M., and Peterson, J.A. (2001) Pivotal role of water in the mechanism of P450BM-3. *Biochemistry* **40**, 13456-13465.

28. Rouzer, C.A., and Marnett, L.J. (2011) Endocannabinoid oxygen by cyclooxygenases, lipoxygenases, and cytochromes P450: cross-talk between the eicosanoid and endocannabinoid signaling pathways. *Chem. Rev*. **111**, 5899-5921.

29. Maccarrone, M. (2017) Metabolism of the endocannabinoid anandamide: open questions after 25 years. *Front. Mol. Neurosci*. **10**:166.

30. Hermanson, D.J., Gamble-George, J.C., Marnett, L.J., and Patel, S. (2014) Substrate-selective COX-2 inhibition as a novel strategy for therapeutic endocannabinoid augmentation. *Trends Pharmacol. Sci*. **35**, 358-367.

31. Urquhart, P., Nicolaou, A., and Woodward, D.F. (2015) Endocannabinoids and their oxygenation by cyclo-oxygenases, liopoxygenases and other oxygenases. *Biochim. Biophys. Acta* **1851**, 366-376.

32. Burstein, S.H., McQuain, C.A., Ross, A.H., Salmonsen, R.A., and Zurier, R.E. (2011) Resolution of inflammation by *N*-arachidonoylglycine. *J. Cell. Biochem*. **112**, 3227-3233.

33. Succar, R., Mitchell, V.A., and Vaughan, C.W. (2007) Actions of N-arachidonyl-glycine in a rat inflammatory pain model. *Mol. Pain* **3**:24.

34. Al Suleimani, Y.M., and Al Mahruqi, A.S. (2017) The endogenous lipid N-arachidonoyl glycine is hypotensive and nitric oxide-cGMP-dependent vasorelaxant. *Eur. J. Pharmacol*. **794**, 209-215.

35. Bondarenko, A.I., Drachuk, K., Panasiuk, O., Sagach, V., Deak, A.T., Malli, R., and Graier, W.F. (2013) N-arachidonoyl glycine suppresses Na^+/Ca^{2+} exchanger-mediated Ca^{2+} entry into endothelial cells and activated BK_{Ca} channels independently of GPCRs. *Br. J. Pharmacol*. **169**, 933-948.

36. Jeong, H.-J., Vandenberg, R.J., and Vaughan, C.W. (2010) N-arachidonyl-glycine modulates synaptic transmission in superficial dorsal horn. *Br. J. Pharmacol*. **161**, 925-935.

37. Chemin, J., Cazade, M., and Lory, P. (2014) Modulation of T-type calcium channels by bioactive lipids. *Pflugers Arch*. **466**, 689-700.

38. Cascio, M.G., Minassi, A., Ligresti, A., Appendino, G., Burstein, S., and Di Marzo, V. (2004) A structure-activity relationship on *N*-arachidonoyl-amino acids as possible endogenous inhibitors of fatty acid amide hydrolase. *Biochem. Biophys. Res. Commun*. **314**, 192-196.

39. Wiles, A.L., Pearlman, R.-J., Rosvall, M., Aubrey, K.R., and Vandenberg, R.J. (2006) N-Arachidonyl-glycine inhibits the glycine transporter, GLYT2. *J. Neurochem*. **99**, 781-786.

40. Mostyn, S.N., Carland, J.E., Shimmon, S., Ryan, R.M., Rawling, T. and Vandenberg, R.J. (2017) *ACS Chem. Neurosci*. **8**, 1949-1959.

41. Console-Bram, L., Ciuciu, S.M., Zhao, P., Zipkin, R.E., Brailoiu, E., and Abood, M.E. (2017) *N*-Arachidonoylglycine, another endogenous agonist of GPR 55. *Biochem. Biophys. Res. Commun*. **490**, 1389-1393.

42. Oh, D.Y., Yoon, J.M., Moon, M.J., Hwang, J.-I., Choe, H., Lee, J.Y., Kim J.I., Kim, S., Rhim, H., O'Dell, D.K., Walker, J.M., Na. H.S., Lee, M.G., Kwon, H.B., Kim, K., and Seong, J.Y. (2008) Identification of faresyl pyrophosphate and *N*-arachidonoylglycine as endogenous ligands for GPR92. *J. Biol. Chem*. **283**, 21054-21064.

43. Baur, R., Gertsch, J., and Sigel, E. (2013) Do N-arachidonoyl-glycine (NA-glycine) and 2-arachidonoylglycerol (2-AG) share mode of action and the binding site on □$_2$ subunit of $GABA_A$ receptors? *PeerJ* **1**:e149.

44. Ghafouri, Z., Tiger, G., Razdan, R.K., Mahadevan, A., Pertwee, R.G., Martin, B.R., and Fowler, C.J. (2004) Inhibition of monoacylglycerol lipase and fatty acid amide hydrolase by analogues of 2-arachidonoylglycerol. *Br. J. Pharmacol*. **143**, 774-784.

45. Burstein, S.H., Huang, S.M., Petros, T.J., Rossetti, R.G., Walker, J.M., and Zurier, R.B. (2002) Regulation of anandamide tissue levels by *N*-arachidonylglycine. *Biochem. Pharmacol*. **64**, 1147-1150

46. Sheskin, T., Hanuš, L., Slager, J., Vogel, Z., and Mechoulam, R. (1997) Structural requirements for binding of anandamide-type compounds to the brain cannabinoid receptor. *J. Med. Chem*. **40**, 659-667.

47. Kohno, M., Hasegawa, Inoue, A., Muraoka, M., Miyazaki, T., Oka, K., and Yasukawa, M. (2006) Identification of *N*-arachidonoylglycine as the endogenous ligand for orphan G-protein-coupled receptor GPR18. *Biochem. Biophys. Res. Commun*. **347**, 827-832.

48. Console-Bram. L., Brailoiu, E., Brailoiu, G.C., Sharir, H., and Abood, M.E. (2014) Activation of GPR18 by cannbinoid compounds: a tale of biased agonism. *Br. J. Pharmacol*. **171**, 3908-3917.

49. Hanuš, L., Shohami, E., Bab, I., and Mechoulam, R. (2014) *N*-Acyl amino acids and their impact on biological processes. Biofactors **40**, 381-388.

50. Nguyen, S.D., and Sok, D.-E. (2004) Preferential inhibition of paraoxonase activity of human paraoxonase 1 by negatively charged lipids. *J. Lipid Res*. **45**, 2211-2220.

51. Takao, K., Noguchi, K., Hashimoto, Y., Shirahata, A., and Sugita, Y. (2015) Synthesis and evaluation of fatty acid amides on the *N*-oleoylethanolamide-like activation of peroxisome proliferator activated receptor □. *Chem. Pharm. Bull. (Tokyo)* **63**, 278-285.

52. Chaturvedi, S., Driscoll, W.J., Elliot, B.M., Faraday, M.M., Grunberg, N.E., and Mueller, G. P. (2006) *In vivo* evidence that *N*-oleoylglycine acts independently of its conversion to oleamide. *Prostaglandins Other Lipid Mediat.* **81**, 136-49.

53. Wang, S., Xu, Q., Shu, G., Wang, L., Gao, P., Xi, Q., Zhang, Y., Jiang, Q., and Zhu, X. (2015) N-Oleoyl glycine, a lipoamino acid, stimulates adipogenesis associated with activation of CB1 receptor and Akt signaling pathway in 3T3-L1. *Biochem. Biophys. Res. Commun*. **466**, 438-443.

54. Wu, J., Zhu, C., Yang, L., Wang, Z., Wang, L., Wang, S., Gao, P., Zhang, Z., Jiang, Q., Zhu, X., and Shu, G. (2017) *J. Agric. Food Chem*. **65**,1051-1057.

55. Bradshaw, H.B., Raboune, S., and Hollis, J.L. (2013) Opportunistic activation of TRP receptors by endogenous lipids: exploiting lipidomics to understand TRP receptor cellular communcation. *Life Sci*. **92**, 404-409.

56. Burstein, S., McQuain, C., Salmonsen, R.A., and Seicol, B. (2012) N-amino acid linoleoyl conjugates: anti-inflammatory activities. *Bioorg. Med. Chem. Lett*. **22**, 872-875.

57. Bonafé, L., Troxler, H., Kuster, T., Heizmann, C.W., Chamoles, N.A., Burlina, A.B., and Blau, N. (2000) Evaluation of urinary acylglycines by electrospray tandem mass spectrometry in mitochondrial energy metabolism defects and organic acidurias. *Mol. Genet. Metab*. **69**, 302-311.

58. Stanislaus, A., Guo, K., and Li, L. (2012) Development of an isotope labeling ultra-high performance liquid chromatography mass spectrometric method for quantification of acylglycines in human urine. *Anal. Chim. Acta* **750**, 161-172.

59. Resh, M.D. (2016) Fatty acylation of proteins: the long and short of it. *Prog. Lipid Res*. **63**, 120-131.

60. Raju, R.V.S., Datla, R.S.S., Warringto, R.C., and Sharma, R.J. (1998) Effects of L-histidine and its structural analogues on human *N*-myristoyltransferase activity and importance of EEVEH amino acid sequence for enzyme activity. *Biochemistry* **37**, 14928-14936.

61. Burnaevskiy, N., Fox, T.G., Plymire, D.A., Ertelt, J.M., Weigele, B.A., Selyunin, A.S., Way, S.S., Patrie, S.M., and Alto, N.M. (2013) Proteolytic elimination of *N*-myristoyl modifications by the Shigella virulence factor IpaJ. *Nature* **496**, 106-109.

62. Kleuss, C., and Krause, E. (2003) Gas is palmitoylatied at the N-terminal glycine. *EMBO J*. **22**, 826-832.

63. Ji, Y., Bachschmid, M.M., Costello, C.E., and Lin, C. (2016) *S*- to *N*-Palmitoyl transfer during proteomic sample preparation. *J. Am. Soc. Mass Spectrom*. **27**, 677-685.

64. Blaskovic, S., Blanc, M., and van der Goot, F.G. (2013) What does S-palmitoylation do to membrane proteins. *FEBS J*. **280**, 2766-2774.

65. Niphakis, M.J., Lum, K.M., Congetta, A.B. III, Correia, B.E., Ichu, T.-A., Olucha, J., Brown, S.J., Kundu, S., Piscitelli, F., Rosen, H., and Cravatt, B.F. (2015) A global map of lipid-binding proteins and their ligandability in cells. *Cell* **161**, 1668-1680.

APPENDIX B

Bm-iAANAT and its Potential Role in Fatty Acid Amide Biosynthesis in *Bombyx mori*

Ryan L. Anderson, Matthew R. Battistini, Dylan J. Wallis, Christopher Shoji, Brian G. O'Flynn, John E. Dillashaw, and David J. Merkler*

Prostaglandins Leukotrienes and Essential Fatty Acids. 2018. 135; 10-17

Summary

Herein, we detail the successful expression, purification, and characterization of an arylalkylamine *N*-acyltransferase from *Bombyx mori* (*Bm*-iAANAT) in *E. coli*. Our *in vitro* determination of substrate specificity for *Bm*-iAANAT demonstrates that this enzyme will accept long-chain fatty acyl-CoA thioesters as substrates leading to the formation of long chain *N*-acylarylalkylamides. In addition, we show that *Bm*-iAANAT is, most likely, responsible for the *in vivo* biosynthesis of such metabolites in *B. mori* due to the detection of the *Bm*-iAANAT transcripts along with the identification and quantification of several long chain *N*-acylarylalkylamides and other long chain fatty acid amides in *B. mori*.

Abstract

The purpose of this research is to unravel the substrate specificity and kinetic properties of an insect arylalkylamine *N*-acyltransferase from *Bombyx mori* (*Bm*-iAANAT) and to determine if this enzyme will catalyze the formation of long chain *N*-acylarylalkylamides *in vitro*. However, the determination of substrates and products for *Bm*-iAANAT *in vitro* is no guarantee that these same molecules are substrates and products for the enzyme in the organism. Therefore, RT-PCR was performed to detect the *Bm*-iAANAT transcripts and liquid chromatography quadrupole time-of-flight mass spectrometry (LC-QToF-MS) analysis was performed on purified lipid extracts from *B. mori* larvae (fourth instar, Bmi4) to determine if long chain fatty acid amides are produced in *B. mori*. Ultimately, we found that recombinant *Bm*-iAANAT will utilize long-chain acyl-CoA thioesters as substrates and identified *B*m-iAANAT transcripts and long-chain fatty acid amides in Bmi4. Together, these data show *Bm*-iAANAT will catalyze the formation of long-chain *N*-acylarylalkylamides *in vitro* and provide evidence *Bm*-iAANAT has a role in fatty acid amide biosynthesis in *B. mori*, as well.

Keywords

Arylalkylamine *N*-acyltransferase

Dopamine

Fatty acid amide biosynthesis

Serotonin

1. Introduction

Fatty acid amides are a family of structurally related lipids, R-CO-NH-R' (the acyl moiety, R-CO-, is derived from a fatty acid and the R'-NH- moiety is derived from an amine), found in both vertebrates and invertebrates [1], [2], [3]. The existence of the *N*-acylamide bond in biology traces back to the identification of hippurate (*N*-benzoylglycine) as a metabolite derived from benzoate in the early 1840s [4], [5] and the fatty acid amide bond traces back to the 1870s to the work of Thudicum on sphingomyelin and other brain ceramides [6]. The best understood member of the fatty acid amide family is *N*-arachidonoylethanolamine (anandamide), the endogenous ligand to the mammalian cannabinoid receptor, CB_1[7], [8]. Based on our knowledge about anandamide [9], [10], it is generally thought the fatty acid amides are neuroactive [2], [11]. This is consistent with the discovery of oleamide, a sleep-inducing lipid amide, and the existence of a family of long-chain *N*-acylethanolamines in the mammalian brain [12], [13], [14]. Fatty acid amides are found in invertebrates, as well [15], [16], [17], [18], [19], [20], but likely serve different functions in these organisms relative to mammals. For example, *Drosophila* melanogaster do produce fatty acid amides [17], [18], [19], but do not express the cannabinoid receptors [21].

Much remains unknown about the fatty acid amides: many have no clearly defined physiological function, details regarding their metabolism remain elusive (biosynthesis, degradation, and cellular transport), and the receptor(s) targeted by most are unidentified [1], [2], [3], [22]. One focus of our research has been on the identification and characterization of enzymes involved in fatty acid amide biosynthesis and melding *in vitro* substrate specificity data with metabolomicdata [23], [24]. We have proposed *N*-acyltransferases operate in fatty acid amide biosynthesis: acyl-CoA + amine → *N*-acylamide + CoA-SH (Fig. 1) [25]. Such *N*-acyltransferases are likely members of the GCN5-related superfamily of *N*-acetyltransferases (GNATs) [26], [27], which would accept long-chain acyl-

CoA thioesters as substrates. Examples of GNAT enzymes utilizing long-chain acyl-CoA thioesters as substrates include *N*-myristoyl transferase [28], glycine*N*-acyltransferase-like 2 [29], and arylalkylamine *N*-acyltransferase-like 2 (AANATL2) [23].

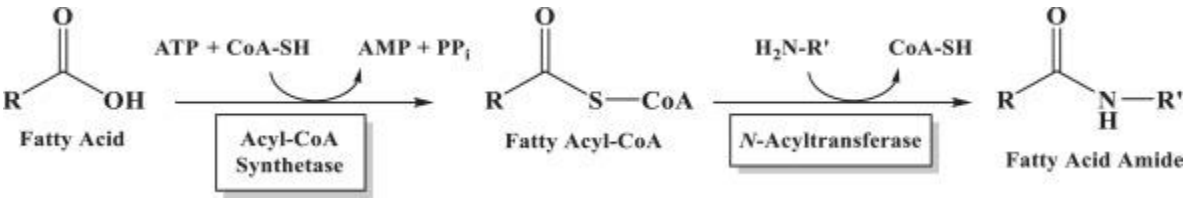

Fig. 1. Proposed Role of *N*-Acyltransferases in Fatty Acid Amide Biosynthesis.

We have employed *Drosophila melanogaster* and mouse neuroblastoma$N_{18}TG_2$ cells in our previous work on the fatty acid amides. Each of these produce fatty acid amides [1], [16], [17], [18], [24], [30], [31] and both express an *N*-acyltransferase that could have a role in fatty acid amide biosynthesis [23], [24]. In *D. melanogaster*, we found the expression profiles of AANATL2 matched well with the metabolomic data showing the presence of the long-chain *N*-acyldopamines and *N*-acylserotonins. Work carried out *in vitro* demonstrated *D. melanogaster* AANATL2 would catalyze the production of long-chain *N*-acyldopamines and *N*-acylserotonins [23]. In the $N_{18}TG_2$ cells, we demonstrated that siRNA-mediated knock-down of glycine *N*-acyltransferase like 3 (GLYATL3) results in the accumulation of long-chain *N*-acylglycines in these cells. These results are consistent with limited *in vitro* substrate specificity data available for GLYATL3 [24]. In sum, our work and that of Waluk et al. [29]strongly suggest *N*-acyltransferases do catalyze key reactions in the fatty acid amide biosynthetic pathway.

We decided to add *Bombyx mor*i, the domesticated silkworm, as a model organism for our fatty acid amide studies. B. *mori* is known to express *Bm*-iAANAT, an enzyme catalyzing the acetyl-CoA-dependent *N*-acetylation of amines and exhibiting a wide tissue distribution [32]. Mutation of *Bm*-iAANAT led to melanism and to the accumulation of dopamine in the silkworm [33], [34]. A more

complete analysis of the substrate specificities of *Bm*-iAANAT seemed warranted to determine if long-chain acyl-CoA thioesters were substrates for this enzyme. If so, the availability of mutants and its broad tissue distribution data point to straightforward metabolomic experiments to evaluate the *in vivo*role of *Bm*-iAANAT in fatty acid amide biosynthesis.

We report, herein, long-chain acyl-CoA thioesters like palmitoyl- and oleoyl-CoA are substrates for *Bm*-iAANAT leading to the formation of fatty acid amides *in vitro*. Also, we find *Bm*-iAANAT accepts many amines as substrates, significantly expanding the list of amine substrates reported for this enzyme [32]. *Bm*-iAANAT is, thus, a "promiscuous generalist" with regards to the acyl-CoA and amine substrates. We identified a set of fatty acid amides in 4th instar larvae of *B. mori*, the first report of these lipid amides in these insects and found *Bm*-iAANAT is expressed in 4th instar larvae. The combination of all our data are consistent with *Bm*-iAANAT functioning in the biosynthesis of fatty acid amides, at least in 4th instar larvae of *B. mori*.

2. Materials and methods

2.1. Materials

Unless otherwise noted, all reagents were obtained from commercial sources. Codon-optimized *Bm*-iAANAT was purchased from Genscript. Oligonucleotideswere purchased from Eurofins MWG Operon BL21 (DE3) *E. coli* cells, XL-10 competent cells, and the *pET28a*(+) vector were purchased from Novagen. PfuUltra High-Fidelity DNA polymerase was purchased from Agilent. XhoI, NdeI, Antarctic phosphatase, and T4 DNA ligase were purchased from New England Biolabs. Kanamycin monosulfate and IPTG were purchased from Gold Biotechnology. ProBond nickel-chelating resin was purchased from Invitrogen. Long and short-chain acyl-CoA thioesters and amine substrates were purchased from Sigma-Aldrich. *N*-Oleoyltryptamine was synthesized from oleoylchloride and tryptamine essentially as described for the synthesis of *N*-heptanoyltryptamine [35]. All other supplies and materials were of the highest quality available from

either Sigma or Fisher Scientific. Spectrophotometric analyses were performed on a Cary 300 Bio UV–Visible spectrophotometer.

2.1. Cloning of Bm-iAANAT

Bm-iAANAT (Accession No. NM_001079654.2) was codon optimized for expression in *E. coli*, with 5′-NdeI and 3′-XhoI restriction sites, included an N-terminal His_6-tag separated from the N-terminal methionine of wildtype enzyme with a 10-amino acid linker (SSGLVPRGSH), and synthesized into a *pUC57*vector. The full-length gene was excised from the *pUC57* vector and ligated into the NdeI and XhoI restriction sites of the *pET-28a* vector. The *Bm-iAANAT- pET28a* vector was then transformed into *E. coli* XL-10 competent cells, plated on a Luria Broth (LB) agar plate supplemented with 50 μg/mL kanamycin and grown overnight at 37°C. A single colony from each vector transformation was cultured overnight in LB media supplemented with 50 μg/mL kanamycin overnight at 37 °C. The *Bm-iAANAT-pET28a* plasmid was purified from the overnight cultures using the Promega Wizard Plus SV Minipreps DNA purification kit, sequenced by Eurofins MWG Operon to confirm correct gene insertion, and finally transformed into *E. coli* BL-21 (DE3) cells for the expression of *Bm*-iAANAT.

2.2. Expression and purification of Bm-iAANAT

The *E. coli* BL-21 (DE3) competent cells containing the *Bm-iAANAT-pET28a*vector were cultured in LB media supplemented with 50 μg/mL kanamycin at 37 °C. Once the cultures reached an absorbance of 0.6 at 600 nm, cells were induced with the addition of 1.0 mM isopropyl β-D-thiogalactopyranoside (IPTG) for 4 hours at 37°C. The final cultures were harvested by centrifugation at 6,000 × g for 10 min at 4°C, and pellets were frozen at −80°C for later analysis. Cell pellets were thawed and suspended in Binding buffer: 20 mM Tris pH 7.9, 500 mM NaCl, and 5 mM imidazole. Cells were lysed by sonication and the cellular debris was pelleted by centrifugation at 16,000 × g for 20 min at 4°C. The supernatant was retained and loaded onto a 5 mL column of ProBond nickel-chelating resin. The column was washed with 5 column volumes (CVs) of Binding buffer, followed by 10 CVs of Wash

buffer: 20 mM Tris pH 7.9, 500 mM NaCl, and 60 mM imidazole. Finally, purified enzyme was eluted from the column in 1 mL fractions with 2–3 CVs of Elution buffer: 20 mM Tris pH 7.9, 500 mM NaCl, and 500 mM imidazole. Fractions were evaluated for purity and protein concentration using 10% sodium dodecyl sulfate polyacrylamide gel electrophoresis (SDS-PAGE) gels and Bradford binding assay, respectively. Fractions containing the purified *Bm*-iAANAT were pooled, dialyzed overnight in 20 mM Tris pH 7.4, 200 mM NaCl, and stored at −80 °C.

2.3. Identification of the amine substrates for Bm-iAANAT

To identify amine substrates, *Bm*-iAANAT activity was measured using either acetyl-CoA (representative of a short-chain acyl-CoA) or oleoyl-CoA (representative of a long-chain acyl-CoA) separately along with sets of different amines grouped together. The amines included in each group are listed in Table S1 (Supplementary Material). The assay solutions used to measure *Bm*-iAANAT activity from the groups of amines consisted of 300 mM Tris pH 8.0, 150 µM DTNB (5,5′-dithiobis (2-nitro-benzoic acid), Ellman's reagent), 500 µM of either acetyl- or oleoyl-CoA and the all the amines grouped together as shown in Table S1 (Supplementary Material, each amine at 60 mM) at 22 °C. Initial velocities were determined by measuring the release of CoA-SH at 412 nm (ε_{412} = 13,600 M^{-1} cm^{-1}) [36], with the reported velocities calculated as the background acyl-CoA thioester hydrolysis rate subtracted from the observed velocity. The rates of background acyl-CoA hydrolysis were determined in absence of *Bm*-iAANAT or after adding heat-denatured (boiled) *Bm*-iAANAT. The background rates of acyl-CoA hydrolysis were the same, within experimental error, for the two control experiments. Any combination of amine group and acyl-CoA displaying a background-corrected rate ≥0.1 µmoles/min/mg was considered a "hit", exhibiting a rate of CoA-SH release ≥3-fold the above background rate. The individual amines within an amine group showing a "hit" were then individually interrogated further at 60 mM in solution with 300 mM Tris pH 8.0, 150 µM DTNB, and 500 µM acetyl-CoA or 500 µM oleoyl-CoA to determine which amines with the group were substrates for *Bm*-iAANAT. Individual amines were considered *Bm*-

iAANAT substrates if the rate of CoA-SH release was ≥0.1 µmoles/min/mg above background acyl-CoA hydrolysis rate.

2.4. Determination of steady-state kinetic constants

Steady-state kinetic characterization of *Bm*-iAANAT was assayed by measuring the release of CoA-SH at 412 nm at 22 °C under the following conditions: 300 mM Tris pH 8.0, 150 µM DTNB, and different initial concentrations of the substrates: an amine and an acyl-CoA. To determine the apparent kinetic constants for the acyl-CoA thioester substrates, the initial tryptamine concentration was 60 mM while the initial concentration of the desired acyl-CoA was varied. To determine the apparent kinetic constants for an amine substrate, the initial acyl-CoA concentration was 100 µM while the initial concentration of the amine was varied. The apparent kinetic constants were determined by fitting the resulting initial rate *vs*. [substrate] data to Eq. (1) using SigmaPlot 12.0: $v_o$represents initial velocity, $V_{max,app}$ is the apparent maximal velocity, $K_{m,app}$ is the apparent Michaelis constant, and [S] is the substrate concentration. Assays were performed in triplicate. The uncertainty for the $(k_{cat}/K_m)_{app}$ values were calculated using Eq. (2), where σ is the standard error of the $k_{cat,app}$ and $K_{m,app}$ values [37].

Equation 1

$$v_o = \frac{V_{max,app}[S]}{K_{m,app} + [S]}$$

Equation 2

$$\sigma\left(\frac{x}{y}\right) = \frac{x}{y}\sqrt{\left(\frac{\sigma_x}{x}\right)^2 + \left(\frac{\sigma_y}{y}\right)^2}$$

2.5 Characterization of the product generated by Bm-iAANAT by LC-QToF-MS

The use of Ellman's reagent to measure CoA-SH release from acetyl-CoA or oleoyl-CoA is no guarantee of *N*-acylamide formation. To confirm *N*-acylamide product formation in a reaction catalyzed by *Bm*-iAANAT, 1 mM tryptamine and 500 µM oleoyl-CoA were incubated with 100 µg of purified enzyme for 1 h in 300 mM Tris pH 8.0. A control lacking enzyme was run in parallel. We determined this ratio of [oleoyl-CoA]/[tryptamine] was ideal for *N*-acylamide production after several optimization experiments because *Bm*-iAANAT can be inhibited by a high concentration of the amine substrate [32]. Following the 1 hr. incubation, the reaction mixture was then passed through a 10 kDa ultrafilter (Millipore) to remove *Bm*-iAANAT. Aliquots (20 µL) of the resulting flow-through solution containing the putative *N*-oleoyltryptamine product from the experiment with enzyme and the control lacking enzyme were injected separately on an Agilent 6540 liquid chromatography/quadrupole time-of-flight mass spectrometer (LC-QTOF-MS) in positive ion mode. The *N*-oleoyltryptamine standard and the enzymatic reaction product characterizations were completed on a Kinetex 2.6 µm C_{18} 100 Å (50 × 2.1 mm) reverse phase column with the following mobile phase gradient with a flow rate of 0.6 mL/min: mobile phase A was 0.1% (v/v) formic acid in water, while mobile phase B was 0.1% (v/v) formic acid in acetonitrile. A linear gradient of 10% mobile phase B increased to 100% B over 5 min, followed by a hold of 3 min at 100% B for the analysis of the product. The column was then equilibrated with 10% mobile phase B for 10 min before subsequent injections. The column was thoroughly washed between injections using the same solvent gradient, but at a flow rate of 1.0 mL/min.

2.6. Detection of Bm-iAANAT transcripts in 4th instar larvae of *B. mori* via RT-PCR

2.6.1. Silkworm culture and isolation of mRNA

B. *mori* eggs were purchased from Carolina Biological and immediately placed into a petri dish upon arrival. Silkworms were cultured with Silkworm Artificial Dry Diet from Carolina Biological and allowed to grow until the fourth instar: after the larvae had molted three times from their original hatch. Total RNA was extracted using the PureLink® RNA Mini Kit from Invitrogen and the mRNA was then

isolated via PolyATtract® mRNA Isolation Systems III from Promega. After the elution of mRNA in nuclease-free water, a 10 kDa centrifugal filter was used to concentrate the heavier nucleic acids (15 min at 12,000 × g). Any traces of remaining genomic DNA were removed using DNase I from Thermo Fisher with the modifications to the recommended protocol, as outlined in Table 1. The reaction mixture was briefly centrifuged, heated at 37°C for 30 min, followed by the addition of 2 µL of 50 mM EDTA, and, lastly, heating for another 10 min at 65°C to inactivate the DNase I.

Table 1. Method for the DNase I-mediated degradation of genomic DNA.

Reagent	Recommended protocol[a]	Modified protocol
mRNA	1 µg	1 µg
DNase I	1 µL	2 µL
DNase I Buffer with $MgCl_2$	1 µL	2 µL
Nuclease-Free Water	to 10 µL	to 18 µL

[a]As recommended by the manufacturer.

2.6.2. Generation of cDNA library and transcripts for Bm-iAANAT and Bm-Alpha Tubulin (TUA1)

A cDNA library from Bmi4 larvae was generated via incubation of isolated mRNA at 45°C for 45 min with reverse transcriptase (MMLV-RT from Promega). PCR was carried out using the thermal cycling conditions noted in Jeffries et al. [19] at an annealing temperature of 60 °C for all amplicons. TUA1 (NM_001043419) was chosen as an endogenous control for the RT-PCRexperiments because this protein is ubiquitously expressed throughout the life of *B. mori*[38]. Forward and reverse primers for TUA1 and *Bm*-iAANAT were designed and ordered from Eurofins Genomics and amplify 99 and 119 bp regions respectively, within the open reading frame of the appropriate gene (Table 2). Separate, one-step RT-PCR reactions for TUA1 and *Bm*-iAANAT were prepared. Each RT-PCR reaction solution contained

25 µL of Access Quick Master Mix from Promega, 320 nM forward primer, 320 nM reverse primer, 250 ng fourth instar larval mRNA, 200 units MMLV reverse transcriptase from Promega, and sufficient nuclease-free water to bring the reaction volume to 50 µL. A no reverse transcriptase control was included to confirm the removal of genomic DNA.

Table 2. Primers used to amplify TUA1 and *Bm*-iAANAT.

Primer	Primer sequence
TUA 1 Forward Primer	AGATGCCCACAGACAAGACC
TUA 1 Reverse Primer	CAAGATCGACGAAGAGAGCA
Bm-iAANAT Forward Primer	CAAAATGTCCGTTCCAGCTT
Bm-iAANAT Forward Primer	GATTGACGGCGAGATTCATT

2.6.3. Analysis of the cDNA products

An aliquot (10 µL) of Blue DNA Loading Dye from New England Biolabs (NEB) was added to each cDNA reaction and the resulting 60 µL RT-PCR reaction solutions were loaded into separate lanes of a 1.8% agarose gel containing ethidium bromide. One lane of the gel was loaded with the 100 bp ladder from NEB. Electrophoresis in 1 × TAE buffer from NEB (diluted from a 50 × stock) allowed for the migration of cDNA products at 50 V over a duration of 90 min. The cDNA bands (Fig. 2) were excised from the gel with a clean razor blade, and the cDNA extracted from the agarose gel slice using the Gel

Extraction_Wizard from Promega. The isolated cDNA was then sequenced commercially by Eurofins Genomics.

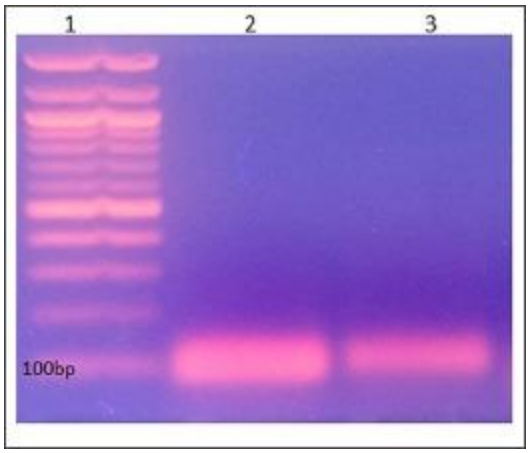

Fig. 2. RT-PCR of *Bm*-iAANAT and *Bm*-TUA1 in the 4th Instar of B. *mori*. Lane 1 contains 100 bp ladder; the band on the bottom denotes 100 bp standard. Lane 2 was loaded with the RT-PCR product for *Bm*-TUA1 (99 bp). Lane 3 was loaded with RT-PCR product for *Bm*-iAANAT (119 bp).
The amplicon product extracted from lane 2 matched the sequence for *Bm*-TUA1, while the amplicon product extracted from lane 3 matched the sequence for *Bm*-iAANAT.

2.7. Extraction and purification of fatty acid amides from 4th instar larvae of B. mori

Bmi4 larvae (3.0 g) were collected on the same day for both mRNA extraction and metabolomic analysis and both collections were carefully assessed to be nearly identical in size and development. The Bmi4 larvae were flash frozen with liquid N_2 and stored at −80 °C until after completion of the RT-PCR experiments. The frozen larvae were ground to a paste in 61 mL of methanol using a mortar and pestle and then were homogenized for 5 min in a clean, glass beaker using a Heidolph Silent Crusher homogenizer at maximum speed (26,000 rpm). The homogenate was divided into three separate samples of equal mass and volume into clean, previously unused vials and all were separately re-homogenized for 5 min at maximum speed. The fatty acid amideswere extracted and purified from these samples using the method of Sultana and Johnson [39], as modified by Jeffries et al. [19]. Blanks were

prepared and treated exactly in the same manner starting with 61 mL of methanol in a clean mortar and pestle without any addition of Bmi4.

2.8. Identification and quantitation of fatty acid amides via LC-QToF-MS

2.8.1. Generation of fatty acid amide standard curves

With the exception of palmitamide-d_{31}, the fatty acid amides used as internal standards, *N*-arachidonoylglycine-d_8, *N*-arachidonoylethanolamide-d_8, palmiticacid-d_{31}, and *N*-oleoylserotonin-d_{17}, were all from Cayman Chemical. Palmitamide-d_{31} was synthesized from palmitic acid-d_{31} as described [1]. Mass spectral analysis of all the deuterated fatty acid amides, obtained commercially or synthesized in-house, were contaminated by <1% of the corresponding unlabeled fatty acid amide (Figure S1, Supplementary Material). Standard curves were made using pure compounds for each fatty acid amide and internal standards at concentrations ranging from 0.1–10 pmoles in methanol:acetonitrile (1:1) (v/v) per 20 µL injection on the LC-QToF-MS. A mixture was made containing 1 µM of each deuterated standard in methanol:acetonitrile (1:1) (v/v).

2.8.2. Sample preparation for LC-QToF-MS

The fatty acid amide-containing extracts from Bmi4 larvae were concentrated using 100 µL C_{18} Zip Tips from Thermo Fisher with the following modifications to the manufacturer's recommended protocol: 0.1% (v/v) trifluoroacetic acid (TFA) was substituted for 0.1% TFA: methanol:acetonitrile (8:1:1) (v/v/v) and the fatty acid amides eluted from the tips in 90 µL of acetonitrile:0.1% (v/v) TFA (95:5). The eluent from the Zip Tip was collected in LC vials with spring inserts and 10 µL of the internal standard mixture was added to make a total volume of 100 µL. Samples were analyzed by LC-QToF-MS as described in Section 2.5. The extraction blank was also prepared in the same manner in order to subtract background concentrations of fatty acid amides that may have accrued during the extraction process or unintentionally added from non-deuterated contaminants of the deuterated internal standards.

2.8.3. Identification and quantification of fatty acid amides in the Bmi4 extracts

All total ion chromatograms for the Bmi4 larval extracts were scanned for *m/z*corresponding to fatty acid amides. The retention times and *m/z* values for metabolites detected in the Bmi4 extracts were compared to those of known standards evaluated under the exact same conditions. The LC column was thoroughly washed (using the same LC method) before the injection of Bmi4 extracts to eliminate false positives. All retention times of detected fatty acid amides were found to be accurate to ±0.1 min of the standard, acceptable deviation of random error from the instrument and the sample matrix effects. These intensity units for each fatty acid amide were converted to pmoles/(gram of tissue) using the standard curves prepared as described in Section 2.8.1.

3. Results

3.1. Cloning, expression, and purification of Bm-iAANAT

Bm-iAANAT from Bombyx *mori* was successfully cloned and expressed in *E.coli*. The recombinant *Bm*-iAANAT we designed possessed a his_6-tag on the N-terminus, allowing for a convenient and facile purification by Ni-chelation chromatography. Our yield of purified *Bm*-iAANAT was 17–18 mg of purified protein per liter of *E. coli* culture. Purity was ≥95% as assessed 10% SDS-PAGE gel (Figure S2, Supplementary Material) and the molecular weight from SDS-PAGE analysis was in good agreement with their predicted mass of *Bm*-iAANAT of 29.6 kDa.

3.2. Substrate specificity of Bm-iAANAT

A screening protocol was used to identify substrates for *Bm*-iAANAT. We pooled together a set of amines (Table S1, Supplementary Material) and evaluated the entire group, at once, for CoA-SH release using a short-chain or long-chain acyl-CoA substrate. The concentration of the individual amines within the pool was high, 60 mM, because of the relatively high K_m (or $K_{m,app}$) value for the amine substrates for some of the GNAT enzymes. For example, the $K_{m,app}$ for glycine for mouse glycine *N*-acyltransferase is 6 mM [40]. A similar protocol could be employed to identify acyl-CoA substrates

for *Bm*-AANAT by evaluating groups of acyl-CoA thioesters against an amine co-substrate for CoA-SH releases, but the acyl-CoA thioesters are expensive and long-chain acyl-CoAthioesters can be inhibitors for *N*-acetyltransferases [41], [42]. As a compromise, we individually screened the amine pools for CoA-SH release using a short-chain or a long-chain acyl-CoA thioester, acetyl-CoA or oleoyl-CoA, as the acyl donor substrate. The benefits of our screening protocol are clear: any combination of pooled amines and acyl-CoA showing no CoA-SH release activity could be reasonably disregarded for further investigation. A false negative is possible if one of the amines in the pool is a *Bm*-iAANAT inhibitor and the degree inhibition by the inhibitor amine is sufficient to mask CoA-SH release activity from a different amine substrate in the pool. A false negative seems unlikely because the *complete* elimination of CoA-SH release activity would require a balance between [amine inhibitor]/K_i ratio, the [amine substrate]/K_m ratio, and would, most likely, occur if the amine substrate exhibits a low k_{cat} value. Conversely, any combination of pooled amines and acyl-CoA that exhibit CoA-SH release can be investigated individually to define the substrate specificity. The application of our screening protocol to *Bm*-iAANAT revealed significant velocities of CoA-SH release from 5 of the amine pools with acetyl-CoA as the acyl donor and 3 of the amine pools with oleoyl-CoA as the acyl donor (Table S2, Supplementary Material). A significant velocity is defined as any rate of CoA-SH release that is ≥3-fold higher than the background rate of acyl-CoA hydrolysis, 0.1 μmoles/min/mg. The background rate of acyl-CoA hydrolysis was the same, within experimental error, for two controls: no added *Bm*-iAANAT or the reaction initiated by the addition of heat-denatured *Bm*-iAANAT. In addition to the amine substrates identified by Tsugehara et al. [32](dopamine, octopamine, norepinephrine, serotonin, tryptamine, and tyramine), we found that *Bm*-iAANAT would accept lysine, histamine, alanine, tyramine, ethanolamine, as well as several polyamines (spermidine, agmatine, cadaverine, and putrescine) as substrates. Because of limited sensitivity of our assay (detection limit of CoA-SH release being ≤1 μM), we could not accurately determine the kinetic constants for the remainder of the newly discovered amine substrates for *Bm*-iAANAT with acetyl-CoA as the co-substrate, due to either a low value for either the $K_{m,app}$ or the $k_{cat,app}$.

Tsugehara et al. [32] employed a more sensitive radiochemical assay with [^{14}C]-acetyl-CoA as a substrate and reported a $K_{m,app}$ value of 0.31 μM for acetyl-CoA.

We repeated the evaluation of the amine pools using oleoyl-CoA as the co-substrate and found that three of the eight amine groups yielded rates of CoA-SH release significantly above background (Table S2, Supplementary Material). Individual interrogation of these groups revealed four amines, tryptamine, tyramine, serotonin, and octopamine, would serve as co-substrates with oleoyl-CoA. With the initial concentration of oleoyl-CoA fixed at 100 μM, tryptamine was the amine with the highest $(k_{cat}/K_m)_{app}$ value, $(1.0 \pm 0.07) \times 10^2$ M^{-1} s^{-1}. Tyramine and octopamine displayed significantly lower $(k_{cat}/K_m)_{app}$ values than tryptamine, attributed both to high $K_{m,app}$ values and lower $k_{cat,app}$ values (Table 3). Qualitatively, the release of CoA-SH was evident when *Bm*-iAANAT was incubated with oleoyl-CoA and serotonin. At the relatively high concentrations of serotonin required to properly measure the formation of *N*-oleoylserotonin, a precipitate formed preventing the accurate quantification of CoA-SH using Ellman's reagent. Thus, we were unable to measure kinetic constants for the *Bm*-iAANAT-catalyzed formation of *N*-oleoylserotonin from serotonin and oleoyl-CoA.

Table 3. Steady-state kinetic constants for different Amine substrates with Oleoyl-CoA as the Acyl Donor.[a,b]

Amine[c]	$K_{m,app}$ (mM)	$k_{cat,app}$ (s^{-1})	$(k_{cat}/K_m)_{app}$ (M^{-1} s^{-1})
Tryptamine	7.0 ± 0.5	0.72 ± 0.01	$(1.0 \pm 0.07) \times 10^2$
Tyramine	84 ± 12	2.7 ± 0.19	32 ± 5.3
Octopamine	65 ± 16	0.31 ± 0.04	4.7 ± 1.2

[a] Reaction conditions were 300 mM Tris pH 8.0, 150 μM DTNB, 100 μM oleoyl-CoA, and varied initial concentrations of the indicated amine.

[b] Kinetic constants are reported with the standard error (n = 3).

[c] Serotonin is an amine substrate when oleoyl-CoA is the acyl donor. However, a precipitate formed during catalysis which interfered with the assay and prevented the accurate determination of the kinetic constants for serotonin.

We employed only acetyl- and oleoyl-CoA in our identification of new amine substrates for *Bm*-iAANAT. There are many potential acyl-CoA substrates for *Bm*-iAANAT and we chose to focus on the unbranched, long chain acyl-CoA substrates that are representative of acyl chains found in biologically-occurring fatty acid amides. With tryptamine held at a constant initial concentration of 60 mM, we found that lauroyl-, myristoyl-, palmitoyl-, and arachidonoyl-CoA (all at an initial concentration of 100 μM) were substrates, yielding a rate of CoA-SH release significantly above the background rate of non-enzymatic acyl-CoA hydrolysis. The kinetic constants for these long-chain acyl-CoA substrates are presented in Table 4. We observed a 6.2-fold decrease in the $(k_{cat}/K_m)_{app}$ value as the length of the acyl chain increased from lauroyl-CoA to arachidonoyl-CoA. The decrease in $(k_{cat}/K_m)_{app}$ values was largely a result in a decrease in the $k_{cat,app}$ value because we found the $K_{m,app}$ values were approximately the same for this set of acyl-CoA substrates, ~1 μM.

Table 4. Steady-state kinetic constants for long-\chain acyl-CoA substrates with tryptamineas the acyl acceptor.[a,b]

Acyl-CoA	$K_{m,app}$ (μM)	$k_{cat,app}$ (s^{-1})	$(k_{cat}/K_m)_{app}$ (M^{-1} s^{-1})
Lauroyl-CoA	0.97 ± 0.12	1.3 ± 0.01	(1.4 ± 0.2) × 10^5
Myristoyl-CoA	0.92 ± 0.20	0.66 ± 0.01	(7.2 ± 1.5) × 10^5
Palmitoyl-CoA	1.1 ± 0.30	0.51 ± 0.01	(4.9 ± 1.4) × 10^5
Oleoyl-CoA	1.7 ± 0.51	0.42 ± 0.02	(2.4 ± 0.70) × 10^5
Arachidonoyl-CoA	1.2 ± 0.67	0.27 ± 0.02	(2.4 ± 1.3) × 10^5

[a] Reaction conditions were 300 mM Tris pH 8.0, 150 μM DTNB, 60 mM tryptamine, and varied initial concentrations of the acyl-CoA.

[b]Kinetic constants are reported with the standard error (n = 3).

To further explore the observed chain length dependence in the kinetic constants, we determined the kinetic constants for tryptamine while holding the initial concentration of several long-chain acyl-CoA thioesters constant at 100 μM (Table S3, Supplementary Material). We observed a similar pattern in the data. The $(K_{m,\ tryptamine})_{app}$ values are all comparable, ranging from 2.5 mM to 7.0 mM. The $(k_{cat}/K_m)_{tryptamine,\ app}$ was highest when the thioester substrate was lauroryl-CoA and declined ~3-fold as the acyl chain length increased to oleoyl-CoA.

3.3. Product characterization of a Bm-iAANAT-catalyzed reaction

The use of Ellman's reagent to detect CoA-SH release does not prove *Bm*-iAANAT has catalyzed the formation of an *N*-acylamide from an acyl-CoA and an amine. While unlikely, CoA-SH release could reflect the amine activation of *Bm*-iAANAT-catalyzed thioester hydrolysis: CoA-S-CO-R + H_2O → R-COOH + CoA-SH. We compared a synthetic standard of *N*-oleoyltryptamine against the product generated by the incubation of *Bm*-iAANAT with tryptamine and oleoyl-CoA. The analysis of the enzymatic product corroborated our kinetic data: the *N*-oleoyltryptamine produced by *Bm*-iAANAT catalysis is consistent with the $[M+H]^+$ peak and retention time (±0.2 min reported error for the LC-QToF-MS) *vs*. the *N*-oleoyltryptamine standard (Table 5). We did not detect any compounds with the retention time or *m/z* of *N*-oleoyltryptamine in the no enzyme-containing (blank) samples.

Table 5. Characterization of the *Bm*-iAANAT-catalyzed reaction via LC-QTOF-MS analysis.

Sample	Retention time (min)	$[M+H]^+$ (*m/z*)
N-Oleoyltryptamine Standard	6.489	425.2588
Bm-iAANAT Product	6.503	425.2574

3.4. Detection of Bm-iAANAT transcript in 4th instar larvae of B. mori *via RT-PCR*

Our *in vitro* studies of purified, recombinant *Bm*-iAANAT suggest this enzyme could have a role in the biosynthesis of fatty acid amides. Our next steps were to determine if fatty acid amides are produced by *B. mori* and, if so, does the presence of these molecules in *B. mori* correlate, at all, to the expression of *Bm*-iAANAT. We identified the presence of *Bm*-iAANAT transcripts by RT-PCR. Primers were prepared to generate a 119 bp *Bm*-iAANAT-derived RT-PCR product and a 99 bp *Bm*-TUA1-derived product (as a control) from a 4th instar larvae *B. mori* cDNA library. After the migration of cDNA products on an agarose gel containing ethidium bromide, the gel was viewed under UV light to illuminate the RT-PCR products. The RT-PCR products match the expected sizes for the *Bm*-iAANAT and *Bm*-TUA1 transcripts, respectively (Fig. 2).

3.5. Detection of a panel of fatty acid amides from Bmi4 via LC-QToF-MS

All total ion chromatograms (TIC) for the 4th instar larvae were scanned for *m/z*similar to the fatty acid amides found in *D. melanogaster*[19]. The retention times and *m/z* values for metabolites detected in the Bmi4 extracts were compared to those of known standards evaluated under the exact same conditions. The intensities for the *m/z* values corresponding to a specific fatty acid amide were converted to pmoles/(gram of tissue) based on standard curves prepared with corresponding authentic fatty acid amide. The fatty acid amides identified from Bmi4 larvae are shown in Table 6.

Table 6. Fatty acid amides detected in 4th instar larvae of *B. mori*.

Fatty Acid Amide	Standard (*m/z*)	4th Instar (*m/z*)	Standard (Retention time)	4th Instar (Retention time)	Amount extracted (pmoles/g)[a]
Palmitamide	256.2645	256.2631	6.214 min.	6.213 min.	28 ± 19
N-Palmitoylserotonin	415.3322	415.2882	6.187 min.	6.125 min.	9.8 ± 0.6
Palmitoleamide	254.2456	254.2463	5.857 min.	5.859 min.	22 ± 13
N-Stearoylserotonin	443.3638	443.3505	6.542 min.	6.576 min.	1.1 ± 0.4
Oleamide	282.2796	282.2786	6.289 min.	6.277 min.	33 ± 2.9
N-Oleoyldopamine	418.3315	418.3306	6.248 min.	6.246 min	6.0 ± 0.3
N-Oleoylethanolamine	326.3057	3.26.3049	6.077 min.	6.074 min	20 ± 15
N-Oleoylglycine	340.2846	340.2847	6.094 min.	5.945 min.	14 ± 1.5
N-Oleoylserotonin	441.3479	441.3483	6.262 min.	6.322 min	3.5 ± 0.6
Linoleamide	280.2643	280.2616	5.979 min.	6.027 min.	22 ± 14
N-Arachidonoylserotonin	463.3326	463.3337	6.071 min.	6.069 min.	14 ± 2.9

[a] Average ± standard deviation for 3 separate measurements.

4. Discussion and conclusions

In this study, we have successfully cloned, expressed, purified, and characterized *Bm*-iAANAT, an arylalkylamine *N*-acyltransferase from Bombyx *mori*. The characterization of *Bm*-iAANAT contributes to the body of knowledge leading to a pest-specific iAANAT inhibitor, important because iAANATs are suggested as new targets for the development of insecticides [43], [44], [45], [46]. The

most important finding from our work was that *Bm*-iAANAT will accept long chain acyl CoA thioesters as substrates. This result coupled to our demonstration that the enzyme is expressed in 4th instar larvae and to our identification of fatty acid amides in the 4th instar larvae of *B. mori* suggests, but does not prove, *Bm*-iAANAT has a role in the biosynthesis of, at least, a few members of the fatty acid amide family in this insect. We have long thought an acyltransferase could function in fatty acid amide production *in vivo*[25]. *Bm*-iAANAT is one of few known acyl-CoA-dependent transferases accepting fatty acyl-CoA thioesters as substrates for the enzymatic production of fatty acid amides; the others being human glycine *N*-acyltransferase like-2 [29], human glycine *N*-acyltransferase like-3 [24], and *D. melanogaster* arylalkylamine *N*-acyltransferase like-2 (AANATL2) [23]. In addition, *N*-myristoyltransferase (NMT) utilizes myristoyl-CoA as the myristoyl donor for the myristoylation of the N-terminus of proteins [28]. The direct conjugation of an amine to an inactivated fatty acid, while thermodynamically unfavorable under biological conditions, has been attributed to the biosynthesis of fatty acid amides [47], [48]. This includes the conjugation of linolenic acid to L-glutamine to yield *N*-linolenoyl-L-glutamine in the caterpillars of *Manduca sexta*[49].

Based on our current understanding of the substrate specificity of *Bm*-iAANAT (Tables 3 and 4 and ref. [32]) and the fatty acid amides identified in Bmi4 (Table 6), *Bm*-iAANAT could serve *in vivo* to generate the *N*-fatty acyl -serotonins and -dopamines. The possibility of *Bm*-iAANAT having a broader role in the biosynthesis of other *N*-fatty acylamides, based on its amine specificity, awaits further work: the identification of other *N*-fatty acylamides in *B. mori*and/or alternations in the fatty acid amidome after the knock down of *Bm*-iAANAT expression. The CRISPR/cas9 system has been used in *B. mori* for the targeted elimination of a protein [50], [51]. We used targeted knockdown methods to demonstrate the glycine *N*-acyltransferase like-3 and peptidylglycine α-amidating monooxygenase function sequentially in mouse neuroblastoma$N_{18}TG_2$ cells to convert fatty acyl-CoA thioesters to the fatty acid primary amides [24].

Another interesting outcome from our work on *Bm*-iAANAT is the influence acyl-CoA substrate chain length has on the affinity of the enzyme for the amine substrate. $K_{m,app}$ values are not

$K_{dissociation}$ values and a discussion of the affinity of *Bm*-iAANAT for the amine substrates assumes that differences in $K_{m,app}$ values for the amines does, at least, approximate the influence of the acyl-CoA substrate on the $K_{dissociation}$ values for an amine. Our work and that of Tsugehara et al. [32] show low $K_{m,app}$ values for the amine substrates when acetyl-CoA is the acyl donor. The $K_{m,app}$ value for tryptamine increases >1,000-fold when the acyl-CoA donor has an acyl chain of 12 carbons or longer (lauroyl-CoA to oleoyl-CoA) (Table 4). We have observed similar trends for other iAANATs, but the effect is more pronounced for *Bm*-iAANAT. For *D. melanogaster* AANATL7, we found the $K_{m,app}$ for histamine increased from 0.52 mM when acetyl-CoA was the acyl donor to 15 mM when hexanoyl-CoA was the acyl donor [42]. For *D. melanogaster* AANATL2, the $K_{m,app}$ for serotonin increased from 7.2 µM for acetyl-CoA to 870 µM for palmitoyl-CoA [23]. We have recently shown the acetyl group of acetyl-CoA shifts the conformational ensemble of *Bm*-iAANAT3 to a high affinity, catalytically efficient conformation [52]. The data presented here on *Bm*-iAANAT is consistent with this conclusion and clearly demonstrates a long acyl chain in the acyl-CoA hinders the most effective positioning of the amine for nucleophilic attack at the thioester bond of the acyl-CoA. A more precise understanding of conformational dynamics and the effects of dynamics on substrate positioning and catalysis in the iAANATs requires structural information. *Bm*-iAANAT could prove the better enzyme in addressing these questions because the amine affinity is more strongly influenced by the length of the acyl chain in the acyl-CoA than in other iAANATs.

Our identification of fatty acid amides in Bmi4 is the first report of these lipid amides in *B. mori*. Long-chain fatty acids are known in *B. mori*[53], [54], [55], [56] and the only report of a related *N*-acylamide in *B. mori* is *N*-acetylglutamate [56]. Fatty acid amides have a long and underappreciated history in insects, starting with the discovery of volicitin, N-(17-hydroxylinolenoyl)-L-glutamine, from *Spodoptera exigua*[15]. Volicitin, volicitin analogs, and other fatty acid amides have been reported in insects other than *B. mori*, including *D. melanogaster*[16], [17], [18], [19], [20]. The function of many fatty acid amides in insects (and many other organisms) remains elusive. The apparent lack of the cannabinoid receptors in *D. melanogaster*[21] despite reports of endocannabinoid-like fatty acid

amides in *D. melanogaster*[17], [18], [19] hints that fatty acid amides serve a different role in insects (and other invertebrates) relative to their functions in vertebrates. This points to a fascinating evolutionary story for these molecules as vertebrates emerged from invertebrates.

Conflicts of interest

The authors declare no conflicts of interest.

Acknowledgments

This work has been supported, in part, by grants from the University of South Florida (a Creative Scholarship grant), the Shirley W. and William L. Griffin Charitable Foundation, the National Institute of Drug Abuse at the National Institutes of Health (R03-DA034323) and the National Institute of General Medical Science of the National Institutes of Health (R15-GM107864) to D.J.M. This work has also received support from the Mass Spectrometry and PeptideFacility, Department of Chemistry, University of South Florida. The authors thank Sydney Balgo for technical assistance with some of the research and Dr. Ioannis Gelis for many helpful discussions throughout this work.

References

[1] E. K. Farrell, Y. Chen, M. Barazanji, K.A. Jeffries, F. Cameroamortegui, D.J. Merkler, Primary fatty acid amide metabolism: conversion of fatty acids and an ethanolamine in $N_{18}TG_2$ and SCP cells, J. Lipid Res. 53 (2012) 247-256, https://doi.org/10.1016/j.drudis.2008.02.006.

[2] F.A. Iannotti, V. Di Marzo, S. Petrosino, Endocannabinoids and endocannabinoid-related mediators: Targets, metabolism and role in neurological disorders, Prog. Lipid Res. 62 (2016) 107-128, http://dx.doi.org/10.1016/j.plipres.2016.02.002.

[3] R. Witkamp, Fatty acids, endocannabinoids, and inflammation, Eur. J. Pharmacol. 785 (2016) 96-107, http://dx.doi.org/10.1016/j.ejphar.2015.08.051.

[4] A Ure, Gouty concretions, with a new method of treatment. Med. Chir. Trans. 24 (1841) 30-35.

[5] W. Keller, Ueber verwandlung der benzoësäure in hippursäure, Justus Liebigs Ann. Chem. 43 (1842) 108-111.

[6] J.D. Spillane, A memorable decade in the history of neurology 1874-84-II, Br. Med. J. 4 (1974) 757-759.

[7] W.A. Devane, L. Hanuš, A. Breuer, R.G. Pertwee, L.A. Stevenson, G. Griffin, D. Gibson, A. Mandelbaum, A. Etinger, R. Mechoulam, Isolation and structure of a brain constituent that binds to the cannabinoid receptor, Science 258 (1992) 1946-1949, http://doi: 10.1126/science.1470919.

[8] T. Hua, K. Vemuri, M. Pu, L. Qu, G.W. Han, Y., Wu, S. Zhao, W. Shui, S. Li, A. Korde, R.B. Laprairie, E.L. Stahl, J.-H. Ho, N. Zvonok, H. Zhou, I. Kufareva, B. Wu,m Q. Zhao, M.A. Hanson, L.M. Bohn, A. Makriyannis, R.C. Stevens, Z.-J. Liu, Crystal structure of the human cannabinoid receptor r, Cell 167 (2016) 750-762, http://dx.doi.org/10.1016/j.cell.2016.10.004.

[9] M. Maccarrone, I. Bab, T. Bíró, G.A. Cabral, S.K. Dey, V. Di Marzo, J.C. Konje, G. Kunos, R. Mechoulam, P. Pacher, K.A. Sharkey, A. Zimmer, Endocannabinoid signaling at the periphery: 50 years after THC, Trends Pharmacol. Sci. 36 (2015) 277-296, http://doi: 10.1016/j.tips.2015.02.008

[10] H.-C. Lu, K. Mackie, An introduction to the endogenous cannabinoid system, Biol. Psychiatry 79 (2016) 516-525, https://doi.org/10.1016/j.biopsych.2015.07.028.

[11] F. Fezza, M. Bari, R. Florio, E. Talamonti, M. Feole, M. Maccarrone, Endocannabinoids, related compounds and their metabolic routes, Molecules 19 (2014) 17078-17106, http://doi:10.3390/molecules191117078.

[12] B.F. Cravatt, O. Prospero-Garcia, G. Siuzdak, N.B. Gilula, S.J. Henriksen, D.L. Boger, R.A. Lerner, Chemical characterization of a family of brain lipids that induce sleep, Science 268 (1995) 1506-1509, http://doi: 10.1126/science.7770779.

[13] P.C. Schmid, R.J. Krebsbach, S.R. Perry, T.M. Dettmer, J.L. Maasson, H.H.O. Schmid, Occurrence and postmorten generation of anandamide and other long-chain *N*-acylethanolamines in mammalian brain, FEBS Lett. 375 (1995) 117-120, http://doi: 10.1016/0014-5793(95)01194-J

[14] M. Maccrrone, M. Attinà, A. Cartoni, M. Bari, A. Finazzi-Agrò, Gas chromatography-mass spectrometry analysis of endogenous cannabinoids in healthy and tumoral human brain and human cells in culture, J. Neurochem. 76 (2001) 594-601, http://doi: 10.1046/j.1471-4159.2001.00092.x.

[15] H.T. Alborn, T.C.J. Turlings, T.H. Jones, G. Stenhagen, J.H. Loughrin, J.H. Tumlinson, An elicitor of plant volatiles from beet armyworm oral secretion, Science 276 (1997) 945-949, http://doi: 10.1126/science.276.5314.945.

[16] F. Fezza, J.W. Dillwith, T. Bisogno, J.S. Tucker, V. Di Marzo, J.R. Sauer, Endocannabinoids and related fatty acid amides, and their regulation, in the salivary gland of the lone star tick, Biochim. Biophys. Acta 1633 (2003) 61-67, http://doi: 10.1016/S1388-1981(03)00087-8.

[17] N. Yoshinaga, T. Aboshi, C. Ishikawa, M. Fukui, M. Shimoda, R. Nishida, C.G. Lait, J.H. Tumlinson, N. Mori, Fatty acid amides, previously identified in caterpillars, found in the cricket *Teleogryllus taiwanemma* and fruit fly *Drosophila melanogaster* larvae, J. Chem. Ecol. 33 (2007) 1376-1381, http://doi 10.1007/s10886-007-9321-2

[18] G. Tortoriello, B.P. Rhodes, S.M. Takacs, J.M. Stuart, A. Basnet, S. Raboune, T.S. Widlanski, P. Doherty, T. Harkany, H.B. Bradshaw, Targeted lipidomics in *Drosophila melanogaster* identifies novel 2-monoacylglycerols and *N*-acyl amides, PLoS One 8 (2013) e67865, https://doi.org/10.1371/journal.pone.0067865

[19] K.A. Jeffries, D.R. Dempsey, A.L. Behari, R.L.Anderson, D.J. Merkler, *Drosophila melanogaster* as a model system to study long-chain fatty acid amide metabolism, FEBS Lett. 588 (2014) 1596-1602, http://doi: 10.1016/j.febslet.2014.02.051.

[20] N. Yoshinaga, C. Ishikawa, I. Seidl-Adams, E. Bosak, T. Aboshi, J.H. Tumlinson, N. Mori, *N*-(18-Hydroxylinolenoyl)-L-glutamine: A newly discovered analog of volicitin in *Manduca sexta* and its elcitior activity in plants, J. Chem. Ecol. 40 (2014) 484-490, http://doi: 10.1007/s10886-014-0436-y

[21] J. McPartland, V. Di Marzo, L. De Petrocellis, A. Mercer, M. Glass, Cannabinoid receptors are absent in insects, J. Comp. Neurol. 436 (2001) 423-429, http://doi: 10.1002/cne.1078.

[22] D.P. Waluk, M.R. Battistini, D.R. Dempsey, E.K. Farrell, K.A. Jeffries, P. Mitchell, L.W. Hernandez, J.C. McBride, D.J. Merkler, M.C. Hunt, Mammalian fatty acid amides of the brain and CNS, in: R.R. Watson, F. DeMeester (Eds.), Omega-3 Fatty Acids in Brain and Neurological Health, Academic Press, London, 2014, 87-107, http://doi: 10.1016/B978-0-12-410527-0.00009-0.

[23] D.R. Dempsey, K.A. Jeffries, R.L. Anderson, A.-M. Carpenter, S. Rodriguez Ospina, D.J., Identification of an arylalkylamine *N*-acyltransferase from *Drosophila melanogaster* that catalyzes the formation of long-chain *N*-acylserotonins, FEBS Lett. 588 (2014) 594-599, http://doi: 10.1016/j.febslet.2013.12.027

[24] K.A. Jeffries, D.R. Dempsey, E.K. Farrell, R.L. Anderson, G.J. Garbade, T.S. Gurina, I. Gruhonjic, C.A Gunderson, D.J. Merkler, Glycine *N*-acyltransferase-like 3 is responsible for long-chain *N*-acylglycine formation in N_{18}TG*2* cells, J. Lipid Res. 57 (2016) 781-790, http://doi: 10.1194/jlr.M062042.

[25] D.J. Merkler, K.A. Merkler, W. Stern, F.F. Fleming, Fatty acid amide biosynthesis: A possible new role for peptidylglycine □-amidating enzyme and acyl-coenzyme A:glycine *N*-acyltransferase, Arch. Biochem. Biophys. 330 (1996) 430-434, http://doi: 10.1006/abbi.1996.0272.

[26] M.W. Vetting, L.P.S. de Carvalho, M. Yu, S.S. Hegde, S. Magnet, S.L. Roderick, J.S. Blanchard, Structure and functions of the GNAT superfamily of acetyltransferases, Arch. Biochem. Biophys. 433 (2005) 212-226, http://doi: 10.1016/j.abb.2004.09.003.

[27] A.I. Ud-Din, A. Tikhomirova, A. Roujeinikova, Structure and functional diversity of GCN5-related *N*-acetyltransferases, Int. J. Mol. Sci. 17 (2016) pii: E1018, http://doi: 10.3390/ijms17071018.

[28] R.V.S. Rajala, R.S.S. Datla, R.N. Moyana, R. Kakkar, S.A. Carlsen, R.K. Sharma, N-myristoyltransferase, Mol. Cell. Biochem. 204 (2000) 135-155, http://doi: 10.1023/A:1007012622030.

[29] D.P. Waluk, N. Schultz, M.C. Hunt, Identification of glycine *N*-acyltransferase-like 2 (GLYATL2) as a transferase that produces *N*-acyl glycines in humans, FASEB J. 24 (2010) 2795-2803, http://doi: 10.1096/fj.09-148551.

[30] V. Di Marzo, L. De Petrocellis, N. Sepe, A. Buono, (1996) Biosynthesis of anandamide and related acylethanolamides in mouse J774 macrophages and N_{18} neuroblastoma cells, Biochem. J. 316 (1996) 977-984, http://doi: 10.1042/bj3160977.

[31] T. Bisogno, N. Sepe, L. De Petrocellis, R. Mechoulam, V. Di Marzo, The sleep inducing factor oleamide is produced by mouse neuroblastoma cells, Biochem. Biophys. Res. Commun. 239 (1997) 473-479, http://doi: 10.1006/bbrc.1997.7431.

[32] T. Tsugehara, S. Iwai, Y. Fujiwara, K. Mita, M. Takeda, Cloning and characterization of insect arylalkylamine *N*-acetyltransferase from *Bombyx mori*, Comp. Biochem. Physiol. B Biochem. Mol. Biol. 147 (2007) 358-366, http://doi: 10.1016/j.cbpb.2006.10.112.

[33] S. Zhan, Q. Guo, M. Li, M. Li, J. Li, X. Miao, Y. Huang, Disruption of an N-acetyltransferase gene in silkworm reveals a novel role in pigmentation, Development 137 (2010) 4083-4090, http:/doi: 10.1242/dev.053678.

[34] F.-y. Dai, L. Qiao, X.-l. Tong, C. Cao, P. Chen, J. Chen, C. Lu, Z.-h. Xiang, Mutations of an arylalkylamine-*N*-acetyltransferase, *Bm*-iAANAT, are responsible for silkworm melanism mutant, J. Biol. Chem. 285 (2010) 19553-19560, http://doi: 10.1074/jbc.M109.096743.

[35] F. Grudmann, V. Dill, A. Dowling, A. Thanwisai, E. Bode, N. Chantratitia, R. ffrench-Constant, H.B. Bode, (2012) Identification and isolation of insecticidal oxazoles from *Pseudomonas* spp., Beilstein J. Org. Chem. 8 (2012) 749-752, http://doi: 10.3762/bjoc.8.85.

[36] G.L. Ellman, Tissue sulfhydryl groups, Arch. Biochem. Biophys. 82 (1959) 70-77, http://doi: 10.1016/0003-9861(59)90090-6.

[37] J.R. Barrante, Applied Mathematics for Physical Chemistry:Third Edition, Pearson Prentice Hall, Upper Saddle River, NJ 2004.

[38] H. Kawasaki, K. Sugaya, G.-X. Quan, J. Nohata, K. Mita, Analysis of □- and □-tubulin genes of *Bombyx mori* using an EST database, Insect Biochem. Mol. Biol. 33 (2003) 131-137, https://doi.org/10.1016/S0965-1748(02)00184-4.

[39] T. Sultana, M.E. Johnson, Sample preparation and gas chromatography of primary fatty acid amides, J. Chromatogr. A 1101 (2006) 278-285, https://doi.org/10.1016/j.chroma.2005. 10.0273.

[40] D.R. Dempsey, J.D. Bond, A.-M. Carpenter, S. Rodriguez Ospina, D.J. Merkler, Expression, purification, and characterization of mouse glycine *N*-acyltransferase in *Escherichia coli*. Protein Expr. Purif. 97 (2014) 23-28, https://doi.org/10.1016/j.pep.2014.02.007.

[41] D.R. Dempsey, K.A. Jeffries, J.D. Bond, A.-M. Carpenter, S. Rodriguez-Ospina, L. Breydo, K.K. Caswell, D.J. Merkler, Mechanistic and structural analysis of *Drosophila melanogaster* arylalkylamine N-acetyltransferases, Biochemistry 53 (2014) 7777-7793, http://dx.doi.org/10.1021/bi5006078

[42] D.R. Dempsey, K.A. Jeffries, S. Handa, A.-M. Carpenter, S. Rodriguez-Ospina, L. Breydo, D.J. Merkler, Mechanistic and structural analysis of a *Drosophila melanogaster* enzyme, arylalkylamine

N-acetyltransferase like 7, an enzyme that catalyzes the formation of *N*-acetylarylakylamides and *N*-acetylhistamine, Biochemistry 54 (2015) 2644-2658, http://doi: 10.1021/acs.biochem.5b00113.

[43] B.G. O'Flynn, A.J. Hawley, D.J. Merkler, Insect Arylalkylamine *N*-Acetyltransferases as Potential Targets for Novel Insecticide Design, Biochem. Mol. Biol. J. 4 (2018) 1:4, In Press

[44] Q. Han, H. Robinson, H. Ding, B.M. Christensen, J. Li, Evolution of insect arylalkylamine *N*-acetyltransferases: Structural evidence from yellow fever mosquito, *Aedes aegypti*. Proc. Natl. Acad. Sci. USA 109 (2012) 11669-11674, http://doi: 10.1073/pnas/1206828109

[45] T. Tsugehara, T. Imai, M. Takeda, Characterization of arylalkylamine *N*-acetyltransferase from silkmoth (*Antheraea pernyi*) and pesticidal drug edesign base on the baculovirus-expressed enzyme, Comp. Biochem. Physiol. C Toxicol. Pharmacol. 157 (2013) 93-102, http://doi: 10.1016/j.cbpc.2012.10.003

[46] B.L.A. Lourenço, M.V.A.S. Silva, E.B. deOliveira, W.R. de Assis Soares, A. Góes-Neto, G. Santos, B.S. Andrade, Virtual screening and molecular docking for arylalkylamine-N-acetyltransferase (aaNAT) inhibitors, a key enzyme of *Aedes* (Stegomyia) *aegypti* (L.) metabolism, Comput. Mol. Biosci. 5 (2015) 35-44, http://dx.doi.org/10.4236/cmb.2015.53005.

[47] N.R. Bachur, S. Udenfriend, Microsomal synthesis of fatty acid amides, J. Biol. Chem. 241 (1966), 1308-1313.

[48] G. Arreaza, W.A. Devane, R.L. Omeir, G. Sajnani, J. Kunz, B.F. Cravatt, D.G. Deutsch, The cloned rat hydrolytic enzyme responsible for the breakdown of anandamide also catalyzes it formation via the condensation of arachidonic acid and ethanolamine, Neurosci. Lett. 234 (1997) 59-62, https://doi.org/10.1016/S0304-3940(97)00673-3.

[49] C.G. Lait, H.T. Alborn, P.E.A. Teal, J.H. Tumlinson III, Rapid biosynthesis of *N*-linolenoyl-L-glutamine, an elicitor of plant volatiles, by membrane-associated enzyme(s) in *Manduca sexta*, Proc. Natl. Acad. Sci. USA 100 (2003) 7027-7032, http://doi: 10.1073/pnas.1232474100.

[50] S. Ma, J. Chang, X. Wang, Y. Liu, J. Zhang, W. Lu, J. Gao, R. Shi, P. Zhao, Q. Xia, CRISPR/Cas9 medicated multiplex genome editing and heritable mutagenesis of *BmKu70* in *Bombyx mori*, Sci Rep. 4 (2014) 4489, http://doi: 10.1038/srep04489.

[51] Y. Liu, S. Ma, J. Chang, T. Zhang, X. Wang, R. Shi, J. Zhang, W. Lu, Y. Liu, and Q. Xia, Tissue-specific genome editing of laminA/C in the posterior silk glands of *Bombyx mori*, J. Genet. Genomics 44 (2017) 451-459, http://dx.doi.org/10.1016/j.jgg.2017.09.003.

[52] A.A. Aboalroub, A.B. Bachman, Z. Zhang, D. Keramisanou, D.J. Merkler, I. Gelis, Acetyl group coordinated progression through the catalytic cycle of an arylalkylamine N-acetyltransferase, PLoS One 12 (2017) e0177270, https://doi.org/ 10.1371/journal.pone.0177270.

[53] M.-G. Kwon, D.-S. Kim, J.-H. Lee, S.-W. Park, Y.-K. Choo, Y.-S. Han, J.-S. Kim, K.-A. Hwang, K. Ko, K. Ko, Isolation and analysis of natural compounds from silkworm pupae and effect of its extracts on alcohol detoxification, Entomol. Res. 42 (2012) 55-62, http://doi: 10.1111/j.1748-5967.2011.00439.x.

[54] D. Paul, S. Dey, Essential amino acids, lipid profile and fat-soluble vitamins of the edible silkworm *Bombyx mori* (Lepidoptera: Bombycidae), Int. J. Trop. Insect Sci. 34 (2014) 239-247, http://doi: 10.1017/S1742758414000526.

[55] L. Zhou, H. Li, F. Hao, N. Li, X. Liu, G. Wang, Y. Wang, H. Tang, Developmental changes for the hemolymph metabolome of silkworm (*Bombyx mori* L.), J. Proteome Res. 14 (2015) 2331-2347, http://doi: 10.1021/acs.jproteome.5b00159.

[56] Y Li, Q. Chen, Y. Hou, Q. Xia, P. Zhao, Metabolomic analysis of the larval head of the silkworm, *Bombyx mori*, Int. J. Mol. Sci. 17 (2016) 1460, http://doi: 10.3390/ijms17091460.